Nuclear parity violation in effective field theory

Shi-Lin Zhu [a,b], C.M. Maekawa [b,c], B.R. Holstein [d,e,*],
M.J. Ramsey-Musolf [b,f,g], U. van Kolck [h,i]

[a] *Department of Physics, Peking University, Beijing 100871, China*
[b] *Kellogg Radiation Laboratory, California Institute of Technology, Pasadena, CA 91125, USA*
[c] *Departamento de Física, Fundação Universidade Federal do Rio Grande,
Campus Carreiros, PO Box 474, 96201 Rio Grande, RS, Brazil*
[d] *Department of Physics-LGRT, University of Massachusetts, Amherst, MA 01003, USA*
[e] *Theory Group, Thomas Jefferson National Accelerator Facility, Newport News, VA 23606, USA*
[f] *Department of Physics, University of Connecticut, Storrs, CT 06269, USA*
[g] *Institute for Nuclear Theory, University of Washington, Seattle, WA 98195, USA*
[h] *Department of Physics, University of Arizona, Tucson, AZ 85721, USA*
[i] *RIKEN-BNL Research Center, Brookhaven National Laboratory, Upton, NY 11973, USA*

Abstract

We reformulate the analysis of nuclear parity violation (PV) within the framework of effective field theory (EFT). To $\mathcal{O}(Q)$, the PV nucleon–nucleon (NN) interaction depends on five a priori unknown constants that parameterize the leading-order, short-range four-nucleon operators. When pions are included as explicit degrees of freedom, the potential contains additional medium- and long-range components parameterized by PV πNN coupling. We derive the form of the corresponding one- and two-pion-exchange potentials. We apply these considerations to a set of existing and prospective PV few-body measurements that may be used to determine the five independent low-energy constants relevant to the pionless EFT and the additional constants associated with dynamical pions. We also discuss the relationship between the conventional meson-exchange framework and the EFT formulation, and argue that the latter provides a more general and systematic basis for analyzing nuclear PV.

* Corresponding author.
E-mail address: holstein@physics.umass.edu (B.R. Holstein).

1. Introduction

The cornerstone of traditional nuclear physics is the study of nuclear forces and, over the years, phenomenological forms of the nuclear potential have become increasingly sophisticated. In the nucleon–nucleon (NN) system, where data abound, the present state of the art is indicated, for example, by phenomenological potentials such as AV18 that are able to fit phase shifts in the energy region from threshold to 350 MeV in terms of ~ 40 parameters [72]. Progress has been made in the description of few-nucleon systems [1], but such a purely phenomenological approach is less efficient in dealing with the components of the nuclear interaction that are not constrained by NN data. At the same time, in recent years a new technique—effective field theory (EFT)—has been used in order to attack this problem by exploiting the symmetries of QCD [2]. In this approach the nuclear interaction is separated into long- and short-distance components. In its original formulation [3], designed for processes with typical momenta comparable to the pion mass, $Q \sim m_\pi$, the long-distance component is described fully quantum mechanically in terms of pion exchange, while the short-distance piece is described in terms of a number of phenomenologically determined contact couplings. The resulting potential [4,5] is approaching [6,7] the degree of accuracy of purely phenomenological potentials. Even higher precision can be achieved at lower momenta, where all interactions can be taken as short ranged, as has been demonstrated not only in the NN system [8,9], but also in the three-nucleon system [10,11]. Precise ($\sim 1\%$) values have been generated also for low-energy, astrophysically important cross sections of reactions such as $n + p \rightarrow d + \gamma$ [12]. Besides providing reliable values for such quantities, the use of EFT techniques allows for a realistic estimation of the size of possible corrections.

Over the past nearly half century there has also developed a series of measurements attempting to illuminate the parity-*violating* (PV) nuclear interaction. Indeed, the first experimental paper was that of Tanner in 1957 [13], shortly after the experimental confirmation of parity violation in nuclear beta decay by Wu et al. [14]. Following the seminal theoretical work by Michel in 1964 [15] and that of other authors in the late 1960s [16–18], the results of such experiments have generally been analyzed in terms of a meson-exchange picture, and in 1980 the work of Desplanques, Donoghue, and Holstein (DDH) developed a comprehensive and general meson-exchange framework for the analysis of such interactions in terms of seven parameters representing weak parity-violating meson–nucleon couplings [19]. The DDH interaction has become the standard setting by which hadronic and nuclear PV processes are now analyzed theoretically.

It is important to observe, however, that the DDH framework is, at heart, a *model* based on a meson-exchange picture. Provided one is interested primarily in near-threshold phenomena, use of a model is unnecessary, and one can instead represent the PV nuclear interaction in a model-independent effective-field-theoretic fashion. The purpose of the present work is to formulate such a systematic, model-independent treatment of PV NN interactions. We feel that this is a timely goal, since such PV interactions are interesting not

only in their own right but also as effects entering atomic PV measurements [21] as well as experiments that use parity violation in electromagnetic interactions to probe nucleon structure [23].

In our reformulation of nuclear PV, we consider two versions of EFT, one in which the pions have been "integrated out" and the other including the pion as an explicit degree of freedom. In the pionless theory, the PV nuclear interaction is entirely short-ranged, and the most general potential depends at leading order on five independent operators parameterized by a set of five a priori unknown low-energy constants (LECs). When applied to low-energy ($E_{cm} \lesssim 50$ MeV) two-nucleon PV observables—such as the neutron spin asymmetry in the capture reaction $\vec{n} + p \rightarrow d + \gamma$—it implies that there are five independent PV amplitudes, which may be determined by an appropriate set of measurements. We therefore recover previous results obtained without effective field theory by Danilov [24] and Desplanques and Missimer [25]. Making contact with these known results is an important motivation for us to consider this pionless EFT. Going beyond this, in next (non-vanishing) order in the EFT, there are several additional independent operators. By contrast, the DDH meson-exchange framework amounts to a model in which the short-range physics is codified into six independent operators. On one hand, the heavy-meson component of the DDH potential is a redundant representation of the leading-order EFT. On the other, it does not provide the most complete parameterization of the short-ranged PV NN force to subleading order, because it is based on a truncation of the QCD spectrum after inclusion of the lowest-lying octet of vector mesons. It may, therefore, not be entirely physically realistic, and we feel that a more general treatment using EFT is warranted.

When we are interested in observables at higher energies, we need to account for pion propagation explicitly, simultaneously removing its effects from the contact interactions. Inclusion of explicit pions introduces a long-range component into the PV NN interaction, whose strength is set at the lowest order by the PV πNN Yukawa coupling, $h^1_{\pi NN}$. This long-range component, which is formally of lower-order than shorter-range interactions, is identical to the long-range, one-pion-exchange (OPE) component of the DDH potential. However, in addition, inclusion of pions leads to several new effects that do not arise explicitly in the DDH picture:

- A medium-range, two-pion-exchange (TPE) component in the potential that arises at the same order as the leading short-range potential and that is also proportional to $h^1_{\pi NN}$. This medium-range component was considered some time ago in Ref. [18] but could not be systematically incorporated into the treatment of nuclear PV until the advent of EFT. As a result, such piece has not been previously included in the analysis of PV observables. We find that the two-pion terms introduce a qualitatively new aspect into the problem and speculate that their inclusion may modify the $h^1_{\pi NN}$ sensitivity of various PV observables.
- Next-to-next-to-leading-order (NNLO) PV πNN operators. In principle, there exist several such operators that contribute to the PV NN interaction at the same order as the leading short-range potential. In practice, however, effects of all but one of the independent NNLO PV πNN operators can be absorbed via a suitable redefinition of the short-range operator coefficients and $h^1_{\pi NN}$. The coefficient of the remaining, independent NNLO operator—$k^{1a}_{\pi NN}$—must be determined from experiment. Addi-

tional terms are generated in the potential at $\mathcal{O}(Q)$ by higher-order corrections to the strong πNN coupling (here, Q denotes a small momentum or pion mass). These terms have also not been included in previous treatments of the PV NN interaction. Their coefficients are fixed by either reparameterization invariance or measurements of other parity-conserving pion–nucleon observables.

- A new electromagnetic operator. For PV observables involving photons, the explicit incorporation of pions requires inclusion of a PV $NN\pi\gamma$ operator that is entirely absent from the DDH framework and whose strength is characterized by a constant $\bar{C}_\pi$.

In short, for the low-energy processes of interest here, the most general EFT treatment of PV observables depends in practice on eight a priori unknown constants when the pion is included as an explicit degree of freedom: five independent combinations of $\mathcal{O}(Q)$ short-range constants and those associated with the effects of the pion: $h^1_{\pi NN}$, $\bar{C}_\pi$, and the NNLO PV πNN coupling $k^{1a}_{\pi NN}$. In order to determine these PV low-energy constants (LECs), one therefore requires a minimum of five independent, low-energy observables for the pionless EFT and eight for the EFT with dynamical pions. Given the theoretical ambiguities associated with interpreting many-body nuclear observables (see below), one would ideally attempt to determine the PV LECs from measurements in few-body systems. Indeed, the state of the art in few-body physics allows one perform ab initio computations of few-body observables [1], thereby making the few-body system a theoretically clean environment in which to study the effects of hadronic PV. At present, however, there exist only two measurements of few-body PV observables: A^{pp}_L, the longitudinal analyzing power in polarized proton–proton scattering, and $A^{p\alpha}_L$, the longitudinal analyzing power for $\vec{p}\alpha$ scattering. In what follows, we outline a prospective program of additional measurements that would afford a complete determination of the PV LECs through $\mathcal{O}(Q)$.

Completion of this low-energy program would serve two additional purposes. First, it would provide hadron structure theorists with a set of benchmark numbers that are in principle calculable from first principles. This situation would be analogous to what one encounters in chiral perturbation theory for pseudoscalar mesons, where the experimental determination of the ten LECs appearing in the $\mathcal{O}(Q^4)$ Lagrangian presents a challenge to hadron-structure theory. While many of the $\mathcal{O}(Q^4)$ LECs are saturated by t-channel exchange of vector mesons, it is not clear a priori that the analogous PV NN constants are similarly saturated (as is assumed implicitly in the DDH model). Moreover, analysis of the PV NN LECs involves the interplay of weak and strong interactions in the strangeness-conserving sector. A similar situation occurs in $\Delta S = 1$ hadronic weak interactions, and the interplay of strong and weak interactions in this case is both subtle and only partially understood, as evidenced, e.g., by the well-known $\Delta I = 1/2$ rule enigma. The additional information in the $\Delta S = 0$ sector provided by a well-defined set of experimental numbers would undoubtedly shed light on this fundamental problem.

The information derived from the low-energy few-nucleon PV program could also provide a starting point for a reanalysis of PV effects in many-body systems. Until now, one has attempted to use PV observables obtained from both few- and many-body systems in order to determine the seven PV meson–nucleon couplings entering the DDH potential, and several inconsistencies have emerged. The most blatant is the vastly different value for $h^1_{\pi NN}$ obtained from the PV γ-decays of ^{18}F and from the combination of the $\vec{p}p$ asym-

metry and the Cesium anapole moment. Although combinations of coupling constants can be found that fit partial sets of experiments (see, e.g., Ref. [20]), it seems difficult to describe all experiments consistently with theory (see, e.g., Ref. [21] and references therein). The origin of this clash could be due to any one of a number of factors. Using the operator constraints derived from the few-body program as input into the nuclear analysis could help clarify the situation. It may be, for example, that the medium-range TPE potential or higher-order operators relevant only to nuclear PV processes play a more significant role in nuclei than implicitly assumed by the DDH framework. Alternatively, the treatment of the many-body system—such as the truncation of the model space in shell-model approaches to the Cesium anapole moment—may be the culprit. (For an example of the relevance of nucleon–nucleon correlations to parity violation in nuclei, see Ref. [22].) In any case, approaching the nuclear problem from a more systematic perspective and drawing upon the results of few-body studies would undoubtedly represent an advance for the field.

In the remainder of the paper, then, we describe in detail the EFT reformulation of nuclear PV and the corresponding program of study. In Section 2, we briefly review the conventional, DDH analysis and summarize the key differences with the EFT approach. In particular, we write down the various components of the PV EFT potential here, relegating its derivation to subsequent sections. In Section 3, we outline the phenomenology of the low-energy few-body PV program, providing illustrative relationships between various observables and the five relevant, independent combinations of short-range LECs. We emphasize that the analysis presented in Section 3 is intended to demonstrate *how* one would go about carrying out the few-body program rather than to give precise numerical formulas. Obtaining the latter will require more sophisticated few-body calculations than we are able to undertake here. Section 4 contains the derivation of the PV potential in the EFT without explicit pions. We then extend the framework to include pions explicitly in Section 5. In Section 6 we discuss the relationship between the PV LECs and the PV meson–nucleon couplings entering the DDH framework, and illustrate how this relationship depends on one's truncation of the QCD spectrum. Section 7 contains some final observations. Various details pertaining to the calculations contained in the text appear in the appendices.

2. Nuclear PV: old and new

The essential idea behind the conventional DDH framework relies on the fairly successful representation of the parity-conserving NN interaction in terms of a single meson-exchange approach. Of course, this requires the use of strong-interaction couplings of the lightest vector (ρ, ω) and pseudoscalar (π) mesons (M),

$$\mathcal{H}_{\text{st}} = -i g_{\pi NN} \bar{N} \gamma_5 \tau \cdot \pi N - g_\rho \bar{N} \left(\gamma_\mu + i \frac{\chi_\rho}{2m_N} \sigma_{\mu\nu} k^\nu \right) \tau \cdot \rho^\mu N$$
$$- g_\omega \bar{N} \left(\gamma_\mu + i \frac{\chi_\omega}{2m_N} \sigma_{\mu\nu} k^\nu \right) \omega^\mu N, \tag{1}$$

whose values are reasonably well determined. The DDH approach to the parity-violating weak interaction utilizes a similar meson-exchange picture, but now with one strong and one weak vertex—cf. Fig. 1.
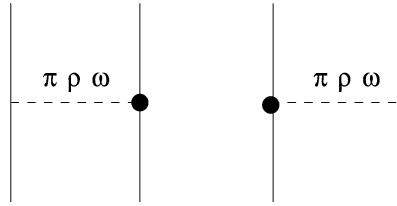
Fig. 1. Parity-violating NN potential generated by meson exchange.

Table 1
Weak NNM couplings as calculated in Refs. [19,28,29]. All numbers are quoted in units of the "sum rule" value $g_\pi = 3.8 \times 10^{-8}$

Coupling	DDH [19] Reasonable range	DDH [19] "Best" value	DZ [28]	FCDH [29]
$h^1_{\pi NN}$	$0 \to 30$	$+12$	$+3$	$+7$
h^0_ρ	$30 \to -81$	-30	-22	-10
h^1_ρ	$-1 \to 0$	-0.5	$+1$	-1
h^2_ρ	$-20 \to -29$	-25	-18	-18
h^0_ω	$15 \to -27$	-5	-10	-13
h^1_ω	$-5 \to -2$	-3	-6	-6

We require then a parity-violating NNM Hamiltonian in analogy to Eq. (1). The process is simplified somewhat by Barton's theorem, which requires that in the CP-conserving limit, which we employ, exchange of neutral pseudoscalars is forbidden [26]. From general arguments, the effective Hamiltonian with fewest derivatives must take the form

$$
\mathcal{H}_{\mathrm{wk}} = \frac{h^1_{\pi NN}}{\sqrt{2}} \bar{N} (\tau \times \pi)_3 N
$$

$$
- \bar{N} \left(h^0_\rho \tau \cdot \rho^\mu + h^1_\rho \rho^\mu_3 + \frac{h^2_\rho}{2\sqrt{6}} \left(3\tau_3 \rho^\mu_3 - \tau \cdot \rho^\mu \right) \right) \gamma_\mu \gamma_5 N
$$

$$
- \bar{N} \left(h^0_\omega \omega^\mu + h^1_\omega \tau_3 \omega^\mu \right) \gamma_\mu \gamma_5 N + h'^1_\rho \bar{N} \left(\tau \times \rho^\mu \right)_3 \frac{\sigma_{\mu\nu} k^\nu}{2m_N} \gamma_5 N. \tag{2}
$$

We see that there exist, in this model, seven unknown weak couplings $h^1_{\pi NN}, h^0_\rho, \ldots$. However, quark model calculations suggest that h'^1_ρ is quite small [27], so this term is usually omitted, leaving parity-violating observables described in terms of just six constants. DDH attempted to evaluate such PV couplings using basic quark-model and symmetry techniques, but they encountered significant theoretical uncertainties. For this reason their results were presented in terms of an allowable range for each, accompanied by a "best value" representing their best guess for each coupling. These ranges and best values are listed in Table 1, together with predictions generated by subsequent groups [28,29].

Before making contact with experimental results, however, it is necessary to convert the NNM couplings generated above into a parity-violating NN potential. Inserting the

strong and weak couplings, defined above, into the meson-exchange diagrams shown in Fig. 1 and taking the Fourier transform, one finds the DDH parity-violating NN potential

$$
\begin{aligned}
V_{\mathrm{DDH}}^{\mathrm{PV}}(\vec{r}) = {} & i\frac{h_{\pi NN}^{1} g_A m_N}{\sqrt{2} F_\pi}\left(\frac{\tau_1 \times \tau_2}{2}\right)_3 (\vec\sigma_1 + \vec\sigma_2)\cdot\left[\frac{\vec p_1 - \vec p_2}{2m_N}, w_\pi(r)\right] \\
& - g_\rho\left(h_\rho^0 \tau_1\cdot\tau_2 + h_\rho^1\left(\frac{\tau_1 + \tau_2}{2}\right)_3 + h_\rho^2\frac{(3\tau_1^3\tau_2^3 - \tau_1\cdot\tau_2)}{2\sqrt{6}}\right) \\
& \times\left((\vec\sigma_1 - \vec\sigma_2)\cdot\left\{\frac{\vec p_1 - \vec p_2}{2m_N}, w_\rho(r)\right\}\right. \\
& \left. + i(1+\chi_\rho)\vec\sigma_1\times\vec\sigma_2\cdot\left[\frac{\vec p_1 - \vec p_2}{2m_N}, w_\rho(r)\right]\right) - g_\omega\left(h_\omega^0 + h_\omega^1\left(\frac{\tau_1 + \tau_2}{2}\right)_3\right) \\
& \times\left((\vec\sigma_1 - \vec\sigma_2)\cdot\left\{\frac{\vec p_1 - \vec p_2}{2m_N}, w_\omega(r)\right\}\right. \\
& \left. + i(1+\chi_\omega)\vec\sigma_1\times\vec\sigma_2\cdot\left[\frac{\vec p_1 - \vec p_2}{2m_N}, w_\omega(r)\right]\right) \\
& - \left(g_\omega h_\omega^1 - g_\rho h_\rho^1\right)\left(\frac{\tau_1 - \tau_2}{2}\right)_3(\vec\sigma_1 + \vec\sigma_2)\cdot\left\{\frac{\vec p_1 - \vec p_2}{2m_N}, w_\rho(r)\right\} \\
& - g_\rho h_\rho'^1 i\left(\frac{\tau_1\times\tau_2}{2}\right)_3(\vec\sigma_1 + \vec\sigma_2)\cdot\left[\frac{\vec p_1 - \vec p_2}{2m_N}, w_\rho(r)\right],
\end{aligned}
\tag{3}
$$

where $\vec p_i = -i\vec\nabla_i$, $\vec\nabla_i$ denoting the gradient with respect to the coordinate $\vec x_i$ of the ith nucleon, $r = |\vec x_1 - \vec x_2|$ is the separation between the two nucleons,

$$
w_i(r) = \frac{\exp(-m_i r)}{4\pi r}
\tag{4}
$$

is the usual Yukawa form, and the strong πNN coupling $g_{\pi NN}$ has been expressed in terms of the axial-current coupling g_A using the Goldberger–Treiman relation: $g_{\pi NN} = g_A m_N/F_\pi$, with $F_\pi = 92.4$ MeV being the pion decay constant.

Nearly all experimental results involving nuclear parity violation have been analyzed using $V_{\mathrm{DDH}}^{\mathrm{PV}}$ for the past twenty-some years. At present, however, there appear to exist discrepancies between the values extracted for the various DDH couplings from experiment. In particular, the values of $h_{\pi NN}^1$ and h_ρ^0 extracted from $\vec p p$ scattering and the γ decay of ^{18}F do not appear to agree with the corresponding values implied by the anapole moment of ^{133}Cs measured in atomic parity violation [30].

These inconsistencies suggest that the DDH framework may not, after all, adequately characterize the PV NN interaction and provides motivation for our reformulation using EFT. The idea of using EFT methods in order to study parity-violating hadronic $\Delta S = 0$ interactions is not new [31,80]. Recently, a flurry of activity (see, for example, Refs. [32–38]) has centered on PV processes involving a single nucleon, such as

$$
ep \to e'p, \quad \gamma p \to \gamma p, \quad \gamma p \to n\pi^+, \quad \text{etc.}
$$

There has also been work on the NN system, with pion exchange treated perturbatively [39,40] or non-perturbatively [41]. However, a comprehensive analysis has yet to take place, and this omission is rectified in the study described below, wherein we generate a systematic framework within which to address PV NN reactions. We utilize the so-called Weinberg formulation [3], wherein the pion, when included explicitly, is treated fully quantum mechanically while shorter-distance phenomena—as would be produced by the exchange of heavier mesons such as ρ, ω, etc.—are represented in terms of simple four-nucleon contact terms. The justification for the non-perturbative treatment of (parts of) pion exchange has been discussed in a recent paper [42].

Although a fully self-consistent procedure would involve use of EFT to compute both the PV operators *and* few-body wavefunctions, equally accurate results can be obtained by drawing upon state-of-the art wave functions obtained from a phenomenological, strong-interaction NN potential, including PV effects perturbatively, and using EFT to systematically organize the relevant PV operators. Such a "hybrid" approach has been followed with some success in other contexts [2] and we adopt it here. In so doing, we truncate our analysis of the PV operators at order Q/Λ_χ, where Q is a small momentum characteristic of the low-energy PV process and $\Lambda_\chi = 4\pi F_\pi \sim 1$ GeV is the scale of chiral symmetry breaking [86,88]. Since realistic wave functions obtained from a phenomenological potential effectively include strong-interaction contributions to all orders in Q/Λ_χ, the hybrid approach introduces some inconsistency at higher orders in Q/Λ_χ. For the low-energy processes of interest here ($E_{\text{cm}} \lesssim 50$ MeV), however, we do not expect the impact of these higher-order problems to be significant. We would not, however, attempt to apply our analysis to higher-energy processes (e.g., the TRIUMF 221 MeV $\vec{p}\,p$ experiment [43]) where inclusion of higher-order PV operators would be necessary.

With these considerations in mind, it is useful to compare $V_{\text{DDH}}^{\text{PV}}$ with the leading-order PV NN EFT potential. In the pionless theory, this potential is entirely short ranged (SR) and has coordinate space form

$$
\begin{aligned}
V_{1,\text{SR}}^{\text{PV}}(\vec{r}) = \frac{2}{\Lambda_\chi^3} &\left\{ \left[C_1 + (C_2 + C_4)\left(\frac{\tau_1 + \tau_2}{2}\right)_3 + C_3 \tau_1 \cdot \tau_2 + \mathcal{I}_{ab} C_5 \tau_1^a \tau_2^b \right] \right. \\
&\times (\vec{\sigma}_1 - \vec{\sigma}_2) \cdot \left\{ -i\vec{\nabla}, f_m(r) \right\} \\
&+ \left[\tilde{C}_1 + (\tilde{C}_2 + \tilde{C}_4)\left(\frac{\tau_1 + \tau_2}{2}\right)_3 + \tilde{C}_3 \tau_1 \cdot \tau_2 + \mathcal{I}_{ab} \tilde{C}_5 \tau_1^a \tau_2^b \right] \\
&\times i(\vec{\sigma}_1 \times \vec{\sigma}_2) \cdot \left[-i\vec{\nabla}, f_m(r) \right] \\
&+ (C_2 - C_4)\left(\frac{\tau_1 - \tau_2}{2}\right)_3 (\vec{\sigma}_1 + \vec{\sigma}_2) \cdot \left\{ -i\vec{\nabla}, f_m(r) \right\} \\
&+ \left. C_6 i\epsilon^{ab3} \tau_1^a \tau_2^b (\vec{\sigma}_1 + \vec{\sigma}_2) \cdot \left[-i\vec{\nabla}, f_m(r) \right] \right\},
\end{aligned}
\tag{5}
$$

where the subscript "1" in the potential denotes the chiral index of the operators[1]

$$\mathcal{I} = \begin{pmatrix} 1 & 0 & 0 \\ 0 & 1 & 0 \\ 0 & 0 & -2 \end{pmatrix}, \tag{6}$$

and $f_m(\vec{r})$ is a function that

 (i) is strongly peaked, with width $\sim 1/m$ about $r = 0$, and
(ii) approaches $\delta^{(3)}(\vec{r})$ in the zero-width ($m \to \infty$) limit.

A convenient form, for example, is the Yukawa-like function

$$f_m(r) = \frac{m^2}{4\pi r} \exp(-mr). \tag{7}$$

Here m is a mass chosen to reproduce the appropriate short-range effects ($m \sim \Lambda_\chi$ in the pionful theory, but $m \sim m_\pi$ in the pionless theory). Note that, since the terms containing $\tilde{C}_2$ and $\tilde{C}_4$ are identical, $V_{\mathrm{SR}}^{\mathrm{PV}}$ nominally contains ten independent operators. As we show below, however, only five combinations of these operators are relevant at low-energies.

For the purpose of carrying out actual calculations, one could just as easily use the momentum-space form of $V_{1,\mathrm{SR}}^{\mathrm{PV}}$, thereby avoiding the use of $f_m(\vec{r})$ altogether. Nevertheless, the form of Eq. (5) is useful when comparing with the DDH potential. For example, we observe that the same set of spin-space and isospin structures appear in both $V_{1,\mathrm{SR}}^{\mathrm{PV}}$ and the vector-meson exchange terms in $V_{\mathrm{DDH}}^{\mathrm{PV}}$, though the relationship between the various coefficients in $V_{1,\mathrm{SR}}^{\mathrm{PV}}$ is more general. In particular, the DDH model is tantamount to taking $m \sim m_\rho, m_\omega$ and assuming

$$\frac{\tilde{C}_1}{C_1} = \frac{\tilde{C}_2}{C_2} = 1 + \chi_\omega, \tag{8}$$

$$\frac{\tilde{C}_3}{C_3} = \frac{\tilde{C}_4}{C_4} = \frac{\tilde{C}_5}{C_5} = 1 + \chi_\rho, \tag{9}$$

assumptions which may not be physically realistic. In Section 6, we give illustrative mechanisms which may lead to a breakdown of these assumptions.

When pions are included explicitly, one obtains in addition the same long-range (LR) component induced by OPE as in $V_{\mathrm{DDH}}^{\mathrm{PV}}$,

$$V_{-1,\mathrm{LR}}^{\mathrm{PV}}(\vec{r}) = i \frac{h_{\pi NN}^1 g_A m_N}{\sqrt{2} F_\pi} \left(\frac{\tau_1 \times \tau_2}{2} \right)_3 (\vec{\sigma}_1 + \vec{\sigma}_2) \cdot \left[\frac{\vec{p}_1 - \vec{p}_2}{2m_N}, w_\pi(r) \right], \tag{10}$$

where $w_\pi(r)$ is given by Eq. (4). Note that, as we will explain in Section 5, $V_{-1,\mathrm{LR}}^{\mathrm{PV}}$ is two orders lower than $V_{1,\mathrm{SR}}^{\mathrm{PV}}$—in contrast to the strong potential where the short- and long-range components first arise formally at the same order. (Even though Eq. (10) has the

---

[1] Roughly speaking, the chiral index corresponds to the order of a given operator in the Q/Λ_χ expansion. A precise definition is given in Section 5 below.

same form as a term in Eq. (5), it has no suppression by powers of Λ_χ or other heavy scales. Therefore, it appears at lower order.)

Furthermore, two new types of contributions to the potential arise at the same order as Eq. (5): (a) a long-range component stemming from higher-order πNN operators, and (b) a medium-range (MR), two-pion-exchange (TPE) contribution, $V_{1,\mathrm{MR}}^{\mathrm{PV}}$. At $\mathcal{O}(Q)$, the TPE potential is proportional to $h_{\pi NN}^1$ and involves two terms having the same spin–isospin structure as the terms in $V_{1,\mathrm{SR}}^{\mathrm{PV}}$ proportional to $\tilde{C}_2$ and C_6 but having a more complicated spatial dependence. In momentum space

$$
V_{1,\mathrm{MR}}^{\mathrm{PV}}(\vec{q})
$$
$$
= -\frac{1}{\Lambda_\chi^3}\left\{ \tilde{C}_2^{2\pi}(q)\frac{\tau_1^z + \tau_2^z}{2}i(\vec{\sigma}_1 \times \vec{\sigma}_2)\cdot\vec{q} + C_6^{2\pi}(q)i\epsilon^{ab3}\tau_1^a\tau_2^b(\vec{\sigma}_1 + \vec{\sigma}_2)\cdot\vec{q} \right\}, \quad (11)
$$

where the functions $\tilde{C}_2^{2\pi}(q)$ and $C_6^{2\pi}(q)$, defined below in Eq. (121), are determined by the leading-order πNN couplings. Again, it is more convenient to compute matrix elements of $V_{1,\mathrm{MR}}^{\mathrm{PV}}$ using the momentum-space form, and we defer a detailed discussion of the latter until Section 5 below. We emphasize, however, the presence of $V_{1,\mathrm{MR}}^{\mathrm{PV}}$ introduces a qualitatively new element into the treatment of nuclear PV with pions not present in the DDH framework.

The NNLO long-range contribution to the potential generated by the new PV πNN operator is

$$
V_{1,\mathrm{LR}}^{\mathrm{PV}} = -i\frac{k_{\pi NN}^{1b}g_A}{2\Lambda_\chi F_\pi^2}\left(\frac{\tau_1 \times \tau_2}{2}\right)_3
$$
$$
\times \left\{ \epsilon_{abc}\sigma_1^c\sigma_2^e\left\{\nabla_1^a, \left[\nabla_r^b\nabla_r^e, w_\pi(r)\right]\right\} + (1 \leftrightarrow 2)\right\} + \cdots, \quad (12)
$$

where ∇_r is the gradient with respect to the relative coordinate $\vec{x}_1 - \vec{x}_2$ and where the $\cdots$ denote long-range, NNLO contributions proportional to $h_{\pi NN}^1$ that are generated by NNLO effects at the strong πNN vertex (see Appendix B).

As we discuss in Section 3, a complete program of low-energy PV measurements includes photo-reactions. In the DDH framework, PV electromagnetic (EM) matrix elements receive two classes of contributions: (a) those involving the standard, parity-conserving EM operators in combination with parity-mixing in the nuclear states, and (b) PV two-body EM operators derived from the amplitudes of Fig. 13. Explicit expressions for these operators in the DDH framework can be found in Ref. [21]. In the case of EFT, the two-body PV EM operators associated with heavy-meson exchange in DDH are replaced by operators obtained by gauging the derivatives in $V_{1,\mathrm{SR}}^{\mathrm{PV}}$ as well as by explicit photon insertions on external legs. The two-body operators associated with $V_{-1,\mathrm{LR}}^{\mathrm{PV}}$ are identical to those appearing in DDH, while the PV currents associated with $V_{1,\mathrm{MR}}^{\mathrm{PV}}$ and $V_{1,\mathrm{LR}}^{\mathrm{PV}}$ are obtained by gauging the derivatives appearing in the potential and by inserting the photon on all charged-particle lines in the corresponding Feynman diagrams.[2] The foregoing two-body currents introduce

---

[2] The derivation of the medium-range two-body operators involves an enormously detailed computation, which we defer to a later publication.

no new unknown constants beyond those already appearing in the potential. However, an additional, independent pion-exchange two-body operator also appears at the same order as the short-range PV two-body currents:

$$\vec{J}(\vec{x}_1, \vec{x}_2, \vec{q}) = \frac{\sqrt{2} g_A \bar{C}_\pi m_\pi^2}{\Lambda_\chi^2 F_\pi} e^{-i\vec{q}\cdot\vec{x}_1} \tau_1^+ \tau_2^- \vec{\sigma}_1 \times \vec{q} \vec{\sigma}_2 \cdot \hat{r} h_\pi(r) + (1 \leftrightarrow 2),$$ (13)

where

$$h_\pi(r) = \frac{\exp(-m_\pi r)}{m_\pi r}\left(1 + \frac{1}{m_\pi r}\right),$$ (14)

and $\bar{C}_\pi$ is an additional LEC parameterizing the leading PV $NN\pi\gamma$ interaction. Any photoreaction sensitive to the short-range PV potential will also depend on $\bar{C}_\pi$ when pions are included explicitly.

Through $\mathcal{O}(Q)$, then the phenomenology of nuclear PV depends on five unknown constants in the pionless theory and eight when pions are included explicitly ($h_{\pi NN}^1$, $k_{\pi NN}^{1a}$, and $\bar{C}_\pi$ in addition to the contact interactions). As we discuss below, an initial low-energy program will afford a determination of the five constants in the pionless theory. Additional low-energy measurements in few-body systems would provide a test of the self-consistency of the EFT at this order. Any discrepancies could indicate the need to including pions as explicit degrees of freedom, thereby necessitating the completion of additional measurements in order to determine the pion contributions to $\mathcal{O}(Q)$. As we discuss below, there exists a sufficient number of prospective measurements that could be used for this purpose. Given the challenging nature of the experiments, a sensible strategy would be to first test for the self-consistency of the pionless EFT with a smaller set of measurements and then to complete the additional measurements needed for EFT with pions if necessary.

3. Parity violation in few-body systems

There exist numerous low-energy experiments that have attempted to explore hadronic parity violation. Some, like the photon asymmetry in the decay of a polarized isomeric state of ^{180}Hf,

$$A_\gamma = -(1.66 \pm 0.18) \times 10^{-2} \quad [44],$$ (15)

or the asymmetry in longitudinally-polarized neutron scattering on ^{139}La,

$$A_z = (9.55 \pm 0.35) \times 10^{-2} \quad [45],$$ (16)

involve F–P shell nuclei wherein the effects of hadronic parity violation are large and clearly observed, but where the difficulty of performing a reliable wave function calculation precludes a definitive interpretation. For this reason, it is traditional to restrict one's attention to S–D shell or lighter nuclei. Here too, there exist a number of experiments, such as the asymmetry in the decay of the polarized first excited state of ^{19}F,

$$A_\gamma\left(\tfrac{1}{2}^-, \ 110 \text{ keV}\right) = -(8.5 \pm 2.6) \times 10^{-5} \quad [46]$$
$$= -(6.8 \pm 1.8) \times 10^{-5} \quad [47],$$ (17)

wherein a clear parity-violating signal is observed, or those such as the circular polarization in the decay of excited levels of ^{21}Ne,

$$P_\gamma\left(\tfrac{1}{2}^-, \ 2.789 \ \text{MeV}\right) = (24 \pm 24) \times 10^{-4} \quad [48]$$
$$= (3 \pm 16) \times 10^{-4} \quad [49], \tag{18}$$

or of ^{18}F,

$$P_\gamma\left(0^-, \ 1.081 \ \text{MeV}\right) = (-7 \pm 20) \times 10^{-4} \quad [50]$$
$$= (3 \pm 6) \times 10^{-4} \quad [51]$$
$$= (-10 \pm 18) \times 10^{-4} \quad [52]$$
$$= (2 \pm 6) \times 10^{-4} \quad [53], \tag{19}$$

wherein a nonzero signal has not been seen, but where the precision of the experiment is high enough that a significant limit can be placed on the underlying parity-violating mechanism.

The reason that a 10^{-4} experiment can reveal information about an effect which is on the surface at the level

$$G_F m_N^2 (p_F/m_N) \sim 10^{-6},$$

where $p_F \sim 270$ MeV is the Fermi momentum, is that the nucleus can act as an PV-amplifier. This occurs when there exist a pair of close-by levels having the same spin but opposite parity, $|J^\pm\rangle$. In this case the parity mixing expected from lowest-order perturbation theory, $|\psi_\pm\rangle \simeq |J^\pm\rangle \pm \epsilon |J^\mp\rangle$, can become anomalously large due to the smallness of the energy difference $E_{J^+} - E_{J^-}$ in the mixing parameter

$$\epsilon \simeq \frac{\langle J^-|H_{\text{weak}}|J^+\rangle}{E_{J^+} - E_{J^-}}. \tag{20}$$

Indeed, when compared with a typical level splitting of ~ 1 MeV, the energy differences exploited in ^{19}F ($\Delta E = 110$ keV), ^{21}Ne ($\Delta E = 5.7$ keV), and ^{18}F ($\Delta E = 39$ keV) lead to expected enhancements at the level of 10, 100, and 25, respectively. However, when interpreted in terms of the best existing nuclear shell-model wave functions, there exists a serious discrepancy between the values of the $\Delta I = 1$ pion coupling required in order to understand the ^{19}F or ^{21}Ne experiments and the upper limit allowed by the ^{18}F result.

Such matters have been extensively reviewed by previous authors [54–56], and we do not intend to revisit these issues here. Instead we suggest that *at the present time* any detailed attempt to understand the parity-violating NN interaction must focus on experiments involving only the very lightest—NN, Nd, $N\alpha$—systems, wherein our ability to calculate the effects of a given theoretical picture are under much better control. As we demonstrate below, there exist a sufficient number of such experiments, either in progress or planned, in order to accomplish this task for either the pionless EFT or the EFT with dynamical pions. Once a reliable set of low-energy constants are in hand, as obtained from such very-light systems, theoretical work can proceed on at least two additional fronts:

(i) experimental results from the heavier nuclear systems—involving P, S–D, and F–P shells and higher levels—can be revisited and any discrepancies hopefully resolved with the confidence that the weak low-energy constants are correct, and

(ii) one can attempt to evaluate the size of the phenomenological weak constants starting from the fundamental quark–quark weak interaction in the Standard Model.

This scheme mirrors the approach that has proven highly successful in chiral perturbation theory (ChPT) [57], wherein phenomenological constants are extracted purely from experimental results, using no theoretical prejudices other than the basic (broken) chiral symmetry of QCD. In the meson sector [58], the phenomenologically determined counter-terms $L_1, L_2, \ldots, L_{10}$ have already become the focus of various theoretical programs attempting to predict their size from fundamental theory. Note that our approach to nuclear parity violation is similar in spirit to the one advocated in a prescient 1978 paper by Desplanques and Missimer [25] that builds on ideas put forward by Danilov [24]. In subsequent work, this approach was superseded by the use of the DDH potential. In our study, then, we are in a sense recasting the ideas of Refs. [24,25] in the modern and theoretically systematic framework of EFT.

3.1. Amplitudes

We now consider the first part of the program—elucidation of the basic weak couplings. We argue that, provided one is working in a region of sufficiently low-energy, the parity-violating NN interaction can be described in terms of just *five* real numbers, which characterize S–P wave mixing in the spin singlet and triplet channels. The arguments in this section borrow heavily from the work of Danilov [24] and Desplanques and Missimer [25]. The following sections will show how to interpret this phenomenology within EFT.

For simplicity we begin with a parity-conserving system of two nucleons. Then the NN scattering matrix can be expressed purely in terms of S-wave scattering at low energies and has the phenomenological form [24]

$$\mathcal{M}(\vec{k}_f, \vec{k}_i) = \langle \vec{k}_f | \hat{T} | \vec{k}_i \rangle = m_t(k) P_1 + m_s(k) P_0, \tag{21}$$

where

$$P_1 = \frac{1}{4}(3 + \vec{\sigma}_1 \cdot \vec{\sigma}_2), \qquad P_0 = \frac{1}{4}(1 - \vec{\sigma}_1 \cdot \vec{\sigma}_2)$$

are spin-triplet and spin-singlet projection operators. All other partial waves can be neglected. We can determine the form of the functions $m_i(k)$ by using the stricture of unitarity,

$$2 \operatorname{Im} \hat{T} = \hat{T}^\dagger \hat{T}. \tag{22}$$

In the S-wave sector this becomes

$$\operatorname{Im} m_i(k) = k \left| m_i(k) \right|^2, \tag{23}$$

whose solution is of the familiar form

$$m_i(k) = \frac{1}{k} e^{i\delta_i(k)} \sin \delta_i(k). \tag{24}$$

Since at zero energy

$$\lim_{k \to 0} m_i(k) = -a_i \tag{25}$$

where a_i is the scattering length, it is clear that unitarity can be enforced by the simple modification

$$m_i(k) = \frac{-a_i}{1 + ika_i}, \tag{26}$$

which is the lowest-order effective-range result. The scattering cross section is found via

$$\frac{d\sigma}{d\Omega} = \mathrm{Tr}\, \mathcal{M}^\dagger \mathcal{M} = \frac{a_i^2}{1 + k^2 a_i^2}, \tag{27}$$

so that at the lowest energy we have the familiar form

$$\lim_{k \to 0} \frac{d\sigma_{s,t}}{d\Omega} = |a_{s,t}|^2. \tag{28}$$

The associated scattering wave functions are given by

$$
\begin{aligned}
\psi_{\vec{k}}^{(+)}(\vec{r}) &= \left[e^{i\vec{k}\cdot\vec{r}} - \frac{m_N}{4\pi} \int d^3 r' \frac{e^{ik|\vec{r}-\vec{r}\,'|}}{|\vec{r}-\vec{r}\,'|} V(\vec{r}\,') \psi_{\vec{k}}^{(+)}(\vec{r}\,') \right] \chi \\
&\xrightarrow{r\to\infty} \left[e^{i\vec{k}\cdot\vec{r}} + \mathcal{M}(-i\vec{\nabla}, \vec{k}) \frac{e^{ikr}}{r} \right] \chi,
\end{aligned}
\tag{29}
$$

where χ is the spin wave function. In the simple Born approximation, then, we can represent the wave function in terms of an effective local potential

$$V_{\mathrm{eff}}^{(0)\mathrm{PC}}(\vec{r}) = \frac{4\pi}{m_N} (a_t P_1 + a_s P_0) \delta^3(\vec{r}), \tag{30}$$

as can be confirmed by substitution into Eq. (29).

Parity mixing can be introduced into this simple representation, as done by Danilov [24], via generalization of the scattering amplitude to include parity-violating structures. Up to laboratory momenta of 140 MeV or so, we can omit all but S- and P-wave mixing, in which case there exist five independent such amplitudes:

(i) $d_t(k)$, representing $^3S_1$–$^1P_1$ mixing;
(ii) $d_s^{0,1,2}(k)$, representing $^1S_0$–$^3P_0$ mixing with $\Delta I = 0, 1, 2$, respectively; and
(iii) $c_t(k)$, representing $^3S_1$–$^3P_1$ mixing,

and, after a little thought, it becomes clear that the low-energy scattering matrix in the presence of parity violation can be generalized to

$$
\begin{aligned}
\mathcal{M}(\vec{k}_f, \vec{k}_i) &= m_t(k) P_1 + m_s(k) P_0 \\
&\quad + \left[\left(d_s^0(k) Q_1 + d_s^1(k) Q_{1+} + d_s^2(k) Q_2 \right) \left(\vec{k}_i \cdot (\vec{\sigma}_1 - \vec{\sigma}_2) P_1 \right. \right. \\
&\quad \left. + P_1 \vec{k}_f (\vec{\sigma}_1 - \vec{\sigma}_2) \right) + d_t(k) \left(\vec{k}_i \cdot (\vec{\sigma}_1 - \vec{\sigma}_2) P_0 + P_0 \vec{k}_f \cdot (\vec{\sigma}_1 - \vec{\sigma}_2) \right) \Big] \\
&\quad + c_t(k) Q_{1-} (\vec{\sigma}_1 + \vec{\sigma}_2) \cdot (\vec{k}_i P_1 + P_1 \vec{k}_f),
\end{aligned}
\tag{31}
$$

where we have introduced the isovector and isotensor operators

$$Q_{1-} = \frac{1}{2}(\tau_1 - \tau_2)_z, \qquad Q_{1+} = \frac{1}{2}(\tau_1 + \tau_2)_z,$$

$$Q_2 = \frac{1}{2\sqrt{6}}(3\tau_{1z}\tau_{2z} - \vec{\tau}_1 \cdot \vec{\tau}_2), \tag{32}$$

and isospin projection operators

$$Q_0 = \frac{1}{4}(1 - \vec{\tau}_1 \cdot \vec{\tau}_2), \qquad Q_1 = \frac{1}{4}(3 + \vec{\tau}_1 \cdot \vec{\tau}_2). \tag{33}$$

Each of the new pieces is indeed odd under spatial inversion ($\vec{\sigma}_i \to \vec{\sigma}_i$ and $\vec{k}_f, \vec{k}_i \to -\vec{k}_f, -\vec{k}_i$) and even under time reversal ($\vec{\sigma}_i \to -\vec{\sigma}_i$ and $\vec{k}_i \cdot (\vec{\sigma}_1 - \vec{\sigma}_2)P_j \leftrightarrow P_j\vec{k}_f \cdot (\vec{\sigma}_1 - \vec{\sigma}_2)$).

Now consider what constraints can be placed on the forms $d_i(k)$, $c_i(k)$. The requirement of unitarity reads

$$\mathrm{Im}\, d_i(k) = k\big[m_i^*(k)d_i(k) + d_i^*(k)m_p(k)\big], \tag{34}$$

where $m_i(k)$, $m_p(k)$ are the scattering amplitudes in the S-, P-wave channels connected by $d_i(k)$. Eq. (34) is satisfied by the solution

$$d_i(k) = \big|d_i(k)\big| \exp i\big[\delta_i(k) + \delta_p(k)\big], \tag{35}$$

i.e., the phase of the transition amplitude is simply the sum of the strong interaction phase shifts in the incoming and outgoing channels.

Danilov [24] suggested that, on account of the short-range of the weak interaction, the energy dependence of the weak couplings $d_i(k)$ should be primarily determined, up to say 50 MeV or so solely by the strong interaction dynamics. Since at very low energy the P-wave scattering can be neglected, he suggested the use of the forms

$$c_t(k) = \rho_t m_t(k), \qquad d_t(k) = \lambda_t m_t(k), \qquad d_s^i(k) = \lambda_s^i m_s(k), \tag{36}$$

which provide the parity-mixing amplitudes in terms of the five phenomenological constants: $\rho_t, \lambda_t, \lambda_s^i$.

We can understand the motivation behind Danilov's assertion by writing down the simplest phenomenological form for a weak low-energy parity-violating NN potential. To do so, one may start with the momentum-space form of $V_{1,\mathrm{SR}}^{\mathrm{PV}}$ given in Eq. (5):

$$
\begin{aligned}
V_{1,\mathrm{SR}}^{\mathrm{PV}}&(\vec{q}, \vec{p}) \\
&= -\frac{1}{\Lambda_\chi^3}\Bigg\{ -\bigg[(C_1 + C_3)Q_1 + (C_1 - 3C_3)Q_0 + (C_2 + C_4)Q_{1+} - \sqrt{\frac{8}{3}}C_5 Q_2 \bigg] \\
&\quad \times (\vec{\sigma}_1 - \vec{\sigma}_2) \cdot \vec{p} \\
&\quad + \bigg[(\tilde{C}_1 + \tilde{C}_3)Q_1 + (\tilde{C}_1 - 3\tilde{C}_3)Q_0 + (\tilde{C}_2 + \tilde{C}_4)Q_{1+} - \sqrt{\frac{8}{3}}\tilde{C}_5 Q_2 \bigg] \\
&\quad \times i(\vec{\sigma}_1 \times \vec{\sigma}_2) \cdot \vec{q} \\
&\quad + [C_2 - C_4]Q_{1-}(\vec{\sigma}_1 + \vec{\sigma}_2) \cdot \vec{p} + C_6 i(\vec{\tau}_1 \times \vec{\tau}_2)_z(\vec{\sigma}_1 + \vec{\sigma}_2) \cdot \vec{q} \Bigg\},
\end{aligned}
\tag{37}
$$

where $p = [(p_1 - p_2) + (p_1' - p_2')]/2$ and $q = [(p_1 - p_2) - (p_1' - p_2')]/2$.

The change in the wave function generated by $V_{1,\mathrm{SR}}^{\mathrm{PV}}(\vec{r})$ is understood to involve the full strong-interaction Green's function and wave functions

$$\delta\psi^{(+)}(\vec{r}) = \int d^3r'\, G_k(\vec{r}, \vec{r}')V_{1,\mathrm{SR}}^{\mathrm{PV}}(\vec{r}')\psi^{(+)}(\vec{r}'), \tag{38}$$

and the connection between the weak PV potential $V_{1,\mathrm{SR}}^{\mathrm{PV}}(\vec{r})$ and the scattering matrix Eq. (31) can be found via

$$d_i(k) \sim -\frac{m_N}{4\pi}\left(\langle\psi_k^{\mathrm{P}(-)}|V_{1,\mathrm{SR}}^{\mathrm{PV}}|\psi_k^{\mathrm{S}(+)}\rangle + \langle\psi_k^{\mathrm{S}(-)}|V_{1,\mathrm{SR}}^{\mathrm{PV}}|\psi_k^{\mathrm{P}(+)}\rangle\right). \tag{39}$$

Now, if we are at very low energy, we may use the plane-wave approximation for the P wave,

$$\psi_k^{\mathrm{P}(-)}(r) \simeq j_1(kr), \tag{40}$$

and we can approximate the S wave by its asymptotic form

$$\psi_k^{\mathrm{S}(+)}(r) \simeq \frac{1}{kr}e^{i\delta_i(k)}\sin\big(kr + \delta_i(k)\big) \xrightarrow{k\to 0} \frac{1}{kr}e^{i\delta_i(k)}\sin\delta_i(k), \tag{41}$$

where we have used the experimental fact that $|\delta_i| \approx |ka_i| \gg k/m$ where $1/m$ is maximum range set by the integration. Then, we can imagine calculating a generic parity-violating amplitude $d_i(k)$ via Eq. (39):

$$d_i(k) \sim \frac{4\pi}{k}C_i\int_0^\infty dr\, r^2 j_1(kr)\left[\frac{\partial}{\partial r}, f_m(r)\right]\frac{1}{kr}e^{i\delta_i(k)}\sin\delta_i(k)$$

$$\equiv \lambda_i\frac{1}{k}e^{i\delta_i}\sin\delta_i = \lambda_i m_i(k), \tag{42}$$

with C_i symbolically indicating the appropriate combination of PV constants appearing in $V_{1,\mathrm{SR}}^{\mathrm{PV}}$ and

$$\lambda_i \sim \frac{4\pi}{k}C_i\int_0^\infty dr\, r j_i(kr)\frac{df_m(r)}{dr} \approx \frac{4\pi}{3}C_i\int_0^\infty dr\, r^2\frac{df_m(r)}{dr}, \tag{43}$$

which is the basic form advocated by Danilov.[3] An analogous relationship holds for ρ_t.

At low energy then it seems prudent to explicitly include the appropriate S-wave scattering length in expressing the effective weak potential, and we can define

$$\lim_{k\to 0} m_{s,t}(k) = -a_{s,t}, \qquad \lim_{k\to 0} c_t(k), d_s(k), d_t(k) = -\rho_t a_t, -\lambda_s^i a_s, -\lambda_t a_t. \tag{44}$$

As emphasized above, the real numbers $\rho_t, \lambda_s^i, \lambda_t$—which can in turn be related to the effective parameters C_i—*completely* characterize the low-energy parity-violating interaction

---

[3] Note that this argument is not quite correct quantitatively. Indeed, since $1/m$ is much smaller than the range of the NN interaction (in the pionful theory), we should really use interior forms of the wave functions. However, when this is done, the same qualitative result is found, but the simple relationship in Eq. (43) is somewhat modified.

and can be determined experimentally, as we shall discuss below. Alternatively, we use an isospin decomposition

$$\lambda_s^{pp} = \lambda_s^0 + \lambda_s^1 + \frac{1}{\sqrt{6}}\lambda_s^2,$$

$$\lambda_s^{np} = \lambda_s^0 - \frac{2}{\sqrt{6}}\lambda_s^2,$$

$$\lambda_s^{nn} = \lambda_s^0 - \lambda_s^1 + \frac{1}{\sqrt{6}}\lambda_s^2, \qquad (45)$$

to write things in terms of the appropriate NN quantities. Now, the explicit connection between the S-matrix elements λ_i, ρ_t and the weak interaction parameters C_i, $\tilde{C}_i$ in our effective Lagrangian must be done carefully using the Eq. (39) and the best possible NN wave functions. This work is underway, but is not yet completed [59]. In the meantime, we may obtain an indication of the connection by using the following simple arguments:

When we restrict ourselves to a model-space containing only the low-energy S, P amplitudes noted above, then several of the operators in Eqs. (5), (37) become redundant. For example, the d_t amplitude involves a $T = 0 \to T = 0$ transition, so only the terms proportional to Q_0 contribute. In this case, the spin-space operators $(\vec{\sigma}_1 - \vec{\sigma}_2) \cdot \vec{p}$ and $i(\vec{\sigma}_1 \times \vec{\sigma}_2) \cdot \vec{q}$ yield identical matrix elements up to an overall constant of proportionality. This feature can be seen by considering the coordinate space potential, which contains the function $f_m(r)$ times derivatives acting on the initial and final states. In the short range limit and in the absence of the NN repulsive core, both the P-wave and first derivative of the S-wave vanish at the origin, whereas the product of the S-wave and first derivative of the P-wave are non-zero. Thus, only the components of $\vec{q}$ and $\vec{p}$ that yield derivatives of the P-wave at the origin contribute, leading to identical matrix elements of these two operators (up to an overall phase). Of course, corrections to this statement occur when $f_m(r)$ is smeared out over some short range $\sim 1/m$. Since $1/m \ll 1/$typical momentum $\sim a$, where a is the scattering length, at low energy such corrections are higher-order in our power counting, going as K^2/m^2, where $K \sim \sqrt{M(E + \bar{V})}$ with $\bar{V} \sim 50$ MeV representing some average depth of the NN potential characterizing the interior region. Similarly, the operators $(\vec{\sigma}_1 - \vec{\sigma}_2)_z$ and $(\vec{\sigma}_1 \times \vec{\sigma}_2)_z$ each transform a spin-triplet into a spin-singlet state, and vice versa. Hence, one may absorb the effect of the term proportional to $(\tilde{C}_1 + \tilde{C}_3)$ into the corresponding term proportional to $(C_1 + C_3)$ by a suitable redefinition of the constants. Related arguments allow one to absorb the remaining terms proportional to the $\tilde{C}_i$—as well as the term containing C_6—into the terms involving $(C_1 - 3C_3)P_1$, $(C_2 + C_4)Q_{1+}$, $(C_2 - C_4)Q_{1-}$, and $C_5 Q_2$ for a net total of *five* independent operators, which in turn generate the five independent low-energy PV amplitudes $\lambda_s^0, \lambda_s^1, \lambda_s^2, \lambda_t, \rho_t$. In the zero-range limit, then, we have

$$\lambda_t \propto (C_1 - 3C_3) - (\tilde{C}_1 - 3\tilde{C}_3),$$
$$\lambda_s^0 \propto (C_1 + C_3) + (\tilde{C}_1 + \tilde{C}_3),$$
$$\lambda_s^1 \propto (C_2 + C_4) + (\tilde{C}_2 + \tilde{C}_4),$$
$$\lambda_s^2 \propto -\sqrt{8/3}(C_5 + \tilde{C}_5),$$

$$\rho_t \propto \frac{1}{2}(C_2 - C_4) - C_6. \tag{46}$$

However, going away from strict threshold values and the use of more realistic wave functions will modify these expectations somewhat, as illustrated by a simple, didactic discussion in Appendix E. We emphasize, however, that what is needed at the present time is a purely empirical evaluation in terms of five independent and precise experiments, and that is what we shall discuss next.

3.2. Relation to observables

The next step of the program—contact between this effective parity-violating inter-action and experimental observables—was initiated by Desplanques and Missimer [25]. Before quoting these results, we sketch the manner by which such a confrontation is per-formed. In doing so, we emphasize that the following analysis does *not* rely on definitive computations employing state-of-the art few-body wave functions—carrying out such cal-culations goes beyond the scope of the present study. Indeed, obtaining precise values for the λ_i and ρ_t will require a concerted effort on the part of both experiment and few-body nuclear theory. What we provide below is intended, rather, to serve as a qualitative roadmap for such a program, setting the context for what we hope will be future experimental and theoretical work.

For simplicity, we begin with an illustrative example of nn scattering, for which the Pauli principle demands that the initial state at low energy must be purely $^1S_0$. One can imagine longitudinally polarizing a neutron of momentum $\vec{p}$ and measuring the total scat-tering cross section from an unpolarized target. Since $\vec{\sigma} \cdot \vec{p}$ is odd under spatial inversion, the cross section can depend on helicity only if parity is violated, and via trace techniques the helicity-correlated cross section can easily be found. Using

$$\mathcal{M}(\vec{k}_f, \vec{k}_i) = m_s(k) P_0 + d_s^{nn}[\vec{k}_i \cdot (\vec{\sigma}_1 - \vec{\sigma}_2) P_0 + P_0 \vec{k}_f \cdot (\vec{\sigma}_1 - \vec{\sigma}_2)] \tag{47}$$

we determine

$$\sigma_\pm = \int d\Omega_f \operatorname{Tr} \mathcal{M}(\vec{k}_f, \vec{k}_i) \frac{1}{2}(1 \pm \vec{\sigma}_1 \cdot \hat{k}_i) \mathcal{M}^\dagger(\vec{k}_f, \vec{k}_i)$$

$$= 4\pi |m_s(k)|^2 \operatorname{Tr} P_0 + 8\pi \operatorname{Re} m_s^*(k) d_s^{nn}(k) \operatorname{Tr} P_0(\vec{\sigma}_1 - \vec{\sigma}_2) \cdot \hat{k}_i (1 \pm \vec{\sigma}_1 \cdot \hat{k}_i) + \cdots$$

$$= 4\pi |m_s(k)|^2 \pm 16\pi \operatorname{Re} m_s^*(k) d_s^{nn}(k) + \cdots. \tag{48}$$

Defining the asymmetry via the sum and difference of such helicity cross sections and neglecting the tiny P-wave scattering, we have then

$$A_L = \frac{\sigma_+ - \sigma_-}{\sigma_+ + \sigma_-} = \frac{4k \operatorname{Re}[m_s^*(k) d_s^{nn}(k)]}{|m_s(k)|^2} \simeq 4k\lambda_s^{nn}. \tag{49}$$

Thus the helicity-correlated nn asymmetry provides a direct measure of the parity-violating parameter λ_s^{nn}. Note that, since the total cross section is involved, some investigators have opted to utilize the optical theorem via [60–62]

$$A_L = 4k \frac{\operatorname{Im} d_s^{nn}(k)}{\operatorname{Im} m_s(k)}, \tag{50}$$

which, using our unitarized forms, is completely equivalent to Eq. (49).

Of course, *nn* scattering is currently just a gedanken experiment, and we have discussed it merely as a warm-up to the real problem: *pp* scattering, which introduces the complications associated with the Coulomb interaction. In spite of this complication, the calculation proceeds quite in parallel to the discussion above with obvious modifications. We find

$$A_L = \frac{\sigma_+ - \sigma_-}{\sigma_+ + \sigma_-} = \frac{4k \, \mathrm{Re}[m_s^*(k) d_s^{pp}(k)]}{|m_s(k)|^2} \simeq 4k \lambda_s^{pp}. \tag{51}$$

In the next section we show how this can be obtained straightforwardly within an EFT approach.

On the experimental side, such asymmetries have been measured both at low energies (13.6 and 45 MeV) as well as at higher energies (221 and 800 MeV). It is only the low-energy results[4]

$$\begin{aligned} A_L^{pp}(13.6\,\mathrm{MeV}) &= -(0.93 \pm 0.20 \pm 0.05) \times 10^{-7} \quad [63], \\ A_L^{pp}(45\,\mathrm{MeV}) &= -(1.50 \pm 0.22) \times 10^{-7} \quad [64], \end{aligned} \tag{53}$$

that are appropriate for our analysis, and from these results we can extract the experimental number for the singlet mixing parameter as

$$\left(\lambda_s^{pp}\right)^{\mathrm{expt}} = -\frac{A_L(45\,\mathrm{MeV})}{4k} = -(4.0 \pm 0.6) \times 10^{-8}\,\mathrm{fm}, \tag{54}$$

where $4k \approx 0.88 m_N$. Note that this Eq. (54) is consistent with that of Desplanques and Missimer [25]

$$\left(\lambda_s^{pp}\right)^{\mathrm{expt}} = -\frac{A_L(45\,\mathrm{MeV})}{0.82 m_N} = -(4.1 \pm 0.6) \times 10^{-8}\,\mathrm{fm}. \tag{55}$$

In a corresponding fashion, as described by Ref. [25], contact can be made between other low-energy observables and the effective parity-violating interaction. Clearly, we require five independent experiments in order to identify the five independent S–P mixing amplitudes. As emphasized above, we consider *only* PV experiments on systems with $A = 4$ or lower, in order that nuclear-model dependence be minimized. We utilize here the results of Desplanques and Missimer [25], but these forms should certainly be updated using state-of-the-art few-body computations. There exist many such possible experiments and we suggest the use of

(i) low-energy *pp* scattering, for which

$$\begin{aligned} pp(13.6\,\mathrm{MeV}): \quad & A_L^{pp} = -0.48 \lambda_s^{pp} m_N, \\ pp(45\,\mathrm{MeV}): \quad & A_L^{pp} = -0.82 \lambda_s^{pp} m_N; \end{aligned} \tag{56}$$

---

[4] Note that the 13.6 MeV Bonn measurement is fully consistent with the earlier but less precise number

$$A_L^{pp}(15\,\mathrm{MeV}) = -(1.7 \pm 0.8) \times 10^{-7} \quad [65] \tag{52}$$

determined at LANL.

(ii) low-energy $p\alpha$ scattering, for which

$$p\alpha(46\,\text{MeV}):\quad A_L^{p\alpha}=\left[-0.48\left(\lambda_s^{pp}+\frac{1}{2}\lambda_s^{pn}\right)-1.07\left(\rho_t+\frac{1}{2}\lambda_t\right)\right]m_N;\quad(57)$$

(iii) threshold np radiative capture, for which there exist two independent observables:

$$\text{circular polarization:}\quad P_\gamma=\left(0.63\lambda_t-0.16\lambda_s^{pn}\right)m_N,$$

$$\text{photon asymmetry:}\quad A_\gamma=-0.107\rho_t m_N;\quad(58)$$

(iv) neutron spin rotation from ^{4}He,

$$\frac{d\phi^{n\alpha}}{dz}=\left[1.2\left(\lambda_s^{nn}+\frac{1}{2}\lambda_s^{pn}\right)-2.68\left(\rho_t-\frac{1}{2}\lambda_t\right)\right]M_n\,\frac{\text{rad}}{\text{m}}.\quad(59)$$

Inverting these results, we can determine the five S–P mixing amplitudes via

$$m_N\lambda_s^{pp}=-1.22A_L^{pp}(45\,\text{MeV}),$$

$$m_N\rho_t=-9.35A_\gamma(np\to d\gamma),\quad(60)$$

$$m_N\lambda_s^{pn}=1.6\,A_L^{pp}(45\,\text{MeV})-3.7A_L^{p\alpha}(46\,\text{MeV})+37A_\gamma(np\to d\gamma)$$
$$-2P_\gamma(np\to d\gamma),$$

$$m_N\lambda_t=0.4\,A_L^{pp}(45\,\text{MeV})-0.7A_L^{p\alpha}(46\,\text{MeV})+7A_\gamma(np\to d\gamma)$$
$$+P_\gamma(np\to d\gamma),$$

$$m_N\lambda_s^{nn}=0.83\frac{d\phi^{n\alpha}}{dz}-33.3A_\gamma(np\to d\gamma)-0.69A_L^{pp}(45\,\text{MeV})$$
$$+1.18A_L^{p\alpha}(46\,\text{MeV})-1.08P_\gamma(np\to d\gamma).\quad(61)$$

At the present time only two of these numbers are known definitively—the longitudinal asymmetry in pp, Eq. (53), and in $p\alpha$ scattering,

$$A_L^{p\alpha}(46\,\text{MeV})=-(3.3\pm0.9)\times10^{-7}\quad[66].\quad(62)$$

However, efforts are underway to measure the photon asymmetry in radiative np capture at LANSCE [67] as well as the neutron spin rotation on ^{4}He at NIST [68]. These measurements are also proposed at the neutron beamline at the Spallation Neutron Source (SNS) under construction at Oak Ridge National Laboratory. An additional, new measurement of the circular polarization in np radiative capture would complete the above program, although this is very challenging because of the difficulty of measuring the photon helicity. Alternatively, one could consider the inverse reaction—the asymmetry in $\vec{\gamma}d\to np$—and this is being considered at Athens [69] and at HIGS at Duke [70].

To the extent that one can neglect inclusion of the π as an explicit degree of freedom, one could use this program of measurements to perform a complete determination of the five independent combinations of $\mathcal{O}(Q)$, PV LECs. Nonetheless, in order to be confident in the results of such a series of measurements, it is useful to note that other light systems can and should also be used as a check of the consistency of the extraction. There are various possibilities in this regard, including

(i) *pd* scattering

$$A_L^{pd}(15\text{ MeV}) = \left(-0.21\rho_t - 0.07\lambda_s^{pp} - 0.13\lambda_t - 0.04\lambda_s^{pn}\right)m_N, \tag{63}$$

(ii) radiative *nd* capture

$$A_\gamma = \left(1.42\rho_t + 0.59\lambda_s^{nn} + 1.18\lambda_t + 0.51\lambda_s^{pn}\right)m_N, \tag{64}$$

(iii) neutron spin rotation on *H*

$$\frac{d\phi^{np}}{dz} = \left(1.26\rho_t - 0.63\lambda_t + 1.8\lambda_s^{np} + 0.45\lambda_s^{pp} + 0.45\lambda_s^{nn}\right)m_N \frac{\text{rad}}{\text{m}}. \tag{65}$$

Note that possible follow-ups of the LANSCE and NIST experiments include the last three processes [71].

We emphasize that the above results have been derived under the assumption that the spin-conserving interaction ρ_t is short-ranged—an assumption applicable at energies well below the pion mass. On the other hand, for the 46 MeV $\vec{p}\alpha$ measurement, the proton momentum is well above m_π, so integrating out the pion may not be justified. In this case, inclusion of the pion will lead to modification of the above formulas, introducing a dependence on $h_{\pi NN}^1$, $k_{\pi NN}^{1a}$, and $\bar{C}_\pi$. Thus, a total of eight low-energy few-body measurements would be needed to determine the relevant set of low-energy constants. In the foregoing discussion, we have identified eight few-body observables that could be used for this purpose. Additional possibilities include the PV asymmetry in near-threshold pion photo- or electro-production [37,38,73] or deuteron photodisintegration [74]. At present, we are unable to write down the complete dependence of the few-body PV observables on $h_{\pi NN}^1$, $k_{\pi NN}^{1a}$, and $\bar{C}_\pi$, since only the effects of the LO OPE PV potential (and associated two-body currents) have been included in previous few-body computations. Obtaining such expressions is a task requiring future theoretical effort. In any case, it is evident from our discussion that there exists ample motivation for several new few-body PV experiments and that a complete determination of the relevant PV low-energy constants is certainly a feasible prospect.

4. EFT without explicit pions

Although the foregoing analysis relied on traditional scattering theory, it is entirely equivalent to an EFT approach. In the following two sections, we present this EFT treatment in greater detail, considering first only processes where the momenta p of all external particles are much smaller than the pion mass. In this regime, the detailed dynamics underlying the NN interaction cannot be resolved, and interactions are represented by simple delta-function potentials. As with any EFT, this approximation is justified by a separation of scales. In this case, one has scales set by the NN scattering lengths—$a_s \sim -20$ fm, $a_t \sim 5$ fm—that are both much larger than the $\sim 1/m_\pi$ range of the pion-exchange component of the NN strong interaction [8,9]. Because of this separation of scales, the deuteron can be described within this pionless EFT. For example, one can calculate the deuteron form factors at momenta up to the pion mass [9]. This pionless EFT is limited in energy, but it is very simple (since all interactions among nucleons are of contact character) and

high-order calculations can be carried out. Therefore, although its expansion parameter is not particularly small, high precision can be reached easily.

In this very-low-energy regime the EFT of the two-nucleon problem is not much more than a reformulation of the analysis in Section 3. The full benefits of an EFT framework will, however, be evident when we consider the regime of momenta comparable to the pion mass in the next section.

4.1. Effective Lagrangian

Nucleons with momenta much smaller than the pion mass are non-relativistic, and in this case, it is convenient to redefine the nucleon fields so as to eliminate the term proportional to m_N from the Lagrangian. In so doing, one obtains an infinite tower of operators proportional to powers of $p/m_N \ll 1$. This widely-used heavy-fermion formalism [75,76], is nothing but a Galilean-covariant expression of the usual non-relativistic expansion. Since the non-relativistic EFT must match the relativistic theory for $p \sim m_N$, Lorentz invariance relates various terms in the tower of $(p/m_N)^k$-suppressed effective operators. Thus, one way to construct the effective Lagrangian is to write the most general rotational-invariant non-relativistic Lagrangian, then to relate parameters by imposing this matching condition, or "reparameterization" invariance [77]. Alternatively, we can simply write a relativistic Lagrangian and then take the non-relativistic limit.

The most general Lagrangian involving two nucleon fields N, $\bar{N}$ and a photon field A_μ that is invariant under Lorentz, parity, time reversal and $U(1)$ gauge symmetries is

$$
\mathcal{L}_{N,\text{PC}} = \bar{N}\left\{ iv \cdot D + \frac{1}{2m_N}\left((v \cdot D)^2 - D^2\right) + [S_\mu, S_\nu][D^\mu, D^\nu] \right.
$$
$$
\left. + \frac{\kappa_0 + \kappa_1 \tau_3}{m_N}\epsilon_{\mu\nu\alpha\beta}v^\alpha S^\beta F^{\mu\nu} + \cdots \right\}N, \tag{66}
$$

where κ_0 (κ_1) is the isoscalar (isovector) anomalous magnetic moment, v^μ and S^μ are the nucleon velocity and spin ($v^\mu = (1, \vec{0})$ and $S^\mu = (0, \vec{\sigma}/2)$ in the nucleon rest frame), $D_\mu = \partial_\mu + ieQ_N A_\mu$ is the electromagnetic covariant derivative, with $Q_N = (1 + \tau_z)/2$ the nucleon charge matrix, and $F^{\mu\nu} = \partial^\mu A^\nu - \partial^\nu A^\mu$. Here, as in the following Lagrangians, "$\cdots$" denote terms with more derivatives, which give rise to other nucleon properties such as polarizabilities.

When we relax the restriction of parity invariance, we can write additional terms, such as

$$
\mathcal{L}_{N,\text{PV}} = \frac{2}{m_N^2}\bar{N}(a_0 + a_1 \tau_z)S_\mu N \partial_\nu F^{\mu\nu} + \cdots, \tag{67}
$$

where a_0 (a_1) is the isoscalar (isovector) anapole moment of the nucleon. These terms were discussed in Refs. [33,34]; they appear in PV electron scattering but not in the processes we focus on here.

For the two-nucleon system, we need to consider contact terms with *four* nucleon fields. The simplest parity-conserving (PC) interactions are

$$
\mathcal{L}_{\text{PC},NN} = -\frac{1}{2}C_S \bar{N}N\bar{N}N + 2C_T \bar{N}S^\mu N\bar{N}S_\mu N + \cdots, \tag{68}
$$

where C_S, C_T are dimensional coupling constants first introduced in Ref. [3]. Their projections onto the two NN S-waves are

$$C_{0s} = C_S - 3C_T, \qquad C_{0t} = C_S + C_T. \tag{69}$$

These parameters are related to the respective scattering lengths, while higher-derivative operators give rise to additional parameters, such as S-wave effective ranges and P-wave scattering volumes [8].

For future reference, it is also useful to write down the first-quantized NN potential arising from $\mathcal{L}_{\mathrm{PC},NN}$. To order $\mathcal{O}(Q)$, we have

$$V_{\mathrm{PC}}^{\mathrm{CT}}(\vec{q}, \vec{p}) = C_S + C_T \vec{\sigma}_1 \cdot \vec{\sigma}_2. \tag{70}$$

Similarly, we can construct PV two-nucleon contact interactions. A detailed derivation appears in Appendix A and leads at $\mathcal{O}(Q)$ to

$$
\begin{aligned}
\mathcal{L}_{\mathrm{PV},NN} = \frac{1}{\Lambda_\chi^3} \Big\{ &-C_1 N^\dagger N N^\dagger \vec{\sigma} \cdot i \vec{D}_- N + C_1 N^\dagger i D_-^i N N^\dagger \sigma^i N \\
&- \tilde{C}_1 i \epsilon^{ijk} N^\dagger i D_+^i \sigma_j N N^\dagger \sigma^k N \\
&- C_2 \, N^\dagger N N^\dagger \tau_3 \vec{\sigma} \cdot i \vec{D}_- N + C_2 N^\dagger i D_-^i N N^\dagger \tau_3 \sigma^i N \\
&- \tilde{C}_2 i \epsilon^{ijk} N^\dagger i D_+^i \sigma_j N N^\dagger \tau_3 \sigma^k N \\
&- C_3 N^\dagger \tau^a N N^\dagger \tau^a \vec{\sigma} \cdot i \vec{D}_- N + C_3 N^\dagger \tau^a i D_-^i N N^\dagger \tau^a \sigma^i N \\
&- \tilde{C}_3 i \epsilon^{ijk} N^\dagger \tau^a i D_+^i \sigma_j N N^\dagger \tau^a \sigma^k N \\
&- C_4 N^\dagger \tau_3 N N^\dagger \vec{\sigma} \cdot i \vec{D}_- N + C_4 N^\dagger \tau_3 i D_-^i N N^\dagger \sigma^i N \\
&- \tilde{C}_4 i \epsilon^{ijk} N^\dagger \tau_3 i D_+^i \sigma_j N N^\dagger \sigma^k N \\
&- C_5 \mathcal{I}_{ab} N^\dagger \tau^a N N^\dagger \tau^b \vec{\sigma} \cdot i \vec{D}_- N + C_5 \mathcal{I}_{ab} N^\dagger \tau^a i D_-^i N N^\dagger \tau^b \sigma^i N \\
&- \tilde{C}_5 \mathcal{I}_{ab} i \epsilon^{ijk} N^\dagger \tau^a i D_+^i \sigma_j N N^\dagger \tau^b \sigma^k N \\
&- C_6 i \epsilon^{ab3} N^\dagger \tau^a N N^\dagger \tau^b \vec{\sigma} \cdot i \vec{D}_+ N \Big\} + \cdots,
\end{aligned}
\tag{71}
$$

where we have introduced the short-hand notation

$$N^\dagger i D_\pm^\mu N \equiv \left(i D^\mu N \right)^\dagger N \pm N^\dagger \left(i D^\mu N \right) \tag{72}$$

(in momentum space, $i D_+^\mu$ and $i D_-^\mu$ give rise to the difference and sum, respectively, of the initial and final nucleon momenta). The effects of the weak interaction are represented by the LECs C_i. We have normalized the operators to a scale $\Lambda_\chi = 4\pi F_\pi \sim 1$ GeV, as would appear natural in a pionful theory. One might then anticipate that the C_i are of order $G_F \Lambda_\chi^2 \sim 10^{-5}$. In fact, as discussed in Section 5, naive dimensional analysis (NDA) suggests that these quantities have the magnitude $C_i \sim (\Lambda_\chi / F_\pi)^2 g_\pi$, where $g_\pi = 3.8 \times 10^{-8}$ sets the scale for non-leptonic weak interactions. One may also attempt to predict such constants using models (see Section 6) and compare with the experimentally determined linear combinations discussed above.

The $\mathcal{O}(Q)$ Lagrangian $\mathcal{L}_{\mathrm{PV},NN}$ gives rise to the potential in Eq. (5), which generates energy-independent S–P wave mixing as discussed earlier. Higher-derivative PV operators lead both to energy-dependence in the S–P mixing amplitudes as well as mixing involving

higher partial waves. Given the level of complexity already appearing at $\mathcal{O}(Q)$, we will *not* consider these higher-order terms.

4.2. Amplitudes

In processes involving a single nucleon, amplitudes can be expanded in loops. The situation is more subtle when two or more nucleons are present [3]. This is due to the fact that intermediate states that differ from initial states only by nucleon kinetic energies receive $O(m_N/p)$ enhancements. A resummation then must be performed, leading, e.g., to nuclear bound states, and it is not immediately obvious that such resummations can be done while maintaining the derivative expansion necessary to retain predictive power order by order. The large values for the NN scattering lengths, however, provide justification for such a procedure [8,9]. Before considering PV effects, it is helpful to review what resummation technique yields for the case of the strong NN interaction.

In lowest order, the S-wave NN interaction can be represented via a contact term

$$T_{0i} = C_{0i}(\mu). \tag{73}$$

Including the rescattering corrections, the full T-matrix is found to be

$$
\begin{aligned}
T_i(k) &= C_{0i}(\mu) + C_{0i}(\mu)G_0(k)C_{0i}(\mu) + \cdots \\
&= \frac{C_{0i}(\mu)}{1 - C_{0i}(\mu)G_0(k)} = -\frac{4\pi}{m_N}\frac{1}{-\frac{4\pi}{m_N C_{0i}(\mu)} - \mu - ik},
\end{aligned} \tag{74}
$$

where

$$G_0(k) = \lim_{\vec{r},\vec{r}' \to 0} G_0(\vec{r},\vec{r}') = \int \frac{d^3 s}{(2\pi)^3} \frac{1}{\frac{k^2}{m_N} - \frac{s^2}{m_N} + i\epsilon} = -\frac{m_N}{4\pi}(\mu + ik) \tag{75}$$

is the zero-range Green's function, which displays the large nucleon mass in the numerator. Identifying the scattering length via

$$-\frac{1}{a_i} = -\frac{4\pi}{m_N C_{0i}(\mu)} - \mu \tag{76}$$

and using the relation

$$m_i(k) = -\frac{m_N}{4\pi} T_i(k) \tag{77}$$

connecting the scattering and T-matrices, we find

$$m_i(k) = \frac{1}{-\frac{1}{a_i} - ik} = -\frac{a_i}{1 + ika_i}. \tag{78}$$

It is important to note here that since a_i is a physical quantity, it cannot depend on the scale parameter μ and this invariance is observed in Eq. (76), wherein the μ dependence of the Green's function is canceled by the corresponding scale dependence in $-4\pi/m_N C_{0i}(\mu)$.

We observe that the resummation is at this order completely equivalent to the unitarization that lead to Eq. (26), and one can show similarly that in the NN system inclusion

of higher-derivative operators reproduces higher powers of energy in the effective-range expansion [8,9].

It is straightforward to generalize the above calculation to account for electromagnetic interactions. As shown in Ref. [78] (see also Ref. [79]) the unitarized pp scattering amplitude has the form

$$m_s(k) = -\frac{m_N}{4\pi} \frac{C_{0s}(\mu)C_\eta^2(\eta_+(k))e^{2i\sigma_0}}{1 - C_{0s}(\mu)G_C(k)}, \tag{79}$$

where $\eta_+(k) = M\alpha/2k$,

$$C_\eta^2(x) = \frac{2\pi x}{e^{2\pi x} - 1} \tag{80}$$

is the usual Sommerfeld factor, $\sigma_0 = \arg\Gamma(\ell + 1 + i\eta_+(k))$ is the Coulomb phase shift, and the free Green's function $G_0(k)$ has also been replaced by its Coulomb analog

$$G_C(k) = \int \frac{d^3s}{(2\pi)^3} \frac{C^2(\eta_+(k))}{\frac{k^2}{m_N} - \frac{s^2}{m_N} + i\epsilon}. \tag{81}$$

Remarkably, this integral can be performed analytically, yielding

$$G_C(k) = -\frac{m_N}{4\pi}\left[\mu + m_N\alpha\left(H(i\eta_+(k)) - \log\frac{\mu}{m_N\pi\alpha} - \zeta\right)\right]. \tag{82}$$

Here ζ is defined in terms of the Euler constant γ_E via $\zeta = 2\pi - \gamma_E$ and

$$H(x) = \psi(x) + \frac{1}{2x} - \log x. \tag{83}$$

The resultant scattering amplitude has the form

$$\begin{aligned}
m_s(k) &= \frac{C_\eta^2(\eta_+(k))e^{2i\sigma_0}}{-\frac{4\pi}{m_N C_{0s}(\mu)} - \mu - m_N\alpha\left[H(i\eta_+(k)) - \log\frac{\mu}{m_N\pi\alpha} - \zeta\right]} \\
&= \frac{C_\eta^2(\eta_+(k))e^{2i\sigma_0}}{-\frac{1}{a_{0s}} - m_N\alpha\left[h(\eta_+(k)) - \log\frac{\mu}{m_N\pi\alpha} - \zeta\right] - ikC_\eta^2(\eta_+(k))},
\end{aligned} \tag{84}$$

where we have defined, as before,

$$-\frac{1}{a_{0s}(\mu)} = -\frac{4\pi}{MC_{0s}(\mu)} - \mu, \tag{85}$$

and

$$h(\eta_+(k)) = \text{Re}\,H(i\eta_+(k)). \tag{86}$$

The experimental scattering length a_{Cs} in the presence of the Coulomb interaction is defined via

$$-\frac{1}{a_{Cs}} = -\frac{1}{a_{0s}(\mu)} + m_N\alpha\left(\log\frac{\mu}{m_N\pi\alpha} - \zeta\right), \tag{87}$$

in which case the scattering amplitude takes its traditional lowest-order form

$$m_s(k) = \frac{C_\eta^2(\eta_+(k))e^{2i\sigma_0}}{-\frac{1}{a_{Cs}} - m_N\alpha H(i\eta_+(k))}. \tag{88}$$

Of course, Eq. (88) requires that the Coulomb-corrected scattering length be different from its non-Coulomb partner, and comparison of the experimental pp scattering length—$a_{pp} = -7.82$ fm—with its nn analog—$a_{nn} = -18.8$ fm—is roughly consistent with Eq. (87) if a reasonable cutoff is chosen (e.g., $\mu \sim 1$ GeV).

Having unitarized the strong scattering amplitude, we can now proceed analogously for its parity-violating analog. The lowest-order S–P mixing amplitude is

$$T_{0\mathrm{SP}} = W_{0\mathrm{SP}}(\mu). \tag{89}$$

Inclusion of S-wave rescattering effects while neglecting P-wave scattering and Coulomb contributions yields the result

$$T_{\mathrm{SP}}(k) = W_{0\mathrm{SP}}(\mu) + W_{0\mathrm{SP}}(\mu)G_0(k)C_{0i}(\mu) + \cdots = \frac{W_{0\mathrm{SP}}(\mu)}{1 - G_0(k)C_{0i}(\mu)}. \tag{90}$$

Writing Eq. (90) in the form

$$d_i(k) = -\frac{m_N}{4\pi}T_{\mathrm{SP}}(k) = \frac{\frac{W_{0\mathrm{SP}}(\mu)}{C_{0i}(\mu)}}{-\frac{4\pi}{m_N C_{0i}(\mu)} - \mu - ik}$$

$$= \frac{\lambda_i}{-\frac{1}{a_i} - ik} = \lambda_i m_i(k), \tag{91}$$

we identify the *physical* (μ-independent) S–P wave mixing amplitude via

$$\lambda_i = \frac{W_{0\mathrm{SP}}(\mu)}{C_{0i}(\mu)}. \tag{92}$$

Similarly, including the Coulomb interaction, we find for the unitarized weak amplitude

$$T_{0\mathrm{SP}} = \frac{W_{0\mathrm{SP}}(\mu)C_\eta^2(\eta_+(k))e^{i(\sigma_0+\sigma_1)}}{(1 - C_{0s}(\mu)G_C(k))} \equiv \frac{\lambda_{\mathrm{SP}}^{pp}C_\eta^2(\eta_+(k))e^{i(\sigma_0+\sigma_1)}}{-\frac{1}{a_{Cs}} - m_N\alpha a_{Cs}H(i\eta_+(k))}, \tag{93}$$

where we have again neglected the P-wave scattering, and have identified

$$\lambda_{\mathrm{SP}}^{pp} = \frac{W_{0\mathrm{SP}}(\mu)}{C_{0s}(\mu)} \tag{94}$$

as the physical mixing parameter.

Having obtained fully unitarized forms, we can now proceed to evaluate the helicity-correlated cross sections, finding, as before, at the very lowest energies,

$$A_L = \frac{\sigma_+ - \sigma_-}{\sigma_+ + \sigma_-} = \frac{4k\,\mathrm{Re}(d_s^*(k)m_s^{pp}(k))}{|m_s(k)|^2} \simeq 4k\lambda_s^{pp}. \tag{95}$$

Somewhat more involved, of course, are processes involving more than two nucleons. Besides the inherent calculational difficulty, interesting new physics arises when three nucleons can overlap. When pions are integrated out of the theory, three-nucleon interactions

become significant. In fact, it has been shown [11] that its strong running requires that the non-derivative contact three-body force be included at *leading* order in the EFT, together with the non-derivative contact two-body forces considered above. This three-nucleon force acts only on the $S_{1/2}$ channel, and provides a mechanism for triton saturation. The existence of one three-body parameter in leading order is the reason behind the phenom-enological Phillips line. Note that most three-nucleon channels are free of a three-nucleon force up to high order, and can therefore be predicted to high accuracy with two-nucleon input only [10]. Similar renormalization might also take place in the four-nucleon system. It remains to be seen whether the same phenomenon also enhances PV few-body forces. We defer a detailed treatment of $A \geqslant 3$ PV forces and related renormalization issues to a future study.

5. EFT with explicit pions

For processes in which $p \sim m_\pi$, it is no longer sufficient to integrate the pions out of the effective theory. Incorporation of the pion as an explicit degree of freedom requires use of consistent PV chiral Lagrangian, which we develop in this section.

5.1. Effective Lagrangian

Chiral perturbation theory (χPT) provides a systematic expansion of physical observ-ables in powers of small momenta and pion mass for systems with at most one nucleon [58, 76]. The interactions obtained from χPT can be used to build four-nucleon operators aris-ing from pion exchange, though care must be taken to avoid double-counting the effects of multi-pion exchange in both operators and wave functions (see below). In the approach we follow here, pionic effects are generally included non-perturbatively. Strong πN inter-actions are derivative in nature, and thus scale as powers of p/Λ_χ. As a result, one can include them while maintaining a systematic derivative expansion [57]. By contrast, weak πN interactions need not involve derivatives, but the small scale associated with hadronic weak interactions (g_π) implies that one needs at most one weak vertex. In addition, explicit chiral symmetry-breaking effects associated with the up- and down-quark masses also en-ter perturbatively, since $m_\pi \ll \Lambda_\chi$. To incorporate all these effects, we require the most general effective Lagrangian to a given order in p containing local interactions parameter-ized by a priori unknown low-energy constants (LECs). The corrections from quark masses and loops are then included order by order.

We give here the basic ingredients to our discussion. (For a review, see Ref. [82].) The nucleon mass m_N is much larger than the pion mass m_π, so we continue to employ a heavy-nucleon field. The pion fields π^a, $a = 1, 2, 3$, enter through

$$\xi = \exp\left(\frac{i\pi^a \tau^a}{2F_\pi}\right), \tag{96}$$

where $F_\pi = 92.4$ MeV is the pion decay constant [83]. This quantity allows us to construct chiral vector and axial-vector currents given by

$$V_\mu = \frac{1}{2}\left(\xi D_\mu \xi^\dagger + \xi^\dagger D_\mu \xi\right),$$

$$A_\mu = -\frac{i}{2}\left(\xi D_\mu \xi^\dagger - \xi^\dagger D_\mu \xi\right) = -\frac{D_\mu \pi}{F_\pi} + O\left(\pi^3\right),$$

respectively.

Chirally-symmetric strong interaction pionic effects can be incorporated into the pionless Lagrangian by substituting $D_\mu \to \mathcal{D}_\mu$, where the chiral covariant derivative is

$$\mathcal{D}_\mu = D_\mu + V_\mu, \tag{97}$$

and by adding interactions involving A_μ. On the other hand, the quark mass matrix $\mathcal{M} = \mathrm{diag}(m_u, m_d)$ generates chiral-symmetry breaking that can be incorporated via

$$\chi_\pm = \xi^\dagger \chi \xi^\dagger \pm \xi \chi^\dagger \xi, \tag{98}$$

where

$$\chi = 2B(s + ip), \tag{99}$$

with B a constant with dimensions of mass, and s, p representing scalar and pseudoscalar source fields. In the present application $s = \mathcal{M}$ and $p = 0$, and in the following, we work in the isospin-symmetric limit, $m_u = m_d = \hat{m}$. Isospin-breaking effects will generate small ($\lesssim 10^{-2}$) multiplicative corrections to the tiny PV effects of interest here, so we safely neglect them. In this case, to leading order in the chiral expansion we have

$$\chi_+ = 2B\hat{m} + O\left(\pi^2\right), \qquad \chi_- = 2B\hat{m}\frac{i\pi}{F_\pi} + O\left(\pi^3\right). \tag{100}$$

The building blocks for including a Δ field in the Lagrangian can be found in Ref. [84]. For simplicity we here integrate out Δ isobars. It is straightforward but tedious to use these building blocks to extend the results of our paper by including explicit Δ effects.

We group terms in Lagrangians $\mathcal{L}^{(\nu)}$ labeled by the chiral index $\nu = d + f/2 - 2$, where d is the number of derivatives and powers of the pion mass and f the number of fermion fields. We only display terms that are relevant for the arguments that follow.

Parity-conserving πN Lagrangian

We then arrive at

$$\mathcal{L}^{(0)}_{\pi N, \mathrm{PC}} = \bar{N}\left[iv \cdot \mathcal{D} + 2g_A^0 S \cdot A\right]N, \tag{101}$$

with the lowest index. Similarly, we have for the next to leading order (NLO) Lagrangian

$$\begin{aligned}
\mathcal{L}^{(1)}_{\pi N, \mathrm{PC}} = \frac{1}{2m_N}\bar{N}\Big\{ &(v \cdot \mathcal{D})^2 - \mathcal{D}^2 + [S_\mu, S_\nu][\mathcal{D}^\mu, \mathcal{D}^\nu] \\
&- 2ig_A^0(S \cdot \mathcal{D}v \cdot A + v \cdot A S \cdot \mathcal{D}) \\
&+ 2(\kappa_0 + \kappa_1 \tau_3)\epsilon_{\mu\nu\alpha\beta}v^\alpha S^\beta F^{\mu\nu}\Big\}N + \cdots
\end{aligned} \tag{102}$$

and the next-to-next-to-leading order (NNLO) terms

$$\mathcal{L}_{\pi N,\text{PC}}^{(2)} = \bar{N} \left\{ \frac{g_A^0}{4m_N^2} \left[\mathcal{D}^\mu, [\mathcal{D}_\mu, S \cdot A] \right] - \frac{g_A^0}{2m_N^2} v \cdot \overleftarrow{\mathcal{D}} S \cdot A v \cdot \mathcal{D} \right.$$
$$- \frac{g_A^0}{2m_N^2} \left(\{ S \cdot \mathcal{D}, v \cdot A \} v \cdot \mathcal{D} + \text{h.c.} \right) - \frac{g_A^0}{4m_N^2} \left(S \cdot A \mathcal{D}^2 + \text{h.c.} \right)$$
$$- \frac{g_A^0}{2m_N^2} \left(S \cdot \overleftarrow{\mathcal{D}} A \cdot \mathcal{D} + \text{h.c.} \right) + 2\hat{d}_{16} S \cdot A \langle \chi_+ \rangle$$
$$\left. + 2\hat{d}_{17} \langle S \cdot A \chi_+ \rangle + i\hat{d}_{18} [S \cdot \mathcal{D}, \chi_-] + i\hat{d}_{19} [S \cdot \mathcal{D}, \langle \chi_- \rangle] \right\} N + \cdots . \quad (103)$$

Here the ellipses denote counter-terms not relevant in our present calculation, a complete list of which is given in Ref. [85]. The superscript "0" in g_A and μ_N indicates that these quantities must be appended by the corresponding loop contributions in order to obtain the physical (renormalized) axial coupling and nucleon magnetic moment.

Parity-conserving NN Lagrangian

For nuclear systems, we require the PC Lagrangian involving more than two nucleon fields. Here we will only need the lowest index ($\nu = 0$) terms, containing four nucleon fields. The relevant Lagrangian has the same form as Eq. (68),

$$\mathcal{L}_{NN,\text{PC}}^{(0)} = -\frac{1}{2} C_S \bar{N} N \bar{N} N + 2 C_T \bar{N} S^\mu N \bar{N} S_\mu N + \cdots , \quad (104)$$

but here C_S, C_T are constants whose numerical values are different from the ones in the pionless theory. This is because we are now removing soft-pion contributions from the counter-terms, and including them explicitly.

The NLO four-nucleon corrections occur at $\nu = 2$, which will not be used since in this work we truncate the chiral expansion of the PV potential at $\mathcal{O}(Q)$. Likewise, six-nucleon PC interactions first appear at $\nu = 1$ so their contribution to PV observables will be at higher order in loop diagrams.

Parity-violating πN Lagrangian

The lowest-index ($\nu = -1$) PV interaction arises from the πNN Yukawa interaction,

$$\mathcal{L}_{\pi N,\text{PV}}^{(-1)} = -\frac{h_{\pi NN}^1}{2\sqrt{2}} \bar{N} X_-^3 N$$
$$= -i h_{\pi NN}^1 (\bar{p} n \pi^+ - \bar{n} p \pi^-) + \cdots , \quad (105)$$

where

$$X_-^3 = \xi^\dagger \tau^3 \xi - \xi \tau^3 \xi^\dagger , \quad (106)$$

and the "$\cdots$" denote the terms in this operator containing additional (odd) numbers of pions. At $\nu = 0$ there exist also PV vector and axial-vector πNN interactions, detailed expressions for which can be found in Refs. [31,32]. However, as discussed in Ref. [38], the effects of the vector operators can be eliminated through $\mathcal{O}(Q)$ by using the equations of motion and by suitably redefining the constant $\bar{C}_\pi$ (defined below). The PV axial-vector couplings involve two or more pions, and, as pointed out in Ref. [32], such couplings

renormalize $h^1_{\pi NN}$ at $\mathcal{O}(Q^3)$. Consequently, their contribution to the PV NN potential appears at $\mathcal{O}(Q^2)$, via loop effects.

At NNLO ($\nu = 1$) we find several new PV πNN operators that will contribute to the PV NN potential at $\mathcal{O}(Q)$. In principle, these operators can be expressed in terms of the quantities $X^q_{L,R}$ defined in Ref. [31], thereby allowing one to determine the full, non-linear dependence on the pion fields. For our purposes, however, it is sufficient to truncate the expansion of these operators at one power of the pion field, since terms containing additional pion fields only contribute to the PV NN interaction beyond $\mathcal{O}(Q)$. After implementing the strictures of reparameterization invariance, we obtain the Lagrangian

$$\mathcal{L}^1_{\pi NN,\mathrm{PV}} = \frac{2ik^{1a}_{\pi NN}}{\Lambda_\chi F_\pi} \epsilon_{\mu\nu\alpha\beta} \bar{N} \overleftarrow{D}^\mu (\vec{\tau} \times \vec{\pi})_3 \overrightarrow{D}^\nu v^\alpha S^\beta N$$
$$+ \frac{k^{1b}_{\pi NN}}{\Lambda_\chi F_\pi} \bar{N} [D^\lambda D_\lambda, (\vec{\tau} \times \vec{\pi})_3] N + \frac{k^{1c}_{\pi NN} m_\pi^2}{\Lambda_\chi F_\pi} \bar{N} (\vec{\tau} \times \vec{\pi})_3 N + \cdots, \tag{107}$$

where we have chosen a normalization such that the constants $k^{1a-c}_{\pi NN}$ ought to be of order a few times g_π according to naive dimensional analysis (see below) and where the "$\cdots$" indicate terms involving more than one pion field.

Nominally, then, there exist three new, independent operators that contribute to the PV NN potential at $\mathcal{O}(Q)$. A proof of their independence under reparameterization invariance, following the arguments of Ref. [87], will appear in a forthcoming publication and we do not reproduce the full arguments here. Heuristically, however, the existence of these operators can be seen from their correspondence with the independent $\mathcal{O}(Q^2)$ scalars that can be formed from the independent momenta, nucleon spin, and pion mass:[5] $\vec{p} \cdot \vec{p}'$, $\vec{\sigma} \cdot \vec{p} \times \vec{p}'$, $(\vec{p} - \vec{p}')^2$, and m_π^2. Naively, then, one would have expected four independent $\mathcal{O}(Q^2)$ operators, rather than just three as given in Eq. (107), with the operator corresponding to $\vec{p}' \cdot \vec{p}$ given by

$$\bar{N} \overleftarrow{D}^\lambda (\vec{\tau} \times \vec{\pi})_3 \overrightarrow{D}_\lambda N. \tag{108}$$

However, in a relativistic formulation of the theory, the corresponding operator can be rewritten in terms of $\bar{N}(\vec{\tau} \times \vec{\pi})_3 N$ and $\bar{N}[D^\lambda D_\lambda, (\vec{\tau} \times \vec{\pi})_3] N$ through suitable integrations by parts and application of the LO equations of motion;[6] consequently, it cannot exist as an independent operator in the heavy baryon formulation. Indeed, similar arguments eliminate an analogous term, $\bar{N} \overleftarrow{D}^\lambda S \cdot A \overrightarrow{D}_\lambda N$, from the parity conserving Lagrangian. In contrast, the remaining terms in $\mathcal{L}^1_{\pi NN,\mathrm{PV}}$ cannot be eliminated in the relativistic theory via such arguments and, thus, must exist as independent terms in the non-relativistic case.

We also note that in order for EFT with non-relativistic nucleon fields to match the fully relativistic theory, the coefficients $k^{1a-c}_{\pi NN}$ in general receive contributions proportional to $h^1_{\pi NN}$ that arise from a non-relativistic reduction of the LO PV πNN Yukawa interaction in addition to contributions that represent *bona fide* $\mathcal{O}(Q^2)$ effects. This situation is analogous to what occurs for the $\mathcal{O}(Q^2)$ nucleon magnetic moment operator, whose coefficient

---

[5] The presence of the single pion field leads to a pseudoscalar interaction with the nucleon.

[6] We thank Vincenzo Cirigliano for discussions on this point.

$\mu_N = Q_N + \kappa_N$ receives a contribution (the Dirac term) that is dictated by relativity and that is proportional to the $\mathcal{O}(Q)$ constant (Q_N) and a genuine, a priori unknown $\mathcal{O}(Q^2)$ contribution (the Pauli term) parameterized by the anomalous magnetic moment. In the present case, only $k_{\pi NN}^{1a,b}$ receive contributions proportional to $h_{\pi NN}^1$ as dictated by relativity:

$$k_{\pi NN}^{1a} = \frac{h_{\pi NN}^1}{4\sqrt{2}} \frac{\Lambda_\chi F_\pi}{M_N^2} + \cdots, \qquad k_{\pi NN}^{1b} = -\frac{h_{\pi NN}^1}{8\sqrt{2}} \frac{\Lambda_\chi F_\pi}{M_N^2} + \cdots, \tag{109}$$

where the "$\cdots$" indicate the unconstrained $\mathcal{O}(Q^2)$ contributions.

In practical terms, only two of the operators in Eq. (107) are likely to be experimentally distinguishable. In momentum space, the second and third terms can be written as independent linear combinations of $(\vec{p} - \vec{p}')^2 + m_\pi^2$ and m_π^2. The latter acts like a chiral correction to $h_{\pi NN}^1$, so to $\mathcal{O}(Q)$ in the EFT, it cannot be resolved experimentally. When inserted into the PV NN potential, the former cancels the pion propagator, leading effectively to an $\mathcal{O}(Q)$ contact operator that is indistinguishable from the SR operator proportional to C_6. In contrast, the effects of the remaining operator involving $k_{\pi NN}^{1a}$ cannot be absorbed into the LO π exchange potential or any of the short-range $\mathcal{O}(Q)$ operators. Its contribution to the potential has been given in Eq. (12).

Parity-violating $\gamma \pi N$ Lagrangian

Finally, there exists also a contact $\pi \gamma NN$ interaction at $\nu = 1$ [38],

$$\mathcal{L}_{\pi\gamma N,\mathrm{PV}}^{(1)} = -i e \frac{\bar{C}_\pi}{\Lambda_\chi F_\pi} \bar{p} \sigma^{\mu\nu} F_{\mu\nu} n \pi^+ + \mathrm{H.c.} \tag{110}$$

Parity-violating NN Lagrangian and $\gamma \pi NN$ Lagrangian

The $\nu = 1$ PV four-nucleon terms have the same form as in Eq. (71) but with the gauge-covariant derivatives D_μ replaced by $\mathcal{D}_\mu$, the gauge *and* chiral covariant derivatives. In this case, the coefficients C_i, $\tilde{C}_i$ will differ numerically from those appropriate to the pionless theory, since in the latter case, the effects of pion exchange are incorporated into the operator coefficients.

5.2. Power counting

Throughout this work we use power-counting arguments to guide us in the task of identifying the most significant contributions to PV observables. Power counting is carried out under an implicit assumption about the size of the couplings of the EFT. It is assumed that the couplings are neither particularly small nor particularly large compared with "naive dimensional analysis" (NDA) [86], in which LECs scale with F_π and Λ_χ as

$$\left(\frac{D_\mu}{\Lambda_\chi}\right)^d \left(\frac{\pi}{F_\pi}\right)^p \left(\frac{\bar{N}N}{\Lambda_\chi F_\pi^2}\right)^{f/2} \times (\Lambda_\chi F_\pi)^2 \times (g_\pi)^n, \tag{111}$$

where d, p, $f = 2k$, k and n are positive integers and

$$g_\pi \sim \frac{G_F F_\pi^2}{2\sqrt{2}} \sim 3.8 \times 10^{-8}. \tag{112}$$

In the absence of weak interactions ($n = 0$), the LECs scale with a large mass scale as $(\Lambda_\chi)^{-\nu}$, where $\nu = d + f/2 - 2$ is the chiral index defined earlier. Hence, one obtains the ordering of operators in Q/Λ_χ described earlier. At energies that are small compared with the mass of W and Z bosons, weak interactions have a strength given by the Fermi constant $G_F = 1.16639 \times 10^{-5}\,\text{GeV}^{-2}$. The effective operators they entail are proportional to (powers of) the Fermi constant times the square of a mass scale. A natural scale is the pion decay constant, so we assume that these operators have coefficients of order of $G_F F_\pi^2 \sim 10^{-7}$. In Eq. (112), we use $g_\pi = 3.8 \times 10^{-8}$ because this scale appears naturally in quark-model estimates as in Ref. [19].

Here we limit ourselves to $n = 1$. Up to two derivatives, then, we have one PV πNN Yukawa coupling $h_{\pi NN}^1$, three NNLO PV πNN couplings $k_{\pi NN}^{1a-c}$, ten short-distance LECS C_i, $\tilde{C}_i$, and one additional independent PV LEC $\bar{C}_\pi$ if we consider PV photo-reactions. As emphasized earlier, only five independent combinations of C_i and $\tilde{C}_i$ are relevant to low-energy PV observables in few-body systems, while the effects of all but one of the NNLO PV πNN operators can be absorbed into other terms in the potential. In practice, then, the inclusion of pions leads to a total of eight independent LECs. From Eq. (111), the expected size of the relevant PV couplings is

$$h_{\pi NN}^1 \sim \left(\frac{\Lambda_\chi}{F_\pi}\right) g_\pi, \tag{113}$$

$$C_i, \tilde{C}_i \sim \left(\frac{\Lambda_\chi}{F_\pi}\right)^2 g_\pi, \tag{114}$$

$$k_{\pi NN}^{1a-c}, \bar{C}_\pi = g_\pi. \tag{115}$$

The most challenging part of the power counting is to order the strong-interaction effects. Here we count powers of Q, where as above Q denotes a small quantity such as the pion mass m_π, an external momentum p, or the electric charge, e. For example, the strong πNN vertex is counted as $\mathcal{O}(Q)$, the PV Yukawa vertex is $\mathcal{O}(Q^0)$, the pion propagator is $\mathcal{O}(Q^{-2})$, and the four-nucleon vertices proportional to $C_{S,T}$ are also counted as $\mathcal{O}(Q^0)$.

In the one-nucleon system, a loop integral $\int d^4k$ can be simply counted as $\mathcal{O}(Q^4)$. If there are two or more nucleons, this naive counting breaks down. The reason is that within nuclei nucleons are nearly on-shell. Thus, instead of being $\mathcal{O}(Q)$, the q^0 component of the pion four-momentum in the one-pion-exchange (OPE) diagram shown in Fig. 2 is $\mathcal{O}(Q^2)$, since

$$q^0 = p_f^0 - p_i^0 \simeq \frac{\vec{p}_f^2 - \vec{p}_i^2}{2m_N}, \tag{116}$$

where i, f label initial and final states. This simply means that in first approximation OPE is static. Now consider the loop diagram generated by the exchange of two pions between two nucleons, and focus on the dq^0 integral, which is, schematically,

$$\int \frac{dq^0}{2\pi} \frac{i}{\frac{E}{2} + q^0 - \frac{\vec{q}^2}{2m_N} + i\epsilon} \frac{i}{\frac{E}{2} - q^0 - \frac{\vec{q}^2}{2m_N} + i\epsilon} \left(\frac{i}{(q^0)^2 - \vec{q}^2 - m_\pi^2 + i\epsilon}\right)^2$$

$$\sim \frac{i}{E - \frac{\vec{q}^2}{m_N} + i\epsilon} \left(\frac{1}{\vec{q}^2 + m_\pi^2}\right)^2 + \cdots, \tag{117}$$
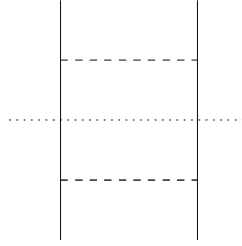
Fig. 2. Parity-conserving iterated one-pion-exchange diagram. A solid (dashed) line represents a nucleon (pion). The dotted line indicates the cut line which picks out the two-nucleon intermediate state.

where $E \sim \mathcal{O}(p^2/m_N)$ is the nucleon kinetic energy. The "$\cdots$" are contributions from the pion poles, which scale according to naive power counting, and other small terms. Yet, the term shown explicitly, stemming from the nucleon pole, represents an $\mathcal{O}(m_N/Q)$ enhancement over naive counting.

This enhancement is more general than the specific diagram considered above. It is present in any diagram that represents a time ordering displaying an intermediate state with nucleons only. Such an intermediate state differs from the initial state only by a difference of nucleon kinetic energies, which is small because of the heavy nature of the nucleons. This type of intermediate state already appeared in the pionless EFT, and led to the resummation (74), which is equivalent to unitarization of the potential, i.e., to the solution of the Schrödinger equation.

To carry out the resummation in the presence of explicit pions, two approaches have been proposed, which differ in the treatment of pion effects relative to the contact interactions. In the simplest approach [89], pion interactions are assumed to be small compared to the non-derivative contact interactions, and only the latter are resummed. Unfortunately, this assumption does not converge for all NN channels at momenta of the order of the pion mass [90]. In the other approach [3], non-derivative contact interactions are assumed to be comparable to OPE, and both interactions are resummed. In its original form, Weinberg's approach was proposed as an expansion of the potential. This approach appears to be successful in accounting for a broad array of nuclear observables [2], but it, too, has problems: iteration of the chiral-symmetry-breaking piece of OPE leads to inconsistent renormalization [42,89].

Progress has been made recently in the understanding of the power counting relevant for NN scattering at $Q \sim m_\pi$ [42]. If an expansion is made around the chiral limit, the aforementioned problems are in principle resolved, and one obtains an expansion that is both consistent and converges. More work is necessary to test the new power counting, but at this stage we can see the reason for its success. The iteration of OPE in the chiral limit, together with the non-derivative contact interactions, makes the NN amplitude numerically similar to Weinberg's original proposal. Therefore, while unnecessarily resumming higher-order terms, Weinberg's power counting can still be used to organize the potential.

With this scheme, we separate Feynman diagrams into two classes: two-particle reducible (2PR) and two-particle irreducible (2PI). Only 2PR diagrams lead to the anomalous enhancement factor after loop integration discussed above. The 2PI diagrams, in contrast, do not contain shallow poles, so they have the same power counting as the one-nucleon

system. With this classification in hand, one can use effective field theory to organize the calculation order by order. The sum of 2PI diagrams yields the potential, which is the kernel for the Lippmann–Schwinger (LS) equation. Through iterations the 2PR diagrams are generated. Solving the LS equation, or equivalently the Schrödinger equation, one arrives at the amplitude from which scattering can be calculated, and whose poles are the NN bound states.

In this work we will follow Weinberg's formalism and derive the PV NN potential up to $\mathcal{O}(Q)$. Only the 2PI PV diagrams are included in the PV potential. All 2PR diagrams can be generated when the PV potential is inserted in the LS equation. In practice, the PV potential is much smaller than the strong potential so it can be treated as a perturbation. One can treat it as a PV operator and calculate the PV matrix element using the wave function from LS equation with the strong potential. The connection with the expansion of Ref. [42] is easily made by further expanding in powers of m_π^2.

5.3. The PV NN potential

Using the above power counting we construct the PV potential, classifying terms according to their size. We truncate the chiral expansion of PV potential at $\mathcal{O}(Q)$, although the procedure can be carried out to higher orders in similar fashion. The PC potential has been derived to $\mathcal{O}(Q^4)$ in Ref. [4].

At $\mathcal{O}(Q^{-1})$, the only contribution comes from OPE diagrams of Fig. 3, where the PV vertex is the LO Yukawa interaction and the strong vertex arises from the operator in Eq. (101). These diagrams give rise to a long-range potential, $V_{\text{LR}}^{\text{PV}}(\vec{k})$:

$$V_{(-1,\text{LR})}^{\text{PV}}(\vec{k}) = -\frac{g_A h_{\pi NN}^1}{2\sqrt{2} F_\pi} i[\vec{\tau}_1 \times \vec{\tau}_2]_3 \frac{(\vec{\sigma}_1 + \vec{\sigma}_2) \cdot \vec{k}}{\vec{k}^2 + m_\pi^2} \tag{118}$$

where the -1 subscript denotes the chiral index of the corresponding amplitude and where $k = p_1 - p_1' = p_2' - p_2$.

Subleading corrections arise from several sources. First, there are corrections to the long-range potential from corrections at the PC vertex (see Fig. 4). As discussed in Appendix B, the corrections involving $\hat{d}_{16,18,19}$ amount to a renormalization of the bare coupling
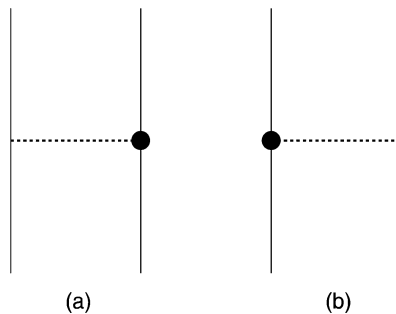

(a)   (b)

Fig. 3. OPE diagram that contributes to the long-range part of the PV potential. The filled circle indicates the PV πNN Yukawa coupling.
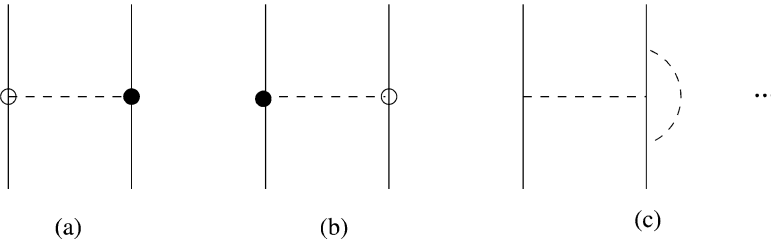
Fig. 4. Corrections to the long-range PV NN potential from insertions of (a), (b) higher-order PC πNN terms, which are denoted by the unfilled circle, and (c) loops.
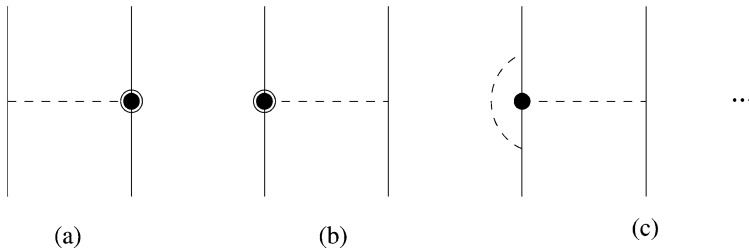
Fig. 5. Corrections to the long-range PV NN potential from insertions of (a), (b) higher-order PV πNN terms, which are denoted by the circled filled circle, and (c) loops.

g_A^0 while the term containing $\hat{d}_{17}$ does not contribute. The remaining terms in Eqs. (102), (103) are proportional to g_A and do not introduce any new unknown constants into the PV potential. Since their contributions are discussed in Appendix B, we do not reproduce them here.

Qualitatively new corrections arise at $\mathcal{O}(Q)$ from long-, medium-, and short-range effects, $V_{1,\mathrm{LR}}^{\mathrm{PV}}$, $V_{1,\mathrm{MR}}^{\mathrm{PV}}$ and $V_{1,\mathrm{SR}}^{\mathrm{PV}}$, respectively. The NNLO long-range contributions arise from inserting the operators in Eq. (107) in the OPE diagrams (see Fig. 5). As noted in above, the effects of the operators proportional to $k_{\pi NN}^{1b,c}$ can be absorbed in the potential through a suitable redefinition of $h_{\pi NN}^1$ and C_6. The momentum space form associated with the remaining operator is

$$V_{1,\mathrm{LR}}^{\mathrm{PV}}(\vec{p}_1,\ldots,\vec{p}_2') = \frac{g_A k_{\pi NN}^{1a}}{\Lambda_\chi F_\pi^2} \left(\frac{\vec{\tau}_1 \times \vec{\tau}_2}{2} \right)_3 \left[\frac{\vec{\sigma}_1 \cdot \vec{p}_1' \times \vec{p}_1 \vec{\sigma}_2 \cdot \vec{q}_1}{\vec{q}_1^2 + m_\pi^2} + (1 \leftrightarrow 2) \right] + \cdots,$$

(119)

where $\vec{p}_i$ ($\vec{p}_i'$) is the initial (final) momentum of the ith nucleon, $\vec{q}_i = \vec{p}_i' - \vec{p}_i$, and the "$\cdots$" denote the $\mathcal{O}(Q)$ contributions generated by corrections to the strong πNN vertex through NNLO (see Eqs. (102), (103)). Taking the Fourier transform of Eq. (119) leads, after some algebra, to the coordinate space potential in Eq. (12). In a similar way, one may evaluate the contributions to $V_{1,\mathrm{LR}}^{\mathrm{PV}}$ generated by order Q^3 contributions to the parity conserving πNN vertex.
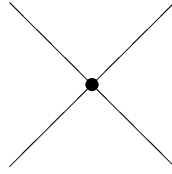
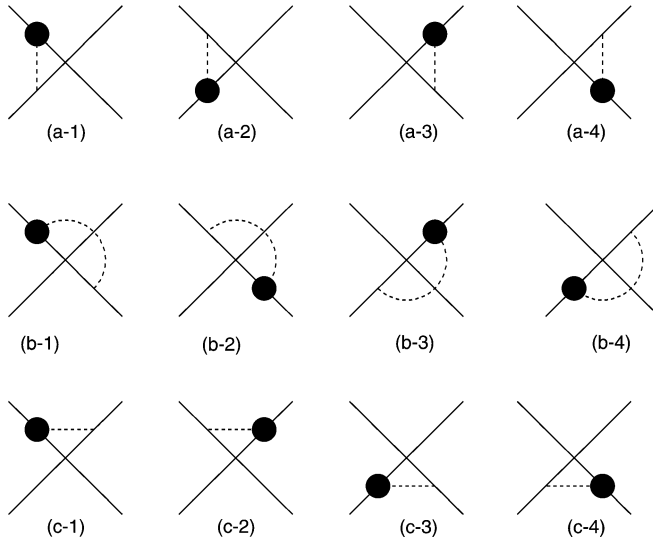Fig. 6. PV NN contact interactions that contribute to the PV short-range potential.

Fig. 7. Possible PV chiral corrections to PC NN couplings $C_{S,T}$.

The short-range part $V_{\text{SR}}^{\text{PV}}$ arises from

 (i) the PV NN contact interactions in Fig. 6 and
(ii) possible chiral corrections to PC NN operators $C_{S,T}$, as shown in Fig. 7.

The contact interactions have exactly the same form as Eq. (5), so we do not reproduce the expression here. Of course, the values of the C_i, $\tilde{C}_i$ differ from those in the pionless theory, where they effectively account for the effects of low-energy pion exchanges. In principle, one would expect these couplings to be renormalized by π loop effects, as in the case of $h_{\pi NN}^1$. As we show in Appendix C, however, such loop effects vanish to $\mathcal{O}(Q)$. Similarly, PV loop corrections to the leading-order PC operators—illustrated in Fig. 7— generate no corrections to the short-range couplings at this order.

The medium-range part $V_{\text{MR}}^{\text{PV}}$ arises from the two-pion-exchange (TPE) diagrams, including

  (i) the triangle diagrams in Fig. 8,
 (ii) the crossed diagrams in Fig. 9, and
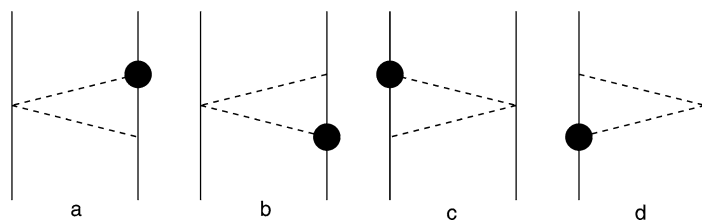(iii) the box diagrams in Fig. 10.

Fig. 8. PV TPE triangle diagrams that contribute to the medium-range PV NN interaction at $\mathcal{O}(Q)$.
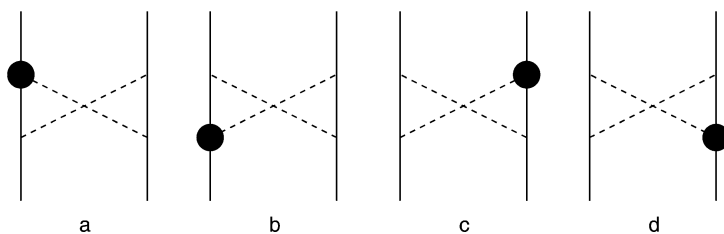

Fig. 9. PV TPE crossed diagrams that contribute to the medium-range PV NN interaction at $\mathcal{O}(Q)$.
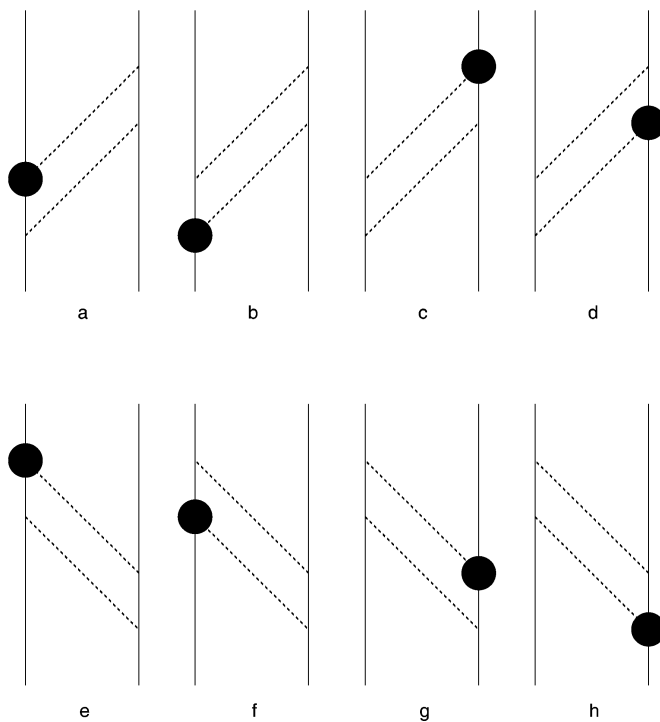

Fig. 10. PV TPE box diagrams that contribute to the medium-range PV NN interaction at $\mathcal{O}(Q)$.

The evaluation of these diagrams is somewhat involved, and we give a detailed discussion in Appendix D. Here, however, we note a few salient features of the calculation. First, the explicit form of the TPE potential is linked to the definition of OPE and the procedure to subtract the iterated OPE from the box diagrams. The slanted box diagrams are meant here as a representation of the full box diagram with the iterated static OPE subtracted (according to the procedure explained in Appendix D). Relativistic corrections (beyond those in OPE) appear at higher orders. Next, we regulate the loop integrals using dimensional regularization. The regulator-dependence is removed by the appropriate counter-terms, which in general have the form given in Eq. (5). The remaining, finite parts of the integrals contain terms "regular"—or polynomial—in momenta and m_π and "irregular", or non-analytic, terms. The former are indistinguishable from operators appearing in Eq. (5) (and higher-order parts of the potential), whereas the latter are uniquely identified with the loop integrals. In principle, one may choose to retain explicitly any portion of the regular terms and absorb the remainder into the short-range LECs appearing in Eq. (5). The meaning of the C_i, $\tilde{C}_i$ is, thus, scheme-dependent. Here, we adopt a scheme in which all of the regular terms are absorbed into the corresponding C_i, $\tilde{C}_i$, leaving only the irregular contributions explicitly in $V_{1,\mathrm{MR}}^{\mathrm{PV}}$:

$$
V_{(1,\mathrm{MR})}^{\mathrm{PV}}(\vec{q}) = -\frac{1}{\Lambda_\chi^3}\left\{ \tilde{C}_2^{2\pi}(q)\frac{\tau_1^z+\tau_2^z}{2}i(\vec{\sigma}_1\times\vec{\sigma}_2)\cdot\vec{q} \right.
$$
$$
\left. + C_6^{2\pi}(q)i\epsilon^{ab3}[\vec{\tau}_1\times\vec{\tau}_2]_3(\vec{\sigma}_1+\vec{\sigma}_2)\cdot\vec{q}\right\}, \tag{120}
$$

where

$$
\tilde{C}_2^{2\pi}(q) = 4\sqrt{2}\pi g_A^3 h_{\pi NN}^1 L(q),
$$
$$
C_6^{2\pi}(q) = -\sqrt{2}\pi g_A h_{\pi NN}^1 L(q) + \frac{3\sqrt{2}}{2}\pi\left[3L(q)-H(q)\right]g_A^3 h_\pi^1, \tag{121}
$$

and

$$
L(q) = \frac{\sqrt{4m_\pi^2+\vec{q}^2}}{|\vec{q}|}\ln\left(\frac{\sqrt{4m_\pi^2+\vec{q}^2}+|\vec{q}|}{2m_\pi}\right), \qquad H(q) = \frac{4m_\pi^2}{4m_\pi^2+\vec{q}^2}L(q). \tag{122}
$$

Thus, the PV TPE amplitudes produce contributions with the same spin–isospin structure as the contact interactions $\tilde{C}_2$, C_6. In fact, since the regulator-dependent and regular parts of the amplitudes can be absorbed into $V_{\mathrm{SR}}^{\mathrm{PV}}$, we would not expect any new spin–isospin dependence to emerge from the divergent TPE amplitudes. The spatial-dependence of the finite, non-analytic part, however, is qualitatively different. We discuss this difference below.

Finally, we observe that there is no PV three-nucleon force to $\mathcal{O}(Q)$. In connecting a third nucleon via a pion-exchange interaction, one increases the order of a given diagram by the same amount as if one added an additional loop. Consequently, the ingredients given in Section 5.1 allow at $\mathcal{O}(Q)$ only tree-level three-nucleon diagrams that involve the leading order PC vertices and the PV Yukawa coupling. However, these diagrams cancel against recoil terms in the iteration of the two-nucleon potential. In fact, the situation here is analogous to the $\mathcal{O}(Q^2)$ PC three-nucleon force, where a similar cancellation occurs

[3,5]. As a result, if one employs an energy-independent potential (as is usually more convenient in few-body calculations), one may omit these three-nucleon diagrams. Non-trivial three-nucleon PV effects should appear only at $\mathcal{O}(Q^2)$, which is beyond the order of our truncation here.

5.4. EFT PV potential: qualitative features

As shown above, the PV NN potential to $\mathcal{O}(Q)$ is given by Eqs. (37), (118), (119), (120). The corresponding coordinate-space $V^{\mathrm{PV}}(r)$ can be obtained straightforwardly by taking the Fourier transform of these expressions. On the basis of the power counting, one would expect the OPE potential $V^{\mathrm{PV}}_{-1,\mathrm{LR}}$ to dominate in those channels where it contributes, unless $h^1_{\pi NN}$ is anomalously small compared with the NDA estimate in Eq. (113). This potential is, of course, not new [16]. Several contributions arise with chiral index $\nu = 1$. Although they are all formally of the same order in power-counting, their effects may nevertheless be distinct due to the different operator structures and spatial ranges. The SR potential has already been discussed extensively in the treatment of the pionless EFT. Qualitatively, the only impact on the SR potential of including the pion as an explicit degree is that the numerical values of relevant combinations of the C_i and $\tilde{C}_i$ will differ for the theory with pions.

The two-pion exchange contribution $V^{\mathrm{PV}}_{1,\mathrm{MR}}$ also appears at $\mathcal{O}(Q)$. The result in Eq. (120) appears to be the first analytic expression for the PV TPE potential that is model-independent and consistent with the symmetries of QCD. Although studies of PV TPE effects have appeared previously in the literature (see, e.g., Ref. [18]), direct comparison with our treatment is difficult. First, we have not been able to find an analytic expression in the literature. Second, two terms in the PV TPE amplitudes that depend strongly on the cutoff would have appeared explicitly had we not used dimensional regularization. This regulator, or cutoff, dependence requires inclusion of short-range counter-terms in order to guarantee that physical observables are regulator-independent. In the analysis of Ref. [18], however, no mention is made of the counter-terms, and we suspect that the corresponding TPE potential is not cutoff-independent. Third, the component of the TPE amplitude unique to the loop diagrams is determined by chiral symmetry, and it is notoriously difficult to maintain this symmetry without using χPT (see Ref. [5] for an illustrative example in the parity conserving three-nucleon sector). The situation for PV interactions closely mirrors the developments in the PC TPE NN potential, whose first derivation in accordance with chiral symmetry was given within EFT [4], and whose form was recently clearly identified in a phase-shift analysis of NN data [91].

The PV TPE contributes two spin–isospin operators. One,

$$O_6 = i[\vec{\tau}_1 \times \vec{\tau}_2]_3(\vec{\sigma}_1 + \vec{\sigma}_2) \cdot \hat{q}, \tag{123}$$

appears also in $V^{\mathrm{PV}}_{-1,\mathrm{LR}}$, but $C^{2\pi,\mathrm{Loop}}_6(q)$ is not a simple Yukawa function. The structure is also the same as the $h^{1'}_{\rho}$ term in the DDH potential, where it is usually neglected. The other spin–isospin structure,

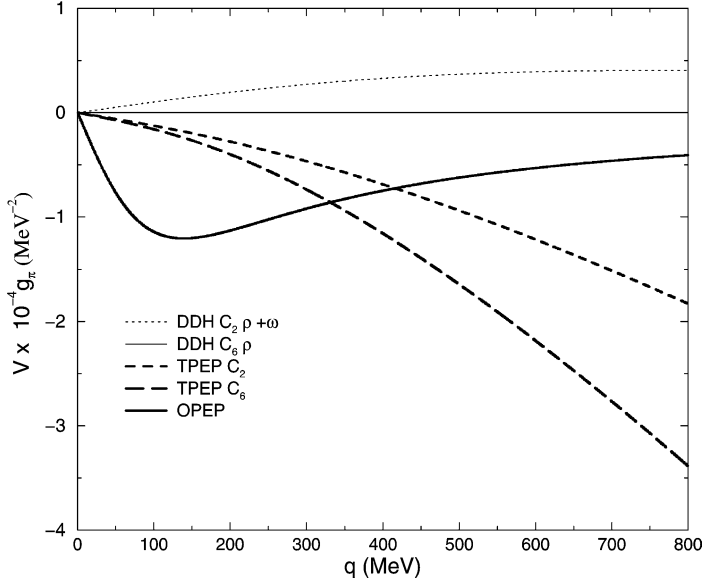$$\tilde{O}_2 = \frac{\tau^z_1 + \tau^z_2}{2} i(\vec{\sigma}_1 \times \vec{\sigma}_2) \cdot \hat{q}, \tag{124}$$

Fig. 11. Components of the PV NN potential (in units of $g_\pi 10^{-4}$ MeV^{-2}) as function of the momentum transferred (in MeV): OPE (thick solid line); C_6 component of TPE (long-dash line); $\tilde{C}_2$ component of TPE (short-dash line); C_6 component of DDH (thin solid line); $\tilde{C}_2$ component of DDH (dotted line).

has the structure of the h_ω^1-term in the DDH potential. In Fig. 11 we plot the momentum-dependence of the coefficients of the operators O_6 (Eq. (123)) and $\tilde{O}_2$ (Eq. (124)) for $V_{1,\mathrm{MR}}^{\mathrm{PV}}$, in comparison with the corresponding components of $V_{-1,\mathrm{LR}}^{\mathrm{PV}}$ and the DDH potential using DDH best values from Table 1.

As expected on the basis of power counting, the OPE potential gives the largest effect for $q \sim m_\pi$. As q increases, the TPE potential grows and eventually overcomes OPE. This feature can be understood simply from the more singular nature of TPE: while $V_{-1,\mathrm{LR}}^{\mathrm{PV}}$ scales as q^{-1} at large q (or r^{-2} at small r), $V_{1,\mathrm{MR}}^{\mathrm{PV}}$ scales as q^1 (or r^{-4}). In comparison with isovector ω-exchange term in DDH, the $\tilde{O}_2$ component of $V_{1,\mathrm{MR}}^{\mathrm{PV}}$ has qualitatively similar behavior at low-q (up to an overall phase). The rise with q is more rapid, however, indicating a longer effective range than for ω-exchange. As pointed out above, the O_6 component at distances $r \lesssim 1/m_\pi$ is missing in DDH, while it is not particularly small in $V_{1,\mathrm{MR}}^{\mathrm{PV}}$. This component will generate an additional energy-dependence in the same channels OPE contributes. Presumably, the conventional practice of neglecting the TPE component leads to inconsistency in the analysis of experiments that probe the $\tilde{O}_6$ operator at different scales. We see no theoretical justification to neglect TPE.

It may, perhaps, be surprising that the TPE contributions to $\tilde{O}_{2,6}$ become numerically non-negligible compared to the OPE effect at relatively low-momentum. For example, when q is of the order of typical Fermi momentum for nuclei (~ 200 MeV), the TPE contribution to $\tilde{O}_6$ is roughly one third the OPE contribution. One may wonder, therefore, whether the EFT converges too slowly to justify truncation at $\mathcal{O}(Q)$. One should keep in mind, however, that TPE effects always appear in tandem with short-range components of

the same order and that the latter properly compensate for the most singular part of the TPE contribution.

New long-range, single pion-exchange terms also arise at subleading order. The structure of the operator associated with $k_{\pi NN}^{1a}$—shown in Eq. (12)—is distinct from those appearing in $V_{-1,\text{LR}}^{\text{PV}}$, $V_{1,\text{MR}}^{\text{PV}}$ and $V_{1,\text{SR}}^{\text{PV}}$ as well as from the operators appearing in the DDH potential. Additional structures are induced by relativistic corrections to the PV πNN Yukawa interaction, which are neglected in the DDH approach (see Appendix B). A consistent power counting, however, requires that one include them along with the SR and MR operators.

Finally, one might also worry that we have not included Δ isobar contributions explicitly since $m_\Delta - m_N$ is comparable to m_π. Indeed, in our treatment, Δ effects are implicit in the LECs. Had we kept the Δ as an explicit degree of freedom, it would contribute to the two-body PV NN interaction solely via loops. Because the PV $\pi N\Delta$ interaction vertices are of D-wave character, loops that contain this new PV interaction are generically two orders higher than the corresponding πN loops containing the PV Yukawa coupling. Similarly, there would also be Δ contributions to the renormalization of h_π^1 appearing in $V_{-1,\text{LR}}^{\text{PV}}$. Since experiments are sensitive only to the renormalized Yukawa couplings, the treatment of Δ loops will only affect the interpretation of h_π^1 and not its extraction from experiment (see the last article in Ref. [38]). The only new contributions from the Δ to the PV NN interaction would be in the TPE potential where the Δ appears between two PC $\pi N\Delta$ vertices.[7] There would also be three-nucleon diagrams that are the PV version of the leading PC three-nucleon force [5]. The calculation of these effects is straightforward, and they introduce no new, a priori unknown PV couplings. We leave the "improved" version of the PV EFT containing these effects for the future when it may be required by phenomenological considerations.

5.5. Currents

As discussed earlier, any experimental program aimed at determining the PV low-energy constants will likely include electromagnetic processes. In order to maintain gauge invariance, one must include the appropriate set of meson-exchange-current operators. Typically in nuclear physics, one expresses the requirements of gauge invariance through the continuity equation

$$\vec{\nabla} \cdot \vec{J} = [\hat{H}, \rho], \tag{125}$$

where $J^\mu = (\rho, \vec{J})$. For the long- and medium-range components of the potential, a minimal set of current operators satisfying Eq. (125) can be obtained by inserting the photon on all charged lines in one- and two-pion-exchange diagrams. The meson exchange current (MEC) operator corresponding to $V_{-1,\text{LR}}^{\text{PV}}$, Fig. 12, is given in Ref. [21]. The operators associated with $V_{1,\text{LR}}^{\text{PV}}$ and $V_{1,\text{MR}}^{\text{PV}}$ are more involved (see Fig. 13(a)–(d)). In particular, construction of the MEC operator associated with $V_{1,\text{MR}}^{\text{PV}}$ is technically arduous, as one must

---

[7] In the two-nucleon PV interaction, these are diagrams analogous to those in Figs. 9, 10 but with the Δ substituted for a nucleon on the line without a filled circle.
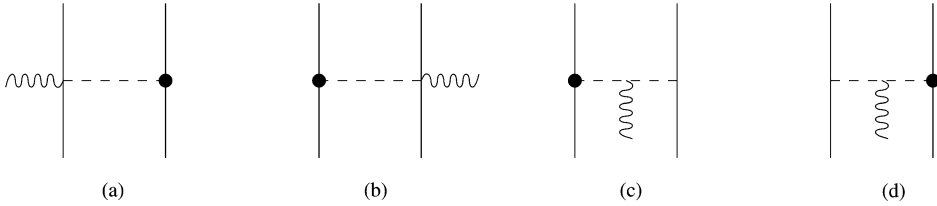
Fig. 12. Long-range PV meson-exchange currents in leading order. A wavy lines represents a photon.
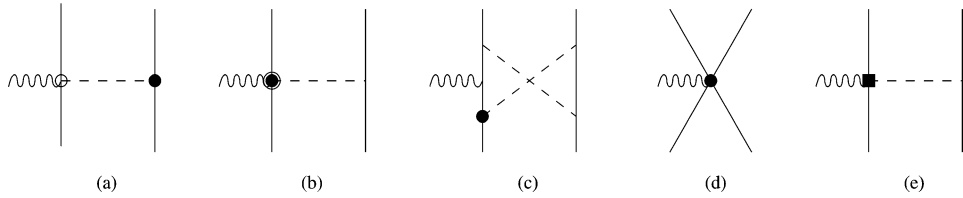

Fig. 13. Corrections to PV meson-exchange currents: OPE from minimal substitution in the sub-leading (a) PC and (b) PV πNN vertices, (c) TPE, (d) short-range contribution from minimal substitution in the PV contact interaction, and (e) OPE from new $\gamma \pi NN$ vertex. Not all ordering and topologies are displayed.

evaluate a large number of Feynman diagrams—a task which goes beyond the scope of the present study. Thus, we defer a derivation of these MEC operators to a future publication.

The foregoing set of MECs constitute a minimal, model-independent set required to ensure that Eq. (125) is satisfied. In addition, one may consider MECs that satisfy Eq. (125) independently from the terms in the potential. At $\mathcal{O}(Q)$, we find that there exists one such MEC that is not determined from V^{PV} by gauge invariance. This operator is obtained by OPE with an insertion of the operator from Eq. (110) (Fig. 13(e)), leading to the momentum space two-body current

$$\vec{J} = -i \left[\frac{\sqrt{2} g_{\pi NN} \bar{C}_\pi}{m_N \Lambda_\chi F_\pi} \right] \tau_1^+ \frac{\vec{\sigma}_2 \cdot \vec{q}_2 \, (\vec{q}_1 + \vec{q}_2) \times \vec{\sigma}_1}{\vec{q}_2^{\,2} + m_\pi^2} + (1 \leftrightarrow 2) \tag{126}$$

and to Eq. (13) in coordinate space.

6. Short-distance archeology: correspondence with DDH and beyond

In the ideal situation, a systematic EFT treatment would use experimental low energy measurements in order to determine the counter-terms λ_t, $\lambda_s^{0,1,2}$, ρ_t, $h_{\pi NN}^1$, $k_{\pi NN}^{1a}$, and $\bar{C}_\pi$ entirely from data. As emphasized earlier, there exists in principle a program of low-energy few-body measurements which will yield at least five linear combinations of these constants. Alternately, one would ultimately hope to gain a theoretical understanding of the values of these constants (and their linear combinations) probed by experiment. However, obtaining reliable theoretical predictions is complicated, since the PV NN interaction involves a non-trivial interplay of weak and non-perturbative strong interactions. Indeed, carrying out a first-principles calculation of the PV LECs is not yet possible, since lattice QCD techniques are not yet sufficiently advanced to address this problem. Consequently,

in order to say anything about the LECs beyond NDA estimates, theorists have of necessity relied on model approaches. In this section we illustrate how the PV LECs can in principle be estimated from details of the short-range dynamics.

Before proceeding further, it is useful to comment on the correspondence with, and difference from, the conventional DDH formalism in the treatment of short-distance PV physics.

(i) The EFT approach is systematic and model-independent. No assumption is made about the dynamics underlying the short-range interactions in the EFT, whereas the DDH formalism relies on a light pseudoscalar- and vector-meson-exchange picture as indicated in Fig. 1.

(ii) The LECs C_{1-5} have a straightforward correspondence with the DDH PV meson–nucleon couplings $h_\omega^{0,1}$, $h_\rho^{0,1,2}$. In the EFT framework, however, C_{1-5} could deviate strongly from the DDH values, as we illustrate below.

(iii) In terms of the DDH meson-exchange language we have the constraints

$$\frac{\tilde{C}_1^{\text{DDH}}}{C_1^{\text{DDH}}} = \frac{\tilde{C}_2^{\text{DDH}}}{C_2^{\text{DDH}}} = 1 + \chi_\omega, \tag{127}$$

$$\frac{\tilde{C}_3^{\text{DDH}}}{C_3^{\text{DDH}}} = \frac{\tilde{C}_4^{\text{DDH}}}{C_4^{\text{DDH}}} = \frac{\tilde{C}_5^{\text{DDH}}}{C_5^{\text{DDH}}} = 1 + \chi_\rho, \tag{128}$$

where $\chi_{\rho,\omega}$ denotes the ratio between tensor and vector couplings of ρ, ω meson–nucleon interaction. In our EFT approach, however, $\tilde{C}_{1-5}$ constitute five LECs whose values need not be related to C_{1-5} as in the DDH picture.

(iv) The DDH parameter $h_\rho'^1$ is generally discarded since its "best value" is tiny. In EFT, on the other hand, $h_\rho'^1$ contributes to C_6, but C_6 need not be small since it can receive a contribution, e.g., from a_0 meson exchange. Moreover, although the operator accompanying C_6 has the same spin–isospin structure as PV pion exchange, these interactions have different ranges and may in principle be distinguished as long as a sufficient range of energies is probed.

6.1. Resonance saturation

One popular model approach—which we adopt here for purely illustrative purposes—assumes that the short-distance dynamics is governed by the exchange of light meson resonances. This "resonance saturation" approach has some theoretical justification from the standpoint of the large-N_c expansion, where N_c denotes the number of colors in QCD [92]. It is also supported by several phenomenological studies. It is well known, for example, that in the $\mathcal{O}(Q^4)$ chiral Lagrangian describing pseudoscalar interactions, the low-energy constants are well described by the exchange of heavy mesons [93]. In particular, the charge radius of the pion receives roughly a 7% long-distance loop contribution, while the remaining 93% is saturated by t-channel exchange of the ρ^0. Similarly, in the baryon sector, dispersion-relation analyses of the isovector and isoscalar nucleon electromagnetic form factors indicate important contributions from the lightest vector mesons [94]. Finally, the primary features of the NN PC potential seem to be well described in such a picture [95].

Thus, it seems reasonable to assume that low-lying-meson exchange may play an important role in the short-distance physics associated with the PV LECs.

With these observations in mind, we invoke resonance saturation to arrive at illustrative estimates for the PV LECs. The relevant Feynman diagram is the same as in Fig. 1, where the exchanged bosons include all possible heavy mesons with appropriate quantum numbers. Here, parity violation enters through one of the meson–nucleon interaction vertices. While the DDH framework includes only the lowest-lying vector mesons to describe the short-distance PV NN interaction, we also consider the exchange of $a_0(980)$, $a_1(1260)$ and $f_1(1285)$, as well as the radial excitations of these systems. Of course, the PV LECs receive additional contributions from higher resonances, correlated meson exchange, *etc*. However, we limit our consideration to this set, as it already suffices to illustrate to what extent the short-distance PV NN interaction can differ from the predictions of the DDH model.

In order to estimate specific values of LECs in the framework of the meson-exchange model we require the corresponding PC and PV meson–nucleon Lagrangians:

Vector-meson exchange

The parity-conserving vector-meson–nucleon interaction Lagrangian reads

$$\mathcal{L}_{\rho NN}^{\text{PC}} = g_{\rho NN}\bar{N}\left[\gamma_\mu + \frac{\chi_\rho}{2m_N}i\sigma_{\mu\nu}q^\nu\right]\tau\cdot\rho^\mu N, \tag{129}$$

$$\mathcal{L}_{\omega NN}^{\text{PC}} = g_{\omega NN}\bar{N}\left[\gamma_\mu + \frac{\chi_\omega}{2m_N}i\sigma_{\mu\nu}q^\nu\right]\omega^\mu N, \tag{130}$$

$$\mathcal{L}_{\phi NN}^{\text{PC}} = g_{\phi NN}\bar{N}\left[\gamma_\mu + \frac{\chi_\phi}{2m_N}i\sigma_{\mu\nu}q^\nu\right]\phi^\mu N. \tag{131}$$

The parity-violating vector-meson–nucleon (VNN) interaction Lagrangian is given in Ref. [19]:

$$\mathcal{L}_{\rho NN}^{\text{PV}} = \bar{N}\gamma^\mu\gamma_5\left[h_\rho^0\tau\cdot\rho_\mu + h_\rho^1\rho_\mu^0 + \frac{h_\rho^2}{2\sqrt{6}}\left(3\tau_3\rho_\mu^0 - \tau\cdot\rho_\mu\right)\right]N$$
$$- \frac{h_\rho'^1}{2m_N}\bar{N}(\vec{\tau}\times\vec{\rho}_\mu)_3\sigma^{\mu\nu}q_\nu\gamma_5 N, \tag{132}$$

$$\mathcal{L}_{\omega NN}^{\text{PV}} = \bar{N}\gamma^\mu\gamma_5\omega_\mu\left[h_\omega^0 + h_\omega^1\tau_3\right]N, \tag{133}$$

$$\mathcal{L}_{\phi NN}^{\text{PV}} = \bar{N}\gamma^\mu\gamma_5\phi_\mu\left[h_\phi^0 + h_\phi^1\tau_3\right]N. \tag{134}$$

Note that we have adopted the convention for γ_5 following Ref. [96], which is *different* from that used in Ref. [19].

To our knowledge, the following contributions to the PV NN short-distance interaction have not been discussed elsewhere in the literature.

$a_0(980)$-meson exchange

$$\mathcal{L}_{a_0 NN}^{\text{PC}} = g_{a_0 NN}\bar{N}\tau\cdot a_0 N, \tag{135}$$

$$\mathcal{L}_{a_0 NN}^{\text{PV}} = h_{a_0}\bar{N}i\gamma_5(\vec{\tau}\times\vec{a}_0)_3 N. \tag{136}$$

a₁(1260)-meson exchange

$$\mathcal{L}^{\mathrm{PC}}_{a_1 NN} = g_{a_1 NN} \bar{N} \gamma_\mu \gamma_5 \tau \cdot a_1^\mu N. \tag{137}$$

Note that the structure $\bar{N} i \sigma_{\mu\nu} q^\nu (\vec{\tau} \cdot \vec{a}_1^\mu) \gamma_5 N$ is analogous to the weak-electricity form factor of nuclear beta decay; it is parity conserving but CP violating and hence is not included. The PV Lagrangian is

$$\mathcal{L}^{\mathrm{PV}}_{a_1 NN} = \bar{N} \gamma_\mu \left[h^0_{a_1} \tau \cdot a_1^\mu + h^1_{a_1} a_{10}^\mu + \frac{h^2_{a_1}}{2\sqrt{6}} \left(3\tau_3 a_{10}^\mu - \tau \cdot a_1^\mu \right) \right] N$$

$$+ \bar{N} \frac{i\sigma_{\mu\nu}q^\nu}{2m_N} \left[h^3_{a_1} \tau \cdot a_1^\mu + h^4_{a_1} a_{10}^\mu + \frac{h^5_{a_1}}{2\sqrt{6}} \left(3\tau_3 a_{10}^\mu - \tau \cdot a_1^\mu \right) \right] N, \tag{138}$$

where a_1^0 is the neutral component of a_1 meson.

f₁(1285)-meson exchange

$$\mathcal{L}^{\mathrm{PC}}_{f_1 NN} = g_{f_1 NN} \bar{N} \gamma_\mu \gamma_5 f_1^\mu N, \tag{139}$$

$$\mathcal{L}^{\mathrm{PV}}_{f_1 NN} = \bar{N} \gamma_\mu \left[h^0_{f_1} f_1^\mu + h^1_{f_1} f_1^\mu \tau^3 \right] N. \tag{140}$$

In principle, one may also include in such a model exchange of the radial excitations of $\rho, \omega, \phi, a_0, a_1, f_1$ mesons is also allowed.

6.2. LECs with DDH framework and beyond

With these couplings in hand, we can identify our predictions for the various low-energy constants.

If we consider only vector-meson exchange à la DDH, we have

$$\frac{\tilde{C}^{\mathrm{DDH}}_i}{C^{\mathrm{DDH}}_i} = 1 + \chi_\omega, \quad i = 1, 2, \qquad \frac{\tilde{C}^{\mathrm{DDH}}_i}{C^{\mathrm{DDH}}_i} = 1 + \chi_\rho, \quad i = 3\text{–}5,$$

$$C^{\mathrm{DDH}}_1 = -\Lambda_\omega h^0_\omega, \qquad C^{\mathrm{DDH}}_2 = -\Lambda_\omega h^1_\omega, \qquad C^{\mathrm{DDH}}_3 = -\Lambda_\rho h^0_\rho,$$

$$C^{\mathrm{DDH}}_4 = -\Lambda_\rho h^1_\rho, \qquad C^{\mathrm{DDH}}_5 = \frac{\Lambda_\rho}{2\sqrt{6}} h^2_\rho, \qquad C^{\mathrm{DDH}}_6 = -\Lambda_\rho g_{\rho NN} h'^1_\rho,$$

where we have defined

$$\Lambda_M = \frac{\Lambda^3_\chi}{2m_N m^3_M}. \tag{141}$$

However, within the context of resonance saturation, these LECs could also receive contributions from radial excitations of rho and omega mesons, and from a_0-, a_1-, f_1-meson exchange. Hence we have, more generally,

$$C_{1,2} = C^{\mathrm{DDH}}_{1,2} + C^{\mathrm{Radial}}_{1,2} + C^{f_1}_{1,2}, \qquad \tilde{C}_{1,2} = \tilde{C}^{\mathrm{DDH}}_{1,2} + \tilde{C}^{\mathrm{Radial}}_{1,2},$$

$$C_{3-5} = C^{\mathrm{DDH}}_{3-5} + C^{\mathrm{Radial}}_{3-5} + C^{a_1}_{3-5}, \qquad \tilde{C}_{3-5} = \tilde{C}^{\mathrm{DDH}}_{3-5} + \tilde{C}^{\mathrm{Radial}}_{3-5} + \tilde{C}^{a_1}_{3-5},$$

$$C_6 = C^{\mathrm{DDH}}_6 + C^{\mathrm{Radial}}_6 + C^{a_0}_6, \tag{142}$$

where

$$
\begin{aligned}
C_1^{f_1} &= -\Lambda_{f_1} g_{f_1 NN} h_{f_1}^0, & C_2^{f_1} &= -\Lambda_{f_1} g_{f_1 NN} h_{f_1}^1, \\
C_3^{a_1} &= -\Lambda_{a_1} g_{a_1 NN} h_{a_1}^0, & \tilde{C}_3^{a_1} &= -\Lambda_{a_1} g_{a_1 NN} \left(h_{a_1}^0 + h_{a_1}^3 \right), \\
C_4^{a_1} &= -\Lambda_{a_1} g_{a_1 NN} h_{a_1}^1, & \tilde{C}_4^{a_1} &= -\Lambda_{a_1} g_{a_1 NN} \left(h_{a_1}^1 + h_{a_1}^4 \right), \\
C_5^{a_1} &= \frac{\Lambda_{a_1}}{2\sqrt{6}} g_{a_1 NN} h_{a_1}^2, & \tilde{C}_5^{a_1} &= -\frac{\Lambda_{a_1}}{2\sqrt{6}} g_{a_1 NN} \left(h_{a_1}^2 + h_{a_1}^5 \right), \\
C_6^{a_0} &= -\Lambda_{a_0} h_{a_0}.
\end{aligned}
\tag{143}
$$

Similar relations will hold for the radial excitations.

6.3. Estimates for C_{1-6}, $\tilde{C}_{1-5}$

As noted above, arriving at reliable theoretical predictions for the PV LECs, even within the context of a model framework, is a formidable task, and one which certainly goes beyond the scope of the present work. Nevertheless, it is useful to have in hand educated guesses for their magnitudes and signs, if for no other reason than to provide benchmarks for comparison with experiment. To that end, we quote below both expectations based on naive dimensional analysis and values obtained from correspondence with the DDH model. Future work could include, for example, computing the weak couplings entering Eq. (143), thereby providing model estimates for the departures of the C_i and $\tilde{C}_i$ from their NDA or DDH values.

There exist various values for the parity-conserving couplings $g_{\rho NN}$, χ_ρ, $g_{\omega NN}$, and χ_ω quoted in the literature [97–99]. Fortunately, the combination $g_{\rho NN}(1 + \chi_\rho)$ takes roughly the same value in different approaches: $g_{\rho NN}(1 + \chi_\rho) \approx 21$. Likewise various approaches consistently yield a very small value for χ_ω. It is thus reasonable to use the values $\chi_\rho = 6$, $g_{\rho NN} = 3$ or $\chi_\rho = 3.7$, $g_{\rho NN} = 4.5$. A word of caution is in order here. The proper accounting of chiral symmetry in multi-pion contributions might affect the extractions of strong couplings. For example, the effect of ω exchange in NN scattering is significantly reduced when correct TPE is considered [91]. As we emphasized earlier, the estimates here should be considered to yield only an educated guess for the order of magnitude of the LECs. The theoretical uncertainty from this exchange model is much larger than the choice of χ_ρ and $g_{\rho NN}$. Here, we simply use $\chi_\rho = 3.7$, $g_{\rho NN} = 4.5$, $\chi_\omega = -0.12$, and $g_{\omega NN} = 14$ to make our best guess. Results are given in Table 2 and should be used with due caution.

7. Conclusions

In summary, we have performed a systematic study of the parity-nonconserving nucleon–nucleon potential, and have suggested ways by which the present confused experimental situation can be resolved. We have proposed breaking this program into two separate pieces:

Table 2
Estimates of ranges and best values for PV coupling constants C_{1-6}, $\tilde{C}_{1-5}$ (in units of $g_\pi = 3.8 \times 10^{-8}$)

LECs	Naive dimensional analysis	Best values	Range
C_1	± 158	32	$-95 \to 172$
$\tilde{C}_1$	± 158	28	$-84 \to 151$
C_2	± 158	17	$13 \to 32$
$\tilde{C}_2$	± 158	15	$11 \to 28$
C_3	± 158	63	$-63 \to 171$
$\tilde{C}_3$	± 158	296	$-296 \to 803$
C_4	± 158	95	$-289 \to 520$
$\tilde{C}_4$	± 158	1	$0 \to 1$
C_5	± 158	-11	$-13 \to -8$
$\tilde{C}_5$	± 158	-51	$-61 \to -28$
C_6	± 158	–	–

(i) Since the low-energy parity-violating potential involves five S–P wave mixing amplitudes, we have constructed a simple local effective potential in order to reliably extract such quantities from experiments involving only the NN, Nd, or $N\alpha$ systems. We have also suggested the critical experiments that are needed in order to successfully complete this task and have given explicit formulas which will express the mixing amplitudes in terms of experimental observables. We have also suggested a two-phase experimental program, where phase one would include six (or possibly seven) measurements needed to test the consistency of the pionless EFT and phase two would involve additional measurements needed to determine the pion-related parameters if necessitated by the results of phase one.

(ii) A second important facet of this program is to confront the extracted phenomenological potential with theoretical expectations. For this task, we have systematically constructed a parity-violating nucleon–nucleon potential $V^{\text{PV}}(\vec{r})$ within the framework of effective field theory using the Weinberg counting scheme up to the order $\mathcal{O}(Q)$. The correspondence with, and difference from, the conventional DDH potential were discussed.

In order for this scheme to come to fruition additional work is required on several fronts. Experimentally it is critical to complete the key experiments, resulting in a confirmed and reliable set of low-energy phenomenological parameters. Once these parameters are known, it is important to use them in order to analyze the heavier nuclear systems and resolve the various existing conflicts. Doing so could have important implications for the applicability of EFT to other electroweak processes in heavy nuclei, such as neutrinoless double β-decay [81]. Future work is also needed to understand the relation between the underlying effective weak potential $V^{\text{PV}}(\vec{r})$ and the effective phenomenological parameters ρ_t, λ_t, λ_s^i and should involve the best available nuclear wave functions. What should result from this program is the resolution of the presently confusing experimental situation and a reliable form for the parity-violating nuclear potential, which we hope will set the standard for future work in this field.

Acknowledgements

Appendix A. The PV NN contact Lagrangian

Since we employ the heavy-fermion formalism, one can build the most general PV operators by using heavy-baryon fields directly. This approach, however, yields redundant operators, which then have to be eliminated by imposing reparameterization invariance. Alternatively, we can obtain the relevant operators starting from the relativistic theory, then performing a non-relativistic expansion. We use ψ_N, $\bar{\psi}_N$ for the relativistic nucleon field and N, $N^{\dagger}$ to denote the nucleon field after non-relativistic reduction. In general, there exist twelve possible PV and CP conserving NN-interaction terms up to one derivative, which we write as

$$\mathcal{O}_1 = \frac{g_1}{\Lambda_\chi^2} \bar{\psi}_N 1 \gamma_\mu \psi_N \bar{\psi}_N 1 \gamma^\mu \gamma_5 \psi_N, \qquad \tilde{\mathcal{O}}_1 = \frac{\tilde{g}_1}{\Lambda_\chi^3} \bar{\psi}_N 1 i \sigma_{\mu\nu} q^\nu \psi_N \bar{\psi}_N 1 \gamma^\mu \gamma_5 \psi_N,$$

$$\mathcal{O}_2 = \frac{g_2}{\Lambda_\chi^2} \bar{\psi}_N 1 \gamma_\mu \psi_N \bar{\psi}_N \tau_3 \gamma_\mu \gamma_5 \psi_N, \qquad \tilde{\mathcal{O}}_2 = \frac{\tilde{g}_2}{\Lambda_\chi^3} \bar{\psi}_N 1 i \sigma_{\mu\nu} q^\nu \psi_N \bar{\psi}_N \tau_3 \gamma_\mu \gamma_5 \psi_N,$$

$$\mathcal{O}_3 = \frac{g_3}{\Lambda_\chi^2} \bar{\psi}_N \tau^a \gamma_\mu \psi_N \bar{\psi}_N \tau^a \gamma_\mu \gamma_5 \psi_N, \qquad \tilde{\mathcal{O}}_3 = \frac{\tilde{g}_3}{\Lambda_\chi^3} \bar{\psi}_N \tau^a i \sigma_{\mu\nu} q^\nu \psi_N \bar{\psi}_N \tau^a \gamma_\mu \gamma_5 \psi_N,$$

$$\mathcal{O}_4 = \frac{g_4}{\Lambda_\chi^2} \bar{\psi}_N \tau_3 \gamma_\mu \psi_N \bar{\psi}_N 1 \gamma_\mu \gamma_5 \psi_N, \qquad \tilde{\mathcal{O}}_4 = \frac{\tilde{g}_4}{\Lambda_\chi^3} \bar{\psi}_N \tau_3 i \sigma_{\mu\nu} q^\nu \psi_N \bar{\psi}_N 1 \gamma_\mu \gamma_5 \psi_N,$$

$$\mathcal{O}_5 = \frac{g_5}{\Lambda_\chi^2} \mathcal{I}^{ab} \bar{\psi}_N \tau_a \gamma_\mu \psi_N \bar{\psi}_N \tau_b \gamma_\mu \gamma_5 \psi_N,$$

$$\tilde{\mathcal{O}}_5 = \frac{\tilde{g}_5}{\Lambda_\chi^3} \mathcal{I}^{ab} \bar{\psi}_N \tau_a i \sigma_{\mu\nu} q^\nu \psi_N \bar{\psi}_N \tau_b \gamma_\mu \gamma_5 \psi_N,$$

$$\mathcal{O}_6 = \frac{g_6}{\Lambda_\chi^2} \epsilon^{ab3} \bar{\psi}_N \tau_a \psi_N \bar{\psi}_N \tau_b i \gamma_5 \psi_N,$$

$$\tilde{\mathcal{O}}_6 = \frac{\tilde{g}_6}{\Lambda_\chi^3} \epsilon^{ab3} \bar{\psi}_N \tau_a \gamma_\mu \psi_N \bar{\psi}_N \tau_b i \sigma_{\mu\nu} q^\nu \gamma_5 \psi_N, \tag{A.1}$$

where $\mathcal{I}^{ab}$ is defined in Eq. (6). In writing down these PV operators, we have assumed that all the isospin violation arises from the weak interaction, thus neglecting isospin violation from up and down quark mass difference and electromagnetic interactions, since corrections from such effects are typically around a few percent and negligible for our purposes. The isospin content of the above terms is transparent: the $1 \cdot 1$, $\tau \cdot \tau$ terms conserve isospin, the piece with $\mathcal{I}^{ab}$ carries $\Delta I = 2$, and all remaining pieces change isospin by one unit.

In order to understand the constraints that relativity imposes, we consider a simple example—the expansion of $\mathcal{O}_1$ and $\tilde{\mathcal{O}}_1$. Up to $\mathcal{O}(Q)$ we have

$$\mathcal{O}_1 = \frac{g_1}{\Lambda_\chi^2} \frac{1}{2m_N} \left[-N^\dagger 1 N N^\dagger 1 \vec{\sigma} \cdot i \vec{D}_- N + N^\dagger 1 i D^i_- N N^\dagger 1 \sigma^i N \right.$$
$$\left. - i \epsilon^{ijk} N^\dagger 1 i D^i_+ \sigma_j N N^\dagger 1 \sigma^k N \right],$$
$$\tilde{\mathcal{O}}_1 = -\frac{\tilde{g}_1}{\Lambda_\chi^3} i \epsilon^{ijk} N^\dagger 1 i D^i_+ \sigma_j N N^\dagger 1 \sigma^k N. \tag{A.2}$$

Note that the *two* relativistic structures $\mathcal{O}_1$ and $\tilde{\mathcal{O}}_1$ together yield *three* distinct non-relativistic spacetime forms. However, only two linear combinations of these forms are independent according to the strictures of relativity. On the other hand, if we had started from the non-relativistic theory and tried to write the most general effective Lagrangian, we would have naively identified each of these three structures as being independent and would have mistakenly postulated three, rather than two, LECs. The requirements imposed on the independence of various non-relativistic operators which follow from consistency with the relativistic theory is known as reparameterization invariance. Physically, this invariance amounts to stating that the non-relativistic theory should not contain more physics (e.g., LECs) than the relativistic one. Analogous situations occur in heavy-quark EFT and in the non-relativistic expansion of the nucleon kinetic operator in heavy-nucleon EFT.

Similar results follow for the operators $\mathcal{O}_{2-5}$ and $\tilde{\mathcal{O}}_{2-5}$ in that each set $\{\mathcal{O}_i, \tilde{\mathcal{O}}_i\}$ generates two *independent* combinations of non-relativistic operators and, thus, two independent LECs. On the other hand, after non-relativistic reduction, $\mathcal{O}_6$ and $\tilde{\mathcal{O}}_6$ yield exactly the *same* form up to $\mathcal{O}(Q)$. Hence, these structures yield only *one* independent LEC in the non-relativistic theory even though there are two different LECs in the original, relativistic theory. The new LEC is a linear combination of g_6 and $\tilde{g}_6$.

The full PV contact heavy-nucleon Lagrangian at $\mathcal{O}(Q)$ in the NN sector can then be written in the form given in Eq. (71), where the LECs C_i are related to the relativistic couplings g_i via

$$C_{1-5} = \frac{\Lambda_\chi}{2m_N} g_{1-5}, \tag{A.3}$$

$$\tilde{C}_{1-5} = \tilde{g}_{1-5} + \frac{\Lambda_\chi}{2m_N} g_{1-5}, \tag{A.4}$$

$$C_6 = \tilde{g}_6 - \frac{\Lambda_\chi}{2m_N} g_6. \tag{A.5}$$

We thus have a total of ten PV LECs describing PV short-distance NN physics. For the purpose of characterizing PV operators in the NN system through $\mathcal{O}(Q)$, these ten constants are sufficient.

Appendix B. Corrections to $V_{-1,\mathrm{LR}}^{\mathrm{PV}}$

There are subleading corrections to OPE that arise from Fig. 4, where the strong vertex comes from subleading PC operators in Eqs. (102), (103). In fact, when the $\nu = 1$ operators from Eq. (102) are inserted in Fig. 4, the resulting PV potential is naively of $\mathcal{O}(Q^0)$. However, with

$$v \cdot q = q_0 = \frac{\vec{p}_{1i}^2 - \vec{p}_{1f}^2}{2m_N} \sim \mathcal{O}(Q^2/m_N), \tag{B.1}$$

with i (f) denoting the initial (final) nucleon, we have

$$V_{1a,\mathrm{LR}}^{\mathrm{PV}} = i \frac{g_A h_{\pi NN}^1}{4\sqrt{2} m_N^2 F_\pi} \left(\frac{\tau_1 \times \tau_2}{2} \right)_3 \frac{(\vec{p}_{1i}^2 - \vec{p}_{1f}^2)\vec{\sigma}_1 \cdot (\vec{p}_{1f} + \vec{p}_{1i}) - (1 \leftrightarrow 2)}{\vec{q}^2 + m_\pi^2}, \tag{B.2}$$

where $q = p_{2f} - p_{2i} = p_{1i} - p_{1f}$. Thus, this contribution enters at $\mathcal{O}(Q)$ and must be included for consistency.

Similarly, the second and third operators from Eq. (103) are nominally $\nu = 2$ but lead to corrections that are $\mathcal{O}(Q^3)$, since they contain two kinetic operators from $v \cdot D$ or $v \cdot A$. However, the insertion of the first, fourth and fifth $\nu = 2$ operators from Eq. (103) in Fig. 4 lead to contributions at $\mathcal{O}(Q)$. We list these terms below. The contribution from the first operator in Eq. (103) reads

$$V_{1b,\mathrm{LR}}^{\mathrm{PV}} = \frac{\vec{q}^2}{8m_N^2} V_{-1,\mathrm{LR}}^{\mathrm{PV}}. \tag{B.3}$$

The contribution from the fourth operator in Eq. (103) is

$$V_{1c,\mathrm{LR}}^{\mathrm{PV}} = -i \frac{g_A h_{\pi NN}^1}{8\sqrt{2} m_N^2 F_\pi} \left(\frac{\tau_1 \times \tau_2}{2} \right)_3 \frac{(\vec{p}_{1i}^2 + \vec{p}_{1f}^2)\vec{\sigma}_1 \cdot \vec{q} + (1 \leftrightarrow 2)}{\vec{q}^2 + m_\pi^2}. \tag{B.4}$$

Finally, the contribution from the fifth operator in Eq. (103) reads

$$V_{1d,\mathrm{LR}}^{\mathrm{PV}} = i \frac{g_A h_{\pi NN}^1}{4\sqrt{2} m_N^2 F_\pi} \left(\frac{\tau_1 \times \tau_2}{2} \right)_3$$
$$\times \frac{(\vec{\sigma}_1 \cdot \vec{p}_{1f})(\vec{q} \cdot \vec{p}_{1i}) + (\vec{\sigma}_1 \cdot \vec{p}_{1i})(\vec{q} \cdot \vec{p}_{1f}) + (1 \leftrightarrow 2)}{\vec{q}^2 + m_\pi^2}. \tag{B.5}$$

Now consider the operators associated with $\hat{d}_{16-19}$. In the isospin-symmetric limit, to leading order in the chiral expansion we have

$$S \cdot A \langle \chi_+ \rangle \sim \frac{m_\pi^2}{F_\pi^2} S \cdot A, \qquad \langle S \cdot A \chi_+ \rangle \sim 0,$$

$$[S \cdot \mathcal{D}, \chi_-] \sim \frac{m_\pi^2}{F_\pi^2} S \cdot A, \qquad \left[S \cdot \mathcal{D}, \langle \chi_- \rangle \right] \sim \frac{m_\pi^2}{F_\pi^2} S \cdot A. \tag{B.6}$$

As a consequence, the LECs $\hat{d}_{16,18,19}$ simply renormalize the bare πNN coupling constant g_A^0 at order $\mathcal{O}(Q^2)$ while LEC $\hat{d}_{17}$ does not contribute. Up to the truncation order $\mathcal{O}(Q)$ the corrections from these LECs to PV NN potential are automatically taken into account as long as we use the renormalized (or physical) g_A in Eq. (118).

Another possible source of corrections to the long-range PV potential is the insertion of subleading PV operators in Fig. 3. As pointed out in the Section 5, the PV vector operator does not contribute due to vector-current conservation. The axial-vector operator involves two pions and leads to loop corrections at $\mathcal{O}(Q^2)$. The contribution from the remaining PV operator proportional to $k_{\pi NN}^{1a}$ has been discussed extensively in the main body of the paper.

Many chiral loops exist at this order, from self-energy and PC- and PV-vertex corrections. The chiral loops do yield contributions $\mathcal{O}(Q)$. However, these effects are included in the renormalization of g_A [82] and of $h_{\pi NN}^1$ [32].

Appendix C. Loop corrections to $V_{1,\mathrm{SR}}^{\mathrm{PV}}$

The contact PV interactions in Fig. 6 appear at $\mathcal{O}(Q)$. From a simple counting of the chiral order of vertices , propagators, and loops, it is clear that loop corrections to these PV LECs, shown in Fig. 14, first appear at $\mathcal{O}(Q^3)$, which is beyond our truncation order.

Potentially more important are the loop corrections to the contact PC interactions, where one vertex is the PV Yukawa coupling of the pion to the nucleon. The relevant Feynman diagrams are shown in Fig. 7.

Take the $C_S NN$ contact interaction as an example. For diagram (a-1), the amplitude is nominally $\mathcal{O}(Q)$, and reads

$$
\begin{aligned}
i M_{a1} &\sim h_{\pi NN}^1 \frac{C_S}{2} \frac{\sqrt{2} g_A}{F_\pi} \int \frac{d^D k}{(2\pi)^D} \frac{i(S_1 \cdot k)}{v_1 \cdot (p_1' + k) + i\epsilon} \frac{i}{v_1 \cdot (p_1 + k) + i\epsilon} \frac{i}{k^2 - m_\pi^2 + i\epsilon} \\
&= -h_{\pi NN}^1 C_S \frac{\sqrt{2} g_A}{F_\pi} S_1^\mu \int_0^\infty s\, ds \int_0^1 du \int \frac{d^D k}{(2\pi)^D} \\
&\quad \times \frac{k_\mu}{[k^2 + s v_1 \cdot k + s(1-u) v_1 \cdot p_1' + u s v_1 \cdot p_1 + m_\pi^2]^3},
\end{aligned}
\tag{C.1}
$$

where s has the dimensions of mass, and where we have Wick-rotated to Euclidean momenta in the second line. From this form it is clear that $i M_{a1} \propto S_1 \cdot v_1 = 0$. The same argument holds for diagrams (a-2)–(a-4).

For diagram (b-1), the amplitude reads

$$
i M_{b1} \sim h_\pi^1 \frac{C_S}{2} \frac{\sqrt{2} g_A}{F_\pi} \int \frac{d^D k}{(2\pi)^D} \frac{i(S_2 \cdot k)}{v_2 \cdot (p_2 + k) + i\epsilon} \frac{i}{v_1 \cdot (p_1' + k) + i\epsilon} \frac{i}{k^2 - m_\pi^2 + i\epsilon}
$$

$$= -h_\pi^1 C_S \frac{\sqrt{2}g_A}{F_\pi} S_2^\mu \int\limits_0^\infty s\,ds \int\limits_0^1 du \int \frac{d^D k}{(2\pi)^D}$$

$$\times \frac{k_\mu}{[k^2 + sv_1 \cdot k + s(1-u)v \cdot p_2 + usv \cdot p_1' + m_\pi^2]^3} = 0, \tag{C.2}$$

where we have used the fact that $v_1 = v_2 = v = (1, \vec{0})$ for low-energy NN interaction. Similarly, (b-2)–(b-4) vanish at $\mathcal{O}(Q)$.

There remains a third class of diagrams, (c-1)–(c-4). These are 2PR diagrams and their amplitudes do not vanish at $\mathcal{O}(Q)$. For example, the amplitude corresponding to diagram (c-1) reads

$$iM_{c1} \sim h_\pi^1 \frac{C_S}{2} \frac{\sqrt{2}g_A}{F_\pi} \int \frac{d^D k}{(2\pi)^D} \frac{i(S_2 \cdot k)}{v_2 \cdot (p_2' - k) + i\epsilon} \frac{i}{v_1 \cdot (p_1' + k) + i\epsilon} \frac{i}{k^2 - m_\pi^2 + i\epsilon}.$$

However, only the 2PI part of these diagrams should be included. In other words, the contribution from the two-nucleon intermediate state should be subtracted from the amplitude. This can be done in old-fashioned time-ordered perturbation theory. Alternatively, we may use the following identity to accomplish the subtraction easily:

$$\frac{i}{-v \cdot k + i\epsilon} = -\frac{i}{v \cdot k + i\epsilon} + 2\pi\delta(v \cdot k). \tag{C.3}$$

The second term corresponds to the two-nucleon pole, while the first term is free of the infrared enhancement discussed earlier. After subtracting the two-nucleon-pole contribution, the modified amplitude for diagram (c-1) becomes

$$i\tilde{M}_{c1} \sim -h_\pi^1 \frac{C_S}{2} \frac{\sqrt{2}g_A}{F_\pi} \int \frac{d^D k}{(2\pi)^D} \frac{i(S_2 \cdot k)}{v_2 \cdot (k - p_2') + i\epsilon} \frac{i}{v_1 \cdot (p_1' + k) + i\epsilon} \frac{i}{k^2 - m_\pi^2 + i\epsilon}$$

$$= 0.$$

Similarly, the 2PI parts of diagrams (c-2)–(c-4) vanish. We see that diagrams (c-1)–(c-4) can be generated from the PC $\mathcal{O}(Q^0)$ $C_{S,T}$ contact potential and leading-order PV OPE potential by iteration in the LS equation.
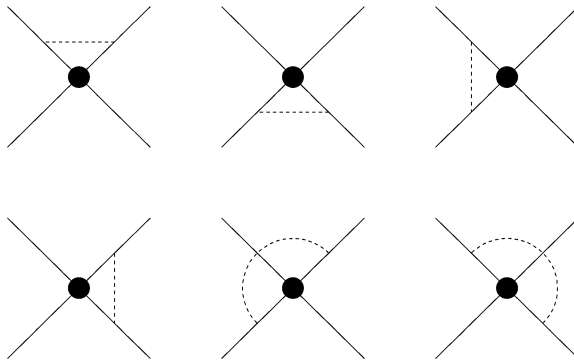

Fig. 14. Possible chiral corrections to PV NN contact interactions.

In summary, the chiral-loop corrections to the PV short-range potential occur at $\mathcal{O}(Q^2)$ or higher.

Appendix D. Derivation of $V_{1,\text{MR}}^{\text{PV}}$

Of course, a consistent calculation in EFT must include all loop diagrams present to a given order. In this appendix we give some details of the evaluation of the diagrams in Figs. 8, 9, 10. We use dimensional regularization for simplicity.

Let us consider first the triangle diagrams in Fig. 8.

Flavor-conserving case

In this case the initial and final state on each nucleon line are the same, i.e., a proton remains a proton and a neutron remains a neutron. Diagrams (c) and (d) are mirror diagrams of (a) and (b) in Fig. 8. We focus on (a) and (b). The sum of their amplitudes reads

$$
\begin{aligned}
i M_{(a)+(b)} &= -\frac{\sqrt{2}g_A h_\pi^1}{4F_\pi^3} \int \frac{d^D k}{(2\pi)^D} \frac{\bar{N}_1 \tau_3^1 v_1 \cdot (2k-q) N_1 \bar{N}_2 1 S_2 \cdot (2k-q) N_2}{v \cdot (p_2+k)(k^2-m_\pi^2)[(k-q)^2-m_\pi^2]} \\
&= -\frac{\sqrt{2}g_A h_\pi^1}{4F_\pi^3} \left\{ 16 \int_0^1 dx \int_0^\infty dy \int \frac{d^D k}{(2\pi)^D} \right. \\
&\quad \times \frac{(v_1 \cdot k)(S_2 \cdot k)}{[k^2-y^2-m_\pi^2-x(1-x)\vec{q}^2]^3} \\
&\quad + 8(S_2 \cdot q) \int_0^\infty y \, dy \int_0^1 dx(1-2x) \int \frac{d^D k}{(2\pi)^D} \\
&\quad \left. \times \frac{1}{[k^2-y^2-m_\pi^2-x(1-x)\vec{q}^2]^3} \right\} = 0.
\end{aligned}
\tag{D.1}
$$

After momentum integration the first term contains a factor $v_1 \cdot S_2 = 0$. The second term vanishes due to the x integration, since the integrand is a total derivative.

Flavor-changing case: $n \leftrightarrow p$

In this case the sum of the amplitude for diagram (a) and (b) reads

$$
\begin{aligned}
i M_{(a)+(b)} &= \frac{\sqrt{2}g_A h_\pi^1}{4F_\pi^3} \int \frac{d^D k}{(2\pi)^D} \frac{(\bar{p}v_1 \cdot (2k-q)n)(\bar{n}S_2 \cdot qp)}{v \cdot (p_2+k)(k^2-m_\pi^2)[(k-q)^2-m_\pi^2]} \\
&= -i\frac{\sqrt{2}g_A h_\pi^1}{\Lambda_\chi^2 F_\pi} L(q)(\bar{p}n)(\bar{n}S_2 \cdot qp),
\end{aligned}
\tag{D.2}
$$

where the function $L(q)$ is defined as in Eq. (122). The sum of the amplitude for diagram (c) and (d) is, likewise,

$$
i M_{(c)+(d)} = i\frac{\sqrt{2}g_A h_\pi^1}{\Lambda_\chi^2 F_\pi} L(q)(\bar{n}p)(\bar{p}S_2 \cdot qn).
\tag{D.3}
$$

Note that $S_2 \cdot q \approx -\frac{1}{2}\vec{\sigma}_2 \cdot \vec{q}$.

Summing the four diagrams and converting to momentum-space operators we get

$$\frac{L(q)}{2\sqrt{2}} \frac{g_A h_\pi^1}{\Lambda_\chi^2 F_\pi} \epsilon^{ab3} (N^\dagger \tau^a N)(N^\dagger \tau^b \vec{\sigma} \cdot \vec{q} N). \tag{D.4}$$

Clearly the sum of triangle diagrams has the same Lorentz, isospin structure as the C_6 contact term.

Consider now the crossed-box diagrams in Fig. 9.

Flavor-conserving case: $pp \to pp$, $nn \to nn$

In Fig. 9, contributions from diagrams (c) and (d) are equal to (a) and (b). For $pp \to pp$ the sum of (a) and (b) leads to

$$i4\sqrt{2}L(q) \frac{g_A^3 h_\pi^1}{\Lambda_\chi^2 F_\pi} (p^\dagger [S_1 \cdot q, S_1^\mu] p)(p^\dagger S_\mu^2 p). \tag{D.5}$$

Note that, for $pp \to pp$, initial particles are identical. The operator form will generate both (a), (b) and their mirror diagrams simultaneously.

For the $nn \to nn$ channel, there is an extra minus sign from PV Yukawa vertex.

$$\sqrt{2}L(q) \frac{g_A^3 h_\pi^1}{\Lambda_\chi^2 F_\pi} \epsilon^{ijk} (n^\dagger q^i \sigma^j n)(n^\dagger \sigma^k n). \tag{D.6}$$

Combining both $pp \to pp$ and $nn \to nn$ channels, we get

$$-\frac{L(q)}{\sqrt{2}} \frac{g_A^3 h_\pi^1}{\Lambda_\chi^2 F_\pi} \epsilon^{ijk} (N^\dagger \tau_3 q^i \sigma^j N)(N^\dagger \sigma^k N),$$

$$-\frac{L(q)}{\sqrt{2}} \frac{g_A^3 h_\pi^1}{\Lambda_\chi^2 F_\pi} \epsilon^{ijk} (N^\dagger q^i \sigma^j N)(N^\dagger \tau_3 \sigma^k N). \tag{D.7}$$

Flavor changing case: $n \to p$, $p \to n$

The sum of diagrams (a)–(d) leads to

$$+\frac{3\sqrt{2}}{16} [-3L(q) + H(q)] \frac{g_A^3 h_\pi^1}{\Lambda_\chi^2 F_\pi} \epsilon^{ab3} (N^\dagger \tau^a N)(N^\dagger \tau^b \vec{\sigma} \cdot \vec{q} N), \tag{D.8}$$

where $H(q)$ is defined as in Eq. (122).

Finally, we discuss the box diagrams. As in Appendix C, we have to subtract the contribution from the two-nucleon intermediate state. The corresponding time-ordered diagrams are shown in Fig. 10. After the subtraction the 2PR part, we find:

Flavor-conserving case: $p \to p$ and $n \to n$

For $np \to np$ the sum of all diagrams leads to

$$i4\sqrt{2}L(q) \frac{g_A^3 h_\pi^1}{\Lambda_\chi^2 F_\pi} (n^\dagger [S_1 \cdot q, S_1^\mu] n)(p^\dagger S_\mu^2 p). \tag{D.9}$$

Note that, for $pn \rightarrow pn$, there is an extra minus sign from the PV Yukawa vertex,

$$-i4\sqrt{2}L(q)\frac{g_A^3 h_\pi^1}{\Lambda_\chi^2 F_\pi}\big(p^\dagger[S_1 \cdot q, S_1^\mu]p\big)\big(n^\dagger S_\mu^2 n\big).$$ (D.10)

Combining both channels, we get

$$\frac{L(q)}{\sqrt{2}}\frac{g_A^3 h_\pi^1}{\Lambda_\chi^2 F_\pi}\epsilon^{ijk}\big(N^\dagger\tau_3 q^i\sigma^j N\big)\big(N^\dagger\sigma^k N\big),$$

$$-\frac{L(q)}{\sqrt{2}}\frac{g_A^3 h_\pi^1}{\Lambda_\chi^2 F_\pi}\epsilon^{ijk}\big(N^\dagger q^i\sigma^j N\big)\big(N^\dagger\tau_3\sigma^k N\big).$$ (D.11)

Flavor-changing case: $n \leftrightarrow p$

The sum of all diagrams leads to the same result as in the crossed-box case,

$$\frac{3\sqrt{2}}{16}\big[-3L(q)+H(q)\big]\frac{g_A^3 h_\pi^1}{\Lambda_\chi^2 F_\pi}\epsilon^{ab3}\big(N^\dagger\tau^a N\big)\big(N^\dagger\tau^b\vec{\sigma}\cdot\vec{q}N\big).$$ (D.12)

In summary, the sum of one-loop, TPE diagrams is

$$\frac{L(q)}{2\sqrt{2}}\frac{g_A h_\pi^1}{\Lambda_\chi^2 F_\pi}\epsilon^{ab3}\big(N^\dagger\tau^a N\big)\big(N^\dagger\tau^b\vec{\sigma}\cdot\vec{q}N\big)$$

$$+\frac{3\sqrt{2}}{8}\big[-3L(q)+H(q)\big]\frac{g_A^3 h_\pi^1}{\Lambda_\chi^2 F_\pi}\epsilon^{ab3}\big(N^\dagger\tau^a N\big)\big(N^\dagger\tau^b\vec{\sigma}\cdot\vec{q}N\big)$$

$$-\sqrt{2}L(q)\frac{g_A^3 h_\pi^1}{\Lambda_\chi^2 F_\pi}\epsilon^{ijk}\big(N^\dagger q^i\sigma^j N\big)\big(N^\dagger\tau_3\sigma^k N\big),$$ (D.13)

which leads to the medium-range potential (120).

Appendix E. Illustrative estimates

Having a form of the weak parity-violating potential $V^{\mathrm{PV}}(r)$ it is, of course, essential to complete the process by connecting with the S-matrix—i.e., expressing the phenomenological parameters λ_i, ρ_t defined in Eq. (36) in terms of the fundamental ones—C_i, $\tilde{C}_i$ defined in Eq. (37). This is a major undertaking and should involve the latest and best NN wave functions such as Argonne V18. The work is underway, but it will be some time until this process is completed [101]. Even after this connection has been completed, the results will be numerical in form. However, it is very useful to have an analytic form by which to understand the basic physics of this transformation and by which to make simple numerical estimates. For this purpose we shall employ simple phenomenological NN wave functions, as described below.

Examination of the scattering matrix Eq. (31) reveals that the parameters $\lambda_{s,t}$ are associated with the short-distance component while ρ_t contains contributions from the both (long-distance) pion exchange as well as short distance effects. In the former case, since the

interaction is short ranged we can use this feature in order to simplify the analysis. Thus, we can determine the shift in the deuteron wavefunction associated with parity violation by demanding orthogonality with the $^3S_1$ scattering state, which yields, using the simple asymptotic form of the bound state wavefunction [102,103]

$$\psi_d(r) = \left[1 + \rho_t(\vec{\sigma}_p + \vec{\sigma}_n) \cdot (-i\vec{\nabla}) + \lambda_t(\vec{\sigma}_p - \vec{\sigma}_n) \cdot (-i\vec{\nabla})\right]\sqrt{\frac{\gamma}{2\pi}}\frac{1}{r}e^{-\gamma r}, \qquad (E.1)$$

where $\gamma^2/M = 2.23$ MeV is the deuteron binding energy. Now the shift generated by $V^{PV}(r)$ is found to be [102,103]

$$\begin{aligned}
\delta\psi_d(\vec{r}) &\simeq \int d^3r' \, G(\vec{r}, \vec{r}')V^{PV}(\vec{r}')\psi_d(r') \\
&= -\frac{M}{4\pi}\int d^3r' \, \frac{e^{-\gamma|\vec{r}-\vec{r}'|}}{|\vec{r}-\vec{r}'|}V^{PV}(\vec{r}')\psi_d(r') \\
&\simeq \frac{M}{4\pi}\vec{\nabla}\left(\frac{e^{-\gamma r}}{r}\right)\cdot\int d^3r' \, \vec{r}' V^{PV}(\vec{r}')\psi_d(r'),
\end{aligned} \qquad (E.2)$$

where the last step is permitted by the short range of $V^{PV}(\vec{r}')$. Comparing Eqs. (E.2) and (E.1) yields then the identification

$$\sqrt{\frac{\gamma}{2\pi}}\lambda_t\chi_t \equiv i\frac{M}{16\pi}\xi_0^\dagger\int d^3r'\,(\vec{\sigma}_1 - \vec{\sigma}_2)\cdot\vec{r}'V^{PV}(\vec{r}')\psi_d(r')\chi_t\xi_0, \qquad (E.3)$$

where we have included the normalized isospin wave function ξ_0 since the potential involves $\vec{\tau}_1, \vec{\tau}_2$. When operating on such an isosinglet np state the PV potential can be written as

$$\begin{aligned}
V^{PV}(\vec{r}') = \frac{2}{\Lambda_\chi^3}\Big[&(C_1 - 3C_3)(\vec{\sigma}_1 - \vec{\sigma}_2)\cdot\left(-i\vec{\nabla}f_m(r) + 2f_m(r)\cdot(-i\vec{\nabla})\right) \\
&+ (\tilde{C}_1 - 3\tilde{C}_3)(\vec{\sigma}_1 \times \vec{\sigma}_2)\cdot\vec{\nabla}f_m(r)\Big],
\end{aligned} \qquad (E.4)$$

where $f_m(r)$ is the Yukawa form

$$f_m(r) = \frac{m^2e^{-mr}}{4\pi r}$$

defined in Eq. (7). Using the identity

$$(\vec{\sigma}_1 \times \vec{\sigma}_2)\frac{1}{2}(1 + \vec{\sigma}_1\cdot\vec{\sigma}_2) = i(\vec{\sigma}_1 - \vec{\sigma}_2) \qquad (E.5)$$

Eq. (E.3) becomes

$$\begin{aligned}
&\sqrt{\frac{\gamma}{2\pi}}\lambda_t\chi_t \\
&\quad\simeq \frac{2M}{16\pi\Lambda_\chi^3}\frac{4\pi}{3}(\vec{\sigma}_1 - \vec{\sigma}_2)^2\chi_t\int\limits_0^\infty dr\,r^3 \\
&\qquad\times\left[-2(3C_3 - C_1)f_m(r)\frac{d\psi_d(r)}{dr} + (3\tilde{C}_3 - 3C_3 - \tilde{C}_1 + C_1)\frac{df_m(r)}{dr}\psi_d(r)\right]
\end{aligned}$$

$$= \sqrt{\frac{\gamma}{2\pi}} \cdot 4\chi_t \frac{1}{12} \frac{2Mm^2}{4\pi \Lambda_\chi^3}$$

$$\times \frac{2m(6C_3 - 3\tilde{C}_3 - 2C_1 + \tilde{C}_1) + \gamma(15C_3 - 3\tilde{C}_3 - 5C_1 + \tilde{C}_1)}{(\gamma + m)^2} \tag{E.6}$$

or

$$\lambda_t \simeq \frac{Mm^2}{6\pi \Lambda_\chi^3} \frac{2m(6C_3 - 3\tilde{C}_3 - 2C_1 + \tilde{C}_1) + \gamma(15C_3 - 3\tilde{C}_3 - 5C_1 + \tilde{C}_1)}{(\gamma + m)^2}. \tag{E.7}$$

In order to determine the singlet parameter λ_s^{np}, we must use the $^1S_0$ np-scattering wave function instead of the deuteron, but the procedure is similar, yielding [102,103]

$$d_s^{np}(k)\chi_s \equiv i \frac{M}{48\pi} \xi_1^\dagger \int d^3r' \, (\vec{\sigma}_1 - \vec{\sigma}_2) \cdot \vec{r}' V^{\mathrm{PV}}(\vec{r}') \psi_{^1S_0}(r')\chi_s\xi_1, \tag{E.8}$$

and we can proceed similarly. In this case the potential becomes

$$V^{\mathrm{PV}}(\vec{r}') = \frac{2}{\Lambda_\chi^3} \Big[(C_1 + C_3 + 4C_5)(\vec{\sigma}_1 - \vec{\sigma}_2) \cdot \big(-i\vec{\nabla} f_m(r) + 2f_m(r) \cdot -(i\vec{\nabla}) \big)$$

$$+ (\tilde{C}_1 + \tilde{C}_3 + 4\tilde{C}_5)(\vec{\sigma}_1 \times \vec{\sigma}_2) \cdot \vec{\nabla} f_m(r) \Big], \tag{E.9}$$

and Eq. (E.8) is found to have the form

$$d_s^{np}(k)\chi_s = \frac{2M}{48\pi \Lambda_\chi^3} \frac{4\pi}{3} (\vec{\sigma}_1 - \vec{\sigma}_2)^2 \chi_s \int\limits_0^\infty dr\, r^3 \Big\{ 2[C_1 + C_3 + 4C_5] f_m(r) \frac{d\psi_{^1S_0}(r)}{dr}$$

$$+ \big[C_1 + \tilde{C}_1 + C_3 + \tilde{C}_3 + 4(C_5 + \tilde{C}_5) \big] \frac{df_m(r)}{dr} \psi_{^1S_0}(r) \Big\}$$

$$= -12\chi_s \frac{1}{36} \frac{2Mm^2}{4\pi \Lambda_\chi^3} e^{i\delta_s} \Big\{ \frac{1}{(k^2 + m^2)^2}$$

$$\times \Big[\cos\delta_s \big[4k^2(C_1 + C_3 + 4C_5)$$

$$+ \big(C_1 + \tilde{C}_1 + C_3 + \tilde{C}_3 + 4(C_5 + \tilde{C}_5) \big) (k^2 + 3m^2) \big]$$

$$+ \frac{2m}{k} \sin\delta_s \big[(C_1 + C_3 + 4C_5)(m^2 + 3k^2)$$

$$+ \big(C_1 + \tilde{C}_1 + C_3 + \tilde{C}_3 + 4(C_5 + \tilde{C}_5) \big) m^2 \big] \Big] \Big\}, \tag{E.10}$$

which, in the limit as $k \to 0$, yields the predicted value for λ_s^{np}:

$$\lambda_s^{np} = -\frac{1}{a_s^{np}} \lim_{k \to 0} d_s^{np}(k)$$

$$= \frac{M}{6\pi a_s^{np} \Lambda_\chi^3} \Big\{ 3\big[C_1 + \tilde{C}_1 + C_3 + \tilde{C}_3 + 4(C_5 + \tilde{C}_5) \big]$$

$$- 2ma_s^{np}\big[2C_1 + \tilde{C}_1 + 2C_3 + \tilde{C}_3 + 4(2C_5 + \tilde{C}_5) \big] \Big\}. \tag{E.11}$$

Similarly, we may identify

$$
\begin{aligned}
\lambda_s^{pp} &= -\frac{1}{a_s^{pp}} \lim_{k \to 0} d_s^{pp}(k) \\
&= \frac{M}{6\pi a_s^{pp} \Lambda_\chi^3} \Big\{ 3\big[C_1 + \tilde{C}_1 + C_2 + \tilde{C}_2 + C_3 + \tilde{C}_3 + C_4 + \tilde{C}_4 - 2(C_5 + \tilde{C}_5) \big] \\
&\quad - 2ma_s^{pp} \big[2C_1 + \tilde{C}_1 + 2C_2 + \tilde{C}_2 + 2C_3 + \tilde{C}_3 + 2C_4 + \tilde{C}_4 - 2(2C_5 + \tilde{C}_5) \big] \Big\}, \\
\lambda_s^{nn} &= -\frac{1}{a_s^{nn}} \lim_{k \to 0} d_s^{nn}(k) \\
&= \frac{M}{6\pi a_s^{nn} \Lambda_\chi^3} \Big\{ 3\big[C_1 + \tilde{C}_1 - C_2 - \tilde{C}_2 + C_3 + \tilde{C}_3 - C_4 - \tilde{C}_4 - 2(C_5 + \tilde{C}_5) \big] \\
&\quad - 2ma_s^{nn} \big[2C_1 + \tilde{C}_1 - 2C_2 - \tilde{C}_2 + 2C_3 + \tilde{C}_3 - 2C_4 - \tilde{C}_4 \\
&\quad - 2(2C_5 + \tilde{C}_5) \big] \Big\}.
\end{aligned}
\tag{E.12}
$$

In order to evaluate the spin-conserving amplitude ρ_t, we shall assume dominance of the long range pion component. The shift in the deuteron wave function is given by

$$
\begin{aligned}
\delta\psi_d(\vec{r}) &= \xi_0^\dagger \int d^3r' \, G_0(\vec{r}, \vec{r}') V_{\text{LR}}^{\text{PV}}(\vec{r}') \psi_d(r') \\
&= -\frac{M}{4\pi} \xi_0^\dagger \int d^3r' \, \frac{e^{-\gamma|\vec{r}-\vec{r}'|}}{|\vec{r}-\vec{r}'|} V_{\text{LR}}^{\text{PV}}(\vec{r}') \psi_d(r') \chi_t \xi_0
\end{aligned}
\tag{E.13}
$$

but now with[8]

$$
V_{\text{LR}}^{\text{PV}}(\vec{r}) = \frac{h_\pi g_{\pi NN}}{\sqrt{2}M} \frac{1}{2} (\tau_1 - \tau_2)_z (\vec{\sigma}_1 + \vec{\sigma}_2) \cdot \big(-i\vec{\nabla} w_\pi(r) \big).
\tag{E.15}
$$

Of course, the meson which is exchanged is the pion so the short range assumption which permitted the replacement in Eq. (E.2) is not valid and we must perform the integration exactly. This process is straightforward but tedious [100]. Nevertheless, we can get a rough estimate by making a "heavy pion" approximation, whereby we can identify the constant ρ_t via

$$
\sqrt{\frac{\gamma}{2\pi}} \rho_t \chi_t \approx -i\frac{M}{32\pi} \int d^3r' \, (\vec{\sigma}_1 + \vec{\sigma}_2) \cdot \vec{r}' V_{\text{LR}}^{\text{PV}}(\vec{r}') \psi_d(r') \chi_t \xi_0
\tag{E.16}
$$

which leads to [105]

$$
\begin{aligned}
\sqrt{\frac{\gamma}{2\pi}} \rho_t \chi_t &\approx -\frac{1}{32\pi} \frac{4\pi}{3} (\vec{\sigma}_1 + \vec{\sigma}_2)^2 \chi_t \frac{h_{\pi NN}^1 g_{\pi NN}}{\sqrt{2}} \int_0^\infty dr \, r^3 \frac{df_\pi(r)}{dr} \psi_d(r) \frac{1}{m_\pi^2} \\
&= \sqrt{\frac{\gamma}{2\pi}} 8\chi_t \frac{1}{96\pi} \frac{h_\pi g_{\pi NN}}{\sqrt{2}} \frac{\gamma + 2m_\pi}{(\gamma + m_\pi)^2}.
\end{aligned}
\tag{E.17}
$$

---

[8] Here we have used the identity

$$
(\vec{\tau}_1 \times \vec{\tau}_2) = -i(\vec{\tau}_1 - \vec{\tau}_2) \frac{1}{2} (1 + \vec{\tau}_1 \cdot \vec{\tau}_2).
\tag{E.14}
$$

We find then the prediction

$$\rho_t = \frac{g_{\pi NN}}{12\sqrt{2}\pi} \frac{\gamma + 2m_\pi}{(\gamma + m_\pi)^2} h^1_{\pi NN}. \tag{E.18}$$

At this point it is useful to obtain rough numerical estimates. This can be done by use of the numerical estimates given in Table 2. To make things tractable, we shall use the best values given therein. Since we are after only rough estimates and since the best values assume the DDH relationship—Eq. (9) between the tilded and non-tilded quantities, we shall express our results in terms of only the non-tilded numbers—a future complete evaluation should include the full dependence. Of course, these predictions are only within a model, but they has the advantage of allowing connection with previous theoretical estimates. In this way, we obtain the predictions

$$\begin{aligned}
\lambda_t &= [-0.092C_3 - 0.014C_1]m_\pi^{-1}, \\
\lambda_s^{np} &= \big[-0.087(C_3 + 4C_5) - 0.037C_1\big]m_\pi^{-1}, \\
\lambda_s^{pp} &= \big[-0.087(C_3 + C_4 - 2C_5) - 0.037(C_1 + C_2)\big]m_\pi^{-1}, \\
\lambda_s^{nn} &= \big[-0.087(C_3 - C_4 - 2C_5) - 0.037(C_1 - C_2)\big]m_\pi^{-1}, \\
\rho_t &= 0.346 h_\pi m_\pi^{-1},
\end{aligned} \tag{E.19}$$

so that, using the best values from Table 2 we estimate

$$\begin{aligned}
\lambda_t &= -2.39 \times 10^{-7} m_\pi^{-1} = -3.41 \times 10^{-7} \text{ fm}, \\
\lambda_s^{np} &= -1.12 \times 10^{-7} m_\pi^{-1} = -1.60 \times 10^{-7} \text{ fm}, \\
\lambda_s^{pp} &= -3.58 \times 10^{-7} m_\pi^{-1} = -5.22 \times 10^{-7} \text{ fm}, \\
\lambda_s^{nn} &= -2.97 \times 10^{-7} m_\pi^{-1} = -4.33 \times 10^{-7} \text{ fm}, \\
\rho_t &= 1.50 \times 10^{-7} m_\pi^{-1} = 2.14 \times 10^{-7} \text{ fm}.
\end{aligned} \tag{E.20}$$

Again we emphasize that in arriving at the foregoing expressions, we have used the DDH relationships between the C_i and $\tilde{C}_i$. In the more general case, one should obtain expressions containing roughly the linear combinations given in Eqs. (46). A similar caveat applies to the expressions below.

At this point we note, however, that λ_s^{pp} is an order of magnitude larger than the experimentally determined number, Eq. (55). The problem here is not with the couplings but with an important piece of physics which has thus far been neglected—short distance effects. There are two issues here. One is that the deuteron and NN wave functions should be modified at short distances from the simple asymptotic form used up until this point in order to account for finite size effects. The second is the well-known feature of the Jastrow correlations that suppress the nucleon–nucleon wave function at short distance.

In order to deal approximately with the short distance properties of the deuteron wave function, we modify the exponential form to become constant inside the deuteron radius R [102,103]

$$\sqrt{\frac{\gamma}{2\pi}} \frac{1}{r} e^{-\gamma r} \to N \begin{cases} \frac{1}{R} e^{-\gamma R}, & r \leqslant R, \\ \frac{1}{r} e^{-\gamma r}, & r > R, \end{cases} \tag{E.21}$$

where

$$N = \sqrt{\frac{\gamma}{2\pi}} \frac{e^{\gamma R}}{\sqrt{1 + \frac{2}{3}\gamma R}}$$

is the modified normalization factor and we use $R = 1.6$ fm. For the NN wave function we use [102,103]

$$\psi_{1S_0}(r) = \begin{cases} A\dfrac{\sin\sqrt{p^2+p_0^2}\,r}{\sqrt{p^2+p_0^2}\,r}, & r \leqslant r_s, \\[2ex] \dfrac{\sin pr}{pr} - \dfrac{1}{\frac{1}{a_s}+ip}\dfrac{e^{ipr}}{r}, & r > r_s, \end{cases} \tag{E.22}$$

where we choose $r_s = 2.73$ fm and $p_o r_s = 1.5$. The normalization constant $A(p)$ is found by requiring continuity of the wave function and its first derivative at $r = r_s$

$$A(p) = \frac{\sqrt{p^2+p_0^2}\,r_s}{\sin\sqrt{p^2+p_0^2}\,r_s} \frac{\sin pr_s - pa_s \cos pr_s}{pr_s(1+ipa_s)}. \tag{E.23}$$

As to the Jastrow correlations we multiply the wave function by the simple phenomenological form [106]

$$\phi(r) = 1 - ce^{-dr^2}, \quad \text{with } c = 0.6, \ d = 3 \text{ fm}^{-2}. \tag{E.24}$$

With these modifications we find the much more reasonable values for the constants $\lambda_s^{pp,np}$ and λ_t

$$\begin{aligned} \lambda_s^{pp} &= \left[-0.011(C_3 + C_4 - 2C_5) - 0.004(C_1 + C_2)\right]m_\pi^{-1}, \\ \lambda_s^{nn} &= \left[-0.011(C_3 - C_4 + 2C_5) - 0.004(C_1 - C_2)\right]m_\pi^{-1}, \\ \lambda_s^{np} &= \left[-0.011(C_3 + 4C_5) - 0.004C_1\right]m_\pi^{-1}, \\ \lambda_t &= [-0.019C_3 - 0.0003C_1]m_\pi^{-1}. \end{aligned} \tag{E.25}$$

Using the best values from Table 2 we find then the benchmark values

$$\begin{aligned} \lambda_s^{pp} &= -4.2 \times 10^{-8} m_\pi^{-1} = -6.1 \times 10^{-8} \text{ fm}, \\ \lambda_s^{nn} &= -3.6 \times 10^{-8} m_\pi^{-1} = -5.3 \times 10^{-8} \text{ fm}, \\ \lambda_s^{np} &= -1.3 \times 10^{-8} m_\pi^{-1} = -1.9 \times 10^{-8} \text{ fm}, \\ \lambda_t &= -4.7 \times 10^{-8} m_\pi^{-1} = -6.7 \times 10^{-8} \text{ fm}. \end{aligned} \tag{E.26}$$

Since ρ_t is a long distance effect, we use the same value as calculated previously as our benchmark number

$$\rho_t = 1.50 \times 10^{-7} \ m_\pi^{-1} = 2.14 \times 10^{-7} \text{ fm}. \tag{E.27}$$

Obviously, the value of λ_s^{pp} is now in much better agreement with the experimental value Eq. (55). Of course, our rough estimate is no substitute for a reliable state of the art

wave function evaluation. This has been done recently by Carlson et al. and yields, using the Argonne V18 wavefunctions [104]

$$\lambda_s^{pp} = \left[-0.008(C_3 + C_4 - 2C_5) - 0.003(C_1 + C_2)\right]m_\pi^{-1} \tag{E.28}$$

in reasonable agreement with the value calculated in Eq. (E.25). Similar efforts should be directed toward evaluation of the remaining parameters using the best modern wave functions.

We end our brief discussion here, but clearly this was merely a simplistic model calculation. It is important to complete this process by using the best contemporary nucleon–nucleon wave functions with the most general EFT potential developed above, in order to allow the best possible restrictions to be placed on the unknown counter-terms.

References

[1] See, e.g., S.C. Pieper, R.B. Wiringa, Annu. Rev. Nucl. Part. Sci. 51 (2001) 53;
    B.R. Barrett, P. Navrátil, W.E. Ormand, J.P. Vary, Acta Phys. Pol. B 33 (2002) 297.
[2] See, e.g., P.F. Bedaque, U. van Kolck, Annu. Rev. Nucl. Part. Sci. 52 (2002) 339.
[3] S. Weinberg, Phys. Lett. B 251 (1990) 288;
    S. Weinberg, Nucl. Phys. B 363 (1991) 3.
[4] C. Ordóñez, U. van Kolck, Phys. Lett. B 291 (1992) 459;
    C. Ordóñez, L. Ray, U. van Kolck, Phys. Rev. C 53 (1996) 2086;
    N. Kaiser, R. Brockmann, W. Weise, Nucl. Phys. A 625 (1997) 758;
    N. Kaiser, S. Gerstendorfer, W. Weise, Nucl. Phys. A 637 (1998) 395;
    N. Kaiser, Phys. Rev. C 65 (2002) 017001, and references therein.
[5] U. van Kolck, Phys. Rev. C 49 (1994) 2932;
    J.L. Friar, D. Hüber, U. van Kolck, Phys. Rev. C 59 (1999) 53.
[6] E. Epelbaum, W. Glöckle, U.-G. Meißner, Nucl. Phys. A 671 (2000) 295, nucl-th/0405048;
    D.R. Entem, R. Machleidt, Phys. Rev. C 68 (2003) 041001.
[7] E. Epelbaum, A. Nogga, W. Glöckle, H. Kamada, U.-G. Meißner, H. Witała, Phys. Rev. C 66 (2002) 064001.
[8] U. van Kolck, Nucl. Phys. A 645 (1999) 273.
[9] J.-W. Chen, G. Rupak, M.J. Savage, Nucl. Phys. A 653 (1999) 386.
[10] P.F. Bedaque, U. van Kolck, Phys. Lett. B 428 (1998) 221;
    P.F. Bedaque, H.-W. Hammer, U. van Kolck, Phys. Rev. C 58 (1998) 641;
    F. Gabbiani, P.F. Bedaque, H.W. Grießhammer, Nucl. Phys. A 675 (2000) 601.
[11] P.F. Bedaque, H.-W. Hammer, U. van Kolck, Nucl. Phys. A 676 (2000) 357;
    P.F. Bedaque, G. Rupak, H.W. Grießhammer, H.-W. Hammer, Nucl. Phys. A 714 (2003) 589.
[12] T.-S. Park, D.-P. Min, M. Rho, Nucl. Phys. A 596 (1996) 515;
    J.-W. Chen, G. Rupak, M.J. Savage, Phys. Lett. B 464 (1999) 1;
    G. Rupak, Nucl. Phys. A 678 (2000) 405;
    T.-S. Park, K. Kubodera, D.-P. Min, M. Rho, Phys. Lett. B 472 (2000) 232.
[13] N. Tanner, Phys. Rev. 107 (1957) 1203.
[14] C.S. Wu, et al., Phys. Rev. 105 (1957) 1413.
[15] F.C. Michel, Phys. Rev. B 133 (1964) 329.
[16] B.H.J. McKellar, Phys. Lett. B 26 (1967) 107.
[17] E. Fischbach, Phys. Rev. 170 (1968) 1398;
    D. Tadic, Phys. Rev. 174 (1968) 1694;
    W. Kummer, M. Schweda, Acta Phys. Aust. 28 (1968) 303;
    B.H.J. McKellar, P. Pick, Phys. Rev. D 7 (1973) 260.

[18] H.J. Pirner, D.O. Riska, Phys. Lett. B 44 (1973) 151.
[19] B. Desplanques, J.F. Donoghue, B.R. Holstein, Ann. Phys. (N.Y.) 124 (1980) 449.
[20] W.S. Wilburn, J.D. Bowman, Phys. Rev. C 57 (1998) 3425.
[21] W.C. Haxton, C.P. Liu, M.J. Ramsey-Musolf, Phys. Rev. C 65 (2002) 045502;
     W.C. Haxton, C.E. Wieman, Annu. Rev. Nucl. Part. Sci. 51 (2001) 261.
[22] G.A. Miller, Phys. Rev. C 67 (2003) 042501(R).
[23] See, e.g., D.H. Beck, B.R. Holstein, Int. J. Mod. Phys. E 10 (2001) 1;
     D.H. Beck, R.D. McKeown, Annu. Rev. Nucl. Part. Sci. 51 (2001) 189.
[24] G.S. Danilov, Phys. Lett. 18 (1965) 40.
[25] B. Desplanques, J. Missimer, Nucl. Phys. A 300 (1978) 286;
     B. Desplanques, Phys. Rep. 297 (1998) 2.
[26] G. Barton, Nuovo Cimento 19 (1961) 512.
[27] B.R. Holstein, Phys. Rev. D 23 (1981) 1618.
[28] V.M. Dubovik, S.V. Zenkin, Ann. Phys. (N.Y.) 172 (1986) 100.
[29] G.B. Feldman, G.A. Crawford, J. Dubach, B.R. Holstein, Phys. Rev. C 43 (1991) 863.
[30] C.S. Wood, et al., Science 275 (1997) 1759.
[31] D.B. Kaplan, M.J. Savage, Nucl. Phys. A 556 (1993) 653.
[32] S.-L. Zhu, S. Puglia, B.R. Holstein, M.J. Ramsey-Musolf, Phys. Rev. D 63 (2001) 033006.
[33] S.-L. Zhu, S. Puglia, B.R. Holstein, M.J. Ramsey-Musolf, Phys. Rev. D 62 (2000) 033008.
[34] C.M. Maekawa, U. van Kolck, Phys. Lett. B 478 (2000) 73;
     C.M. Maekawa, J.S. Veiga, U. van Kolck, Phys. Lett. B 488 (2000) 167.
[35] P.F. Bedaque, M.J. Savage, Phys. Rev. C 62 (2000) 018501.
[36] J.-W. Chen, T.D. Cohen, C.W. Kao, Phys. Rev. C 64 (2001) 055206.
[37] J.-W. Chen, X. Ji, Phys. Rev. Lett. 86 (2001) 4239;
     J.-W. Chen, X. Ji, Phys. Lett. B 501 (2001) 209.
[38] S.-L. Zhu, S. Puglia, B.R. Holstein, M.J. Ramsey-Musolf, Phys. Rev. C 64 (2001) 035502;
     S.-L. Zhu, C.M. Maekawa, B.R. Holstein, M.J. Ramsey-Musolf, Phys. Rev. Lett. 87 (2001) 201802;
     S.-L. Zhu, C.M. Maekawa, G. Sacco, B.R. Holstein, M.J. Ramsey-Musolf, Phys. Rev. D 65 (2002) 033001.
[39] D.B. Kaplan, M.J. Savage, R.P. Springer, M.B. Wise, Phys. Lett. B 449 (1999) 1.
[40] M.J. Savage, R.P. Springer, Nucl. Phys. A 644 (1998) 238;
     M.J. Savage, R.P. Springer, Nucl. Phys. A 657 (1999) 457;
     M.J. Savage, R.P. Springer, Nucl. Phys. A 686 (2001) 413.
[41] C.H. Hyun, T.-S. Park, D.-P. Min, Phys. Lett. B 516 (2001) 321.
[42] S.R. Beane, P.F. Bedaque, M.J. Savage, U. van Kolck, Nucl. Phys. A 700 (2002) 377;
     S.R. Beane, M.J. Savage, Nucl. Phys. A 713 (2003) 148;
     S.R. Beane, M.J. Savage, Nucl. Phys. A 717 (2003) 91.
[43] A.R. Berdoz, et al., Phys. Rev. C 68 (2003) 034004;
     A.R. Berdoz, et al., Phys. Rev. Lett. 87 (2001) 272301.
[44] K.S. Krane, et al., Phys. Rev. C 4 (1971) 1906.
[45] V.W. Yuan, et al., Phys. Rev. C 44 (1991) 2187;
     Y. Masuda, et al., Nucl. Phys. A 504 (1989) 269;
     V.P. Alfimenko, et al., Nucl. Phys. A 398 (1983) 93.
[46] E.G. Adelberger, et al., Phys. Rev. C 27 (1983) 2833.
[47] K. Elsener, et al., Nucl. Phys. A 461 (1987) 579;
     K. Elsener, et al., Phys. Rev. Lett. 52 (1984) 1476.
[48] K.A. Snover, et al., Phys. Rev. Lett. 41 (1978) 145.
[49] E.D. Earle, et al., Nucl. Phys. A 396 (1983) 221.
[50] C.A. Barnes, et al., Phys. Rev. Lett. 40 (1978) 840.
[51] M. Bini, et al., Phys. Rev. Lett. 55 (1985) 795.
[52] G. Ahrens, et al., Nucl. Phys. A 390 (1982) 496.
[53] S.A. Page, et al., Phys. Rev. C 35 (1987) 1119.
[54] B.R. Holstein, Weak Interactions in Nuclei, World Scientific, Singapore, 1989.
[55] E. Adelberger, W.C. Haxton, Annu. Rev. Nucl. Part. Sci. 35 (1985) 501.

[56] W. Haeberli, B.R. Holstein, in: W.C. Haxton, E.M. Henley (Eds.), Symmetries and Fundamental Interactions in Nuclei, World Scientific, Singapore, 1995.
[57] S. Weinberg, Physica A 96 (1979) 327.
[58] J. Gasser, H. Leutwyler, Ann. Phys. (N.Y.) 159 (1984) 142;
    J. Gasser, H. Leutwyler, Nucl. Phys. B 250 (1985) 465.
[59] R. Schiavilla, J. Carlson, private communication.
[60] V.R. Brown, E.M. Henley, F.R. Krejs, Phys. Rev. C 9 (1974) 935.
[61] T. Oka, Prog. Theor. Phys. 66 (1981) 977.
[62] D.E. Driscoll, G.A. Miller, Phys. Rev. C 39 (1989) 1951.
[63] P.D. Evershiem, et al., Phys. Lett. B 256 (1991) 11.
[64] S. Kistryn, et al., Phys. Rev. Lett. 58 (1987) 1616;
    R. Balzer, et al., Phys. Rev. C 30 (1984) 1409.
[65] J.M. Potter, et al., Phys. Rev. Lett. 33 (1974) 1307;
    D.E. Nagle, et al., in: 3rd International Symposium on High Energy Physics with Polarized Beams and Targets, AIP Conf. Proc. 51 (1978) 224.
[66] J. Lang, et al., Phys. Rev. Lett. 54 (1985) 170.
[67] M. Snow, et al., Nucl. Instrum. Methods 440 (2000) 729.
[68] D. Markov, private communication.
[69] C. Papanicholas, private communication.
[70] H. Weller, private communication.
[71] M. Snow, private communication.
[72] R.B. Wiringa, V.G.J. Stoks, R. Schiavilla, Phys. Rev. C 51 (1995) 38.
[73] R. Suleman, S. Kowalski, Jefferson Laboratory proposal PR02-006.
[74] B. Wojtsekhowski, Jefferson Laboratory letter of intent LOI-00-002.
[75] H. Georgi, Phys. Lett. B 240 (1990) 447.
[76] E. Jenkins, A.V. Manohar, Phys. Lett. B 255 (1991) 558;
    E. Jenkins, A.V. Manohar, Phys. Lett. B 259 (1991) 353.
[77] M. Luke, A.V. Manohar, Phys. Lett. B 286 (1992) 348.
[78] B.R. Holstein, Phys. Rev. D 60 (1999) 114030.
[79] X. Kong, F. Ravndal, Nucl. Phys. A 656 (1999) 421.
[80] M.J. Savage, Nucl. Phys. A 695 (2001) 365.
[81] G. Prezeau, M.J. Ramsey-Musolf, P. Vogel, hep-ph/0303205.
[82] V. Bernard, N. Kaiser, U.-G. Meißner, Int. J. Mod. Phys. E 1 (1992) 561.
[83] B.R. Holstein, Phys. Lett. B 244 (1990) 83.
[84] T.R. Hemmert, B.R. Holstein, J. Kambor, J. Phys. G 24 (1998) 1831.
[85] N. Fettes, et al., Ann. Phys. 283 (2000) 273;
    N. Fettes, et al., Ann. Phys. 288 (2001) 249, Erratum.
[86] A. Manohar, H. Georgi, Nucl. Phys. B 234 (1984) 189.
[87] M.E. Luke, A.V. Manohar, Phys. Lett. B 286 (1992) 348.
[88] J.F. Donoghue, E. Golowich, B.R. Holstein, Phys. Rev. D 30 (1984) 587.
[89] D.B. Kaplan, M.J. Savage, M.B. Wise, Phys. Lett. B 424 (1998) 390;
    D.B. Kaplan, M.J. Savage, M.B. Wise, Nucl. Phys. B 534 (1998) 329.
[90] S. Fleming, T. Mehen, I.W. Stewart, Nucl. Phys. A 677 (2000) 313.
[91] M.C.M. Rentmeester, R.G.E. Timmermans, J.L. Friar, J.J. de Swart, Phys. Rev. Lett. 82 (1999) 4992.
[92] E. Witten, Nucl. Phys. B 160 (1979) 57.
[93] G. Ecker, J. Gasser, A. Pich, E. de Rafael, Nucl. Phys. B 321 (1989) 311.
[94] G. Höhler, et al., Nucl. Phys. B 114 (1976) 505.
[95] V.G.J. Stoks, R.A.M. Klomp, C.P.F. Terheggen, J.J. de Swart, Phys. Rev. C 49 (1994) 2950.
[96] J.D. Bjorken, S. Drell, Relativistic Quantum Fields, McGraw–Hill, New York, 1965.
[97] G.E. Brown, R. Machleidt, Phys. Rev. C 50 (1986) 1731.
[98] G. Janssen, K. Holinde, J. Speth, Phys. Rev. C 54 (1996) 2218.
[99] S.-L. Zhu, Phys. Rev. C 59 (1999) 435;
    S.-L. Zhu, Phys. Rev. C 59 (1999) 3455.
[100] B. Desplanques, Nucl. Phys. A 335 (1980) 147.

[101] B.F. Gibson, V.R. Brown, R. Schiavilla, private communications.
[102] Here we follow the approach of: I.B. Khriplovich, R.V. Korkin, Nucl. Phys. A 690 (2001) 610.
[103] I.B. Khriplovich, Phys. At. Nucl. 64 (2001) 516.
[104] J. Carlson, R. Schiavilla, V.R. Brown, B.F. Gibson, Phys. Rev. C 65 (2002) 035502.
[105] B. Desplanques, Phys. Lett. B 512 (2001) 305.
[106] D.O. Riska, G.E. Brown, Phys. Lett. B 38 (1972) 193.